Biogeochemical and kinetics characterization of sulfate reducing microbial communities enriched from mine drainages

By

Karabelo Macmillan Moloantoa

February 2015

University of the Free State

Universiteit van die Vrystaat

Yunivesithi ya Freistata

Biogeochemical and kinetics characterization of sulfate reducing microbial communities enriched from mine drainages

By

Karabelo Macmillan Moloantoa

BSc. Hons. (UFS)

Submitted in fulfilment of the requirements for the degree

MAGISTER SCIENTIAE

In the

Department of Microbial, Biochemical and Food Biotechnology

Faculty of Natural and Agricultural Sciences

University of the Free State

Bloemfontein

South Africa

February 2015

Supervisor: Prof. E. van Heerden

Co-Supervisor: Dr. J. C. Castillo

I hereby dedicate this dissertation to my mother

Judith Letladi Moloantoa, Grandmother Eva Tlou Ramphele,

my two uncles (Christopher Ramphele and Lebogang Ramphele), my

three aunts (Mathea Maponya, Phuti Machaba and Katlego Thobejane)

and Lesego Sebatana for their support and love during my studies.

“With men, this is impossible, but with God all things are possible”

(Mathew 19:29)

ACKNOWLEDGEMENTS

I would like to express my gratitude and appreciation to the following:

- **God:** My creator and father, for giving me life, strength and wisdom to accomplish all tasks presented to me during my studies. (Phillipians 4:19 – 20).

- **Prof. E. van Heerden:** My supervisor, for being the best study leader ever. Thank you for believing in me and never giving up on me even when I was at my worst lows. Thank you for the opportunity to explore my potential in achieving greater things in my life. Your amazing knowledge, assistance, guidance, love and coaching has impacted my life not only academically but personally and intellectually as a scientist.

- **Dr. J. C. Castillo:** My co-supervisor, for your hard work and guidance throughout my bench work and dissertation write up. Thank your for sacrificing most of your personal time including seval evenings we spent in the laboratory. Thank you for being patient with me and always coming to my rescue when I needed scientific help. I highly value and appreciate your support and guidance till the very last day of the preparation of this script.

- **Prof. M. Smith, L. Steyn and T. Mpeyakhe (Department of Biotechnology, UFS, Bloemfontein):** for assistance with the Bioreactors.

- **Prof. P. van Wyk, Dr. C. Swart-Pistor and H. Grobler (Centre for Microscopy, UFS, Bloemfontein)**: for assistance with SEM and TEM analysis.

- **D. Welman-Purchase (Department of Geology, UFS, Bloemfontein)**: for assistance with XRD analysis.

- **Dr. P. Williams, M. Maleke, C. Mulandu, O.O. Kuloyo, A.O. Ojo:** My colleagues, for your assistance when I needed extra pair of hands, eyes and scientific knowledge you imparted during my studies and for proofreading my dissertation in you inconvenient times.

- **L.J. Moloantoa:** My mother, for allowing me to further my studies and supporting me throughout my entire life. I wouldn't have done it without you. I love you mom.

- **Pastor. At Boshof and the CRC pastoral and leadership team (CRC Bloemfontein)**: My spiritual leaders, for the spiritual and moral design in my life. Thank you for your prayers and spiritual guidance and teachings than moulded the person I am today.

- **Lesego Sebatana:** For the support, genuine love and for always being there for me when I needed someone to confide in. You are the best.

- **TIA (Technology Innovation Agency):** for financial support.

DECLARATION

I hereby declare that this dissertation is submitted by me for the Magister Scientiae degree at the University of the Free State. This work is solely my own and has not been previously submitted by me at any other University or Faculty, and the other sources of information used have been acknowledged. I further grant copyright of this dissertation in favour of the University of the Free State.

KM Moloantoa (2007129626) February 2015

TABLE OF CONTENTS

LIST OF ABBREVIATIONS xiv

LIST OF FIGURES xvii

LIST OF TABLES xxiii

CHAPTER 1 1

1. LITERATURE REVIEW 2

1.1. Introduction 2

1.2. Acid Mine Drainage 2

1.2.1. Background of Acid Mine Drainage 2

1.2.2. Acid Mine Drainage formation 3

1.2.3. Properties of Acid Mine Drainage 5

1.3. Acid Mine Drainage treatment options 7

1.3.1. Overall Acid Mine Drainage treatment options 7

1.3.2. Chemical Acid Mine Drainage treatment 8

1.3.3. Biological Acid Mine Drainage treatment 9

1.4. Role of Sulfate-reducing bacteria in Acid Mine Drainage 10

1.4.1. Characteristics and diversity of sulfate-reducing bacteria 11

1.4.2. Factors affecting biological sulfate reduction in AMD 14

1.4.2.1. Electron donor and carbon source selected for SRB growth 14

1.4.2.2. The effect of temperature on SRB 15

1.4.2.3. The effect of pH on sulfate reduction 16

1.4.2.4. Sulfate and sulfide concentrations affecting sulfate reduction 17

1.4.2.5. Effect of high metals concentrations on sulfate-reduction 18
1.5. Conclusions 20
1.6. References 21

CHAPTER 2 27

2. INTRODUCTION TO THE PRESENT STUDY 28
2.1. Introduction 28
2.1.1. Study aims and objectives 29
2.2. References 31

CHAPTER 3 32

3. THE STUDY AND EVALUATION OF MICROBIAL COMMUNITIES FROM ACID MINE DRAINAGES AND NON ACID MINE DRAINAGES FOR THE SULFATE REDUCTION POTENTIAL 33
3.1. Abstract 33
3.2. Introduction 34
3.2.1. Aims and objectives of the chapter 36
3.3. Materials and methods 37
3.3.1. Localization and environmental settings 37
3.3.2. Samples collection 39

3.3.3. Chemical analysis 39
3.3.3.1. Physicochemical parameters 39
3.3.3.2. Sulfate concentrations 40
3.3.3.3. Sulfide concentrations 40
3.3.3.4. Other chemical analysis 42
3.3.4. Microbial characterization 42
3.3.4.1. DAPI staining 42
3.3.4.2. Live/Dead staining 44
3.3.4.3. Gram staining 44
3.3.5. Molecular characterization 45
3.3.5.1. Genomic DNA extraction 45
3.3.5.2. Amplification of the partial 16S rRNA gene fragment 46
3.3.5.3. Denaturation Gradient Gel Electrophoresis (DGGE) 47
3.3.6. Microbial enrichments 51
3.3.6.1. Anaerobic media preparations 52
3.3.6.2. Media inoculation and incubation 53
3.3.6.3. Secondary inoculation into fresh media 54
3.3.6.4. Tertiary inoculation into the fresh media 54
3.3.6.5. Microbial characterization of enriched cultures 55
3.3.6.6. Molecular analysis of the enriched tertiary cultures 55
3.3.6.7. Amplification of the dsrAB gene fragments from gDNA 55
3.3.6.8. Cryopreservation of the enriched cultures 57
3.3.6.9. Scanning Electron Microscopy 57
3.4. Results and discussions 58
3.4.1. Samples description and analysis 58
3.4.2. Microbial characterization results 61
3.4.2.1. Microbial cell counts by DAPI staining 61

3.4.2.2. Bacterial viability test by Live/Dead staining 62
3.4.2.3. Morphological characterization of bacteria by gram staining..... 62
3.4.3. Molecular characterization results 63
3.4.3.1. Genomic DNA extraction..... 63
3.4.3.2. Amplification of the partial 16S rRNA gene fragments 65
3.4.3.3. Denaturation Gradient Gel Electrophoresis (DGGE) analysis..... 65
3.4.4. Microbial enrichments results 70
3.4.4.1. Results analysis of the anaerobic enrichments 70
3.4.4.2. Microbial characterization of tertiary enrichment cultures 71
3.4.5. Molecular analysis of the enriched tertiary cultures 72
3.4.5.1. Genomic DNA extraction of the tertiary enrichment cultures..... 72
3.4.5.2. Amplification results of the partial 16S rRNA fragments from the enrichments gDNA 73
3.4.5.3. Denaturation Gradient Gel Electrophoresis (DGGE) analysis of the enriched cultures 74
3.4.5.4. Amplification results of the dsr gene fragments from the extracted gDNA 77
3.4.5.5. Scanning Electron Microscopy analysis of the enriched cultures... 79
3.5. Conclusions..... 82
3.6. References..... 84

CHAPTER 4 90

4. BEHAVIOURAL STUDIES AND EVALUATION OF ANAEROBIC SULFATE REDUCING COMMUNITIES FOR SULFATE REDUCTION AND METAL PRECIPITATION PROCESSES IN VARIED CONDITIONS 91
4.1. Abstract..... 91

4.2. Introduction 92
4.2.1. Aims and objectives of the chapter 94
4.3. Materials and methods 95
4.3.1. Preparation and maintenance of cultures for the microbial-metal interaction experiments 95
4.3.2. Batch experiments 96
4.3.2.1. Microbial sulfate reduction of inclining concentrations 96
4.3.2.2. Effects of pH and temperature on sulfate reduction 96
4.3.2.2.1. Optical density measurements 97
4.3.2.3. Effects of high metal concentrations on sulfate reduction 97
4.3.3. Bioreactor studies 98
4.3.3.1. Carbon source selection 98
4.3.3.1.1. The Sixfors bioreactor setup 98
4.3.3.1.2. Bioreactors inoculation, start up, operation and termination 100
4.3.3.2. Metal-microbe interactions studies in the bioreactors 101
4.3.3.2.1. Sampling and analysis 101
4.3.3.2.2. Carbon source analysis 102
4.3.3.3. Molecular analysis of metals tolerant microorganisms 103
4.3.3.4. Morphological and mineralogical characterization of precipitates 103
4.3.3.4.1. Samples preparation 103
4.3.3.4.2. Scanning Electron Microscopy coupled to Energy Dispersed X-ray Spectroscopy (SEM-EDS) 103
4.3.3.4.3. Transmission Electron Microscopy coupled to Energy Dispersed X-ray Spectroscopy (TEM-EDS) 104
4.3.3.4.4. X-Ray Diffractometer analysis (XRD) 104
4.4. Results and discussions 105
4.4.1. Culture preparations for the metal-microbe interaction 105
4.4.2. Batch experiments 106

4.4.2.1. Microbial sulfate reduction of inclining concentrations 106
4.4.2.2. Effects of low pH and temperature on sulfate-reduction..... 107
4.4.2.3. Effects of high metal concentrations on sulfate reduction 111
4.4.3. Bioreactor studies..... 114
4.4.3.1. Carbon source selection 114
4.4.3.2. Metal-microbe interactions..... 117
4.4.3.3. Molecular analysis of metals tolerant microorganisms..... 122
4.4.3.3.1. Genomic DNA extraction and 16S rRNA amplification..... 122
4.4.3.3.2. Denaturation Gradient Gel Electrophoresis (DGGE)..... 123
4.4.3.4. Morphological and mineralogical characterization of precipitates 129
4.4.3.4.1. Scanning Electron Microscopy coupled to Energy Dispersed X-ray Spectroscopy (SEM-EDS)..... 130
4.4.3.4.2. Transmission Electron Microscopy coupled to Energy Dispersed X-ray spectroscopy (TEM-EDS)..... 134
4.4.3.4.3. X-Ray Diffraction analysis 136
4.5. Conclusions..... 137
4.6. References..... 139

CHAPTER 5 144
5. SUMMARY 145
5.1. Summary..... 145
5.2. Opsomming..... 148

LIST OF ABBREVIATIONS

ºC	Degrees Celsius
<	less than
>	greater than
%	Percentage
µL	microlitre
AMD	acid mine drainage
ARD	Acid rock drainage
ASRM	anaerobic sulfate reducing medium
BLAST	Basic Local Alignment Search Tool
bp	base pair
DAPI	4',6-diamidino-2-phenylindole
DGGE	Deanaturation Gradient Gel Electrophoresis
dH_2O	distilled water
DNA	Deoxyribonucleic Acid
DO	Dissolved oxygen
DSR	Dissimilatory sulphite reductase enzyme
dsrAB	Dissimilatory sulfite reductase gene
EC	Electrical conductivity
EDS	Energy Dispersive X-ray Spectroscopy
EDTA	Ethylenediaminetetraacetic acid.
EDX	X-ray Diffractometer

EPS	Extracellular olymeric substances
et al.	et alii / and others
EtBr	Ethidium Bromide
Fe_T	Total iron
g	gram
gDNA	Genomic DNA
ha	hectare
HPLC	High Performance Liquid Chromatography
ICP	Inductively Coupled Plasma
IDT	Integrated DNA Technologies
IGS	Institute of Ground water Studies
km	kilometre
kV	kilovolts
L	litre
M	Molar
mg/L	milligram per litre
mL	millilitre
mM	millimolar
mS/m	Millisimens per metre
mV	millivolts
NCBI	National Centre for Biotechnology Information
ng/µL	nanogram per microlitre
nm	nanometer

NMD	Non-acid mine drainage
OD	Optical Density
ORP	Oxidation Reduction Potential
PCR	Polymerase Chain Reaction
pH	Measure of the Acidity or Basicity of a solution
PSGM	Postgate medium
RNA	Ribosamal nucleic acid
SABS	South African Bureau of Standards
SEM	Scanning Electron Microscopy
SOB	Sulfide-oxidizing bacteria
sp.	specie
spp.	species
SRB	sulfate-reducing bacteria
t	ton
TAE	Tris Acetate EDTA
TDS	Total Dissolved Solids
TEM	Transmission Electron Microscopy
UF	Urea Formamide
v/v	volume per volume
w/v	weight per volume
w/w	weight per weight
x g	Acceleration due to Gravity
XRD	X-ray Diffraction

LIST OF FIGURES

Figure 1.1: Biological (biotic) and chemical (abiotic) strategies for acid mine drainage remediation. (Taken from Johnson and Hallberg, 2005).

Figure 1.2: Biological sulfur transformations in natural and artificial environments. (Taken from Sánchez-Adrea *et al.,* 2014).

Figure 1.3: Sulfide speciation as a function of pH at 25ºC. (Taken from Kaksonen and Puhukka, 2007).

Figure 3.1: AMD and NMD chemical formation process and the microbial diversities dominant in them. (Generic figure).

Figure 3.2: South African map indicating selected study sites. Location 1: Site-Ex, Location 2: Site-Ka and Location 3: Site-Po (Taken from McCarthy, 2011).

Figure 3.3: Sampling sites selected for the study. A: Site-Ex, B: Site-Ka and C: Site-Po.

Figure 3.4: Standard curve relating sulfide concentrations to absorbance (670 nm).

Figure 3.5: Anaerobic serum vials containing enrichment media. Left: PSGM, Middle: two vials containing yeast extract and Right: ASRM.

Figure 3.6: DAPI staining images. A: Sludge sample, B: Site-Ex, C: Site-Ka and D: Site-Po. Scale bar = 1 µm.

Figure 3.7: Live/Dead staining images from the three water samples. A: Site-Ex, B: Site-Ka and C: Site-Po.

Figure 3.8: Gram stained bacterial cells from the three water samples. A: Site-Ex, B: Site-Ka and C: Site-Po.

Figure 3.9: Genomic DNA extracts visualized on a 0.8% (w/v) agarose gel. A: representing the water samples and B: representing the two sludge samples.

A. Lane M: DNA standard Marker (O'GeneRuler^{TM} Ladder Mix), Lane 1: Site-Ex, Lane 2: Site-Ka and Lane 3: Site-Po.
B. Lane M: DNA standard Marker (O'GeneRuler^{TM} Ladder Mix), Lane 4: Sludge 1 and Lane 5: Sludge 2.

Figure 3.10: Amplification results of the partial 16S rRNA fragments from the extracted gDNA on a 1% (w/v) agarose gel. Lane M: DNA standard Marker (O'GeneRuler^{TM} Ladder Mix), Lane 1: Sludge 1, Lane 2: Sludge 2, Lane 3: Site-Ex, Lane 4: Site-Ka, Lane 5: Site-Po and Lane 6: Positive control.

Figure 3.11: DGGE profile of the sludge and AMD water samples. Lane 1: Site-Ex, Lane 2: Site-Ka, Lane 3: Site-Po and Lane 4: Sludge sample.

Figure 3.12: Tertiary anaerobic enrichment cultures in both ASRM and PSGM. A1: Sludge in ASRM, A2: Site-Ex in ASRM, A3: Site-Ka in ASRM and A4: Site-Po in ASRM. B1: Sludge in PSGM, B2: Site-Ex in PSGM, B3: Site-Ka in PSGM and B4: Site-Po in PSGM.

Figure 3.13: Microscopic analysis results of tertiary enrichment cultures. A-D: Gram staining (PSGM). A: Sludge in PSGM, B: Site-Ex in PSGM, C: Site-Ka in PSGM and D: Site-Po in PSGM.

E-H: Gram staining (ASRM). E: Sludge in ASRM, F: Site-Ex in ASRM, G: Site-Ka in ASRM and H: Site-Po in ASRM.

I-L: DAPI staining. I: Sludge in PSGM, J: Site-Ex in PSGM, K: Site-Ka in PSGM and L: Site-Po in PSGM.

M-P: Live/Dead staining. M: Sludge in PSGM, N: Site-Ex in PSGM, O: Site-Ka in PSGM and P: Site-Po in PSGM. Scale bar = 1 µm.

Figure 3.14: Amplification results of the partial 16S rRNA fragments from the extracted gDNA of tertiary cultures on a 1% (w/v) agarose gel. Lane M: DNA standard Marker (O'GeneRuler^{TM} Ladder Mix), Lane 1: Sludge in PSGM, Lane 2: Sludge in ASRM, Lane 3: Site-Ex in PSGM, Lane 4: Site-Ex in ASRM, Lane 5: Site-Ka in PSGM, Lane 6: Site-Ka in ASRM, Lane 7: Site-Po in PSGM and Lane 8: Site-Po in ASRM.

Figure 3.15: DGGE profile of tertiary cultures enriched in ASRM and PSGM. Lane 1: Sludge in PSGM, Lane 2: Sludge in ASRM, Lane 3: Site-Ex in PSGM, Lane 4: Site-Ex in ASRM, Lane 5: Site-Ka in PSGM, Lane 6: Site-Ka in ASRM, Lane 7: Site-Po in PSGM and Lane 8: Site-Po in ASRM.

Figure 3.16: Amplification results of the *dsrAB* gene fragments on 1% agarose gels. A: PCR products of the *dsrAB* gene fragments. Lane M: DNA standard Marker (O'GeneRuler^{TM} Ladder Mix), Lane 1: Site-Ex in PSGM, Lane 2: Site-Ka in PSGM, Lane 3: Slidge in PSGM, Lane 4: Sludge in ASRM, Lane 5: Site-Po in ASRM.
B: Gradient PCR amplification of the *dsrAB* gene fragments from sludge samples. Lane M: DNA standard Marker (O'GeneRuler^{TM} Ladder Mix), Group 1 Lanes: Sludge in PSGM and Group 2 Lanes: Sludge in ASRM.

Figure 3.17: Scanning Electron Microscope image showing biofilm and precipitates formed in the tertiary enrichment cultures. A: Biofilm enriched in PSGM, B and C: Higher magnification of subsections of A, D: Biofilm enriched in ASRM, E and F: Back Scattering images of precipitates in culture enriched in PSGM, G: Back Scattering images of precipitates in culture enriched in ASRM, H: Reference image of Pyrite precipitates (Taken from Larrasoaña *et al*., 2014), I: Reference image of the *Desulfovibrio* sp. (Taken from Warthmann *et al.,* 2005).

Figure 4.1: Preparation flow diagram and selected parameters for evaluating sulfate reducing activity of the enriched SRB.

Figure 4.2: Sixfors fermenters (INFORS AG CH-4103 Bottminingen / Switzerland) used for the bioreactor studies.

Figure 4.3: HPLC standard curve relating glycerol peak area to the amount of sample injected into the HPLC column.

Figure 4.4: Live/Dead staining images (A to C): A: Co-cultured consortia in PSGM, B: Co-cultured consortia in ASRM and C: Secondary co-cultured consortia from cultures depicted in A and B. D: Consortia maintained in PSGM for downstream experiments.

Figure 4.5: Parameter profiles monitored in four batch experiments to evaluate the effects of pH and temperature on SRB. A: Microbial growth curves, B: ORP profiles, C: pH profiles, D: sulfate reduction profiles, E: sulfide formation profiles and F: sulfide formation profiles of cultures grown at a pH of 3.5 (25ºC) and two cultures both grown at temperature of 10ºC in pH of 6.5 and 3.5.

Figure 4.6: Vials containing cultures used in batch experiments of the metal effects on sulfate reduction and profiles of monitored parameters. A: Vials containing cultures at day 12. A1: Culture with no metals, A2: Culture with 200 mg/L of Fe^{2+}, A3: Culture with 100 mg/L of Fe^{2+} and 100 mg/L of Zn^{2+}, A4: Culture with 100 mg/L of Zn^{2+} and A5: Culture with 200 mg/L of Zn^{2+}. B: pH profiles, C: sulfate reduction profiles and D: sulfide formation profiles.

Figure 4.7: Profiles showing evolutions of parameters yielded by two cultures with different carbon sources: glycerol and sodium lactate. A: sulfate reduction profiles, B: sulfide formation profiles, C: ORP profiles and D: DO profiles.

Figure 4.8: Profiles showing evolutions of parameters yielded by four cultures with different metal concentrations and pH control effects on bacterial growth. A: sulfate reduction profiles, B: sulfide generation profiles, C: ORP profiles, D: pH profiles, E: Zn^{2+} reduction profile, F: Fe^{2+} reduction

profile, G: DO profiles and H: Glycerol quantification profiles done by HPLC.

Figure 4.9: Amplificons of the 16S rRNA fragments from the extracted gDNA of bioreactor samples on a 1% (w/v) agarose gel stained with EtBr. Group 1: R1 samples, Group 2: R2 samples, Group 3: R3 samples and Group 4: R4 samples. Lane M: DNA standard Marker (O'GeneRuler^{TM} Ladder Mix), Lane 1: day 5, Lane 2: day 10, Lane 3: day 15, Lane 4: day 20 and Lane I: Inoculum used for the bioreactors.

Figure 4.10: DGGE profiles of consortia incubated in reactors with metals (R1: Inoculum, 200 mg/L Zn^{2+} and pH control and R2: Inoculum, 200 mg/L Fe^{2+} and pH control).
Group 1 (Fe^{2+}): Lane 1: R1 – day 5, Lane 2: R1 – day 10, Lane 3: R1 – day 15, Lane 4: R1 – day 20.
Group 2 (Zn^{2+}): Lane 5: R2 – day 5, Lane 6: R2 – day 10, Lane 7: R2 – day 15, Lane 8: R2 – day 20.

Figure 4.11: DGGE profiles of consortia incubated in reactors with (R3: Inoculum, no metals and no pH control and R4: Inoculum, no metals and pH control).
Group 1 (-pH): Lane 1: R3 – day 5, Lane 2: R3 – day 10, Lane 3: R3 – day 15, Lane 4: R3 – day 20.
Group 2 (+pH): Lane 5: R4 – day 5, Lane 6: R4 – day 10, Lane 7: R4 – day 15, Lane 8: R4 – day 20.

Figure 4.12: Centrifuged samples before lyophilisation. A: R1 (Inoculum, 200 mg/L Zn^{2+} and pH control), B: R2, (Inoculum, 200 mg/L Fe^{2+} and pH control), C: R3 (Inoculum, no metals and no pH control) and D: R4 (Inoculum, no metals and pH control).

Figure 4.13: SEM micrographs and EDS spectrum of sample harvested from a bioreactor with 200 mg/L of Zn^{2+} (R1). A and B: SEM micrographs showing bacterial cells, C: magnified red square in B and D: SEM-EDS analysis spectrum of the circled particle.

Figure 4.14: SEM micrographs and EDS spectrum of sample harvested from a bioreactor with 200 mg/L of Fe^{2+} (R2). A and B: SEM micrographs, C: magnified red square in B and D: SEM-EDS analysis spectrum of the circled particle in C.

Figure 4.15: SEM micrographs of samples harvested from bioreactors with no metals. A to C: SEM micrographs showing bacterial biofilm from the bioreactors (R3 and R4).

Figure 4.16: TEM micrographs and EDS spectrum of Zn^{2+} containing sample from a bioreactor with 200 mg/L of Zn^{2+} (R2). A and B: TEM micrographs, C: TEM-EDS analysis spectrum of the encircled area in red.

LIST OF TABLES

Table 1.1: Classification of representative sulfate-reducing bacteria (Taken from Castro *et al.,* 2000).

Table 3.1: PCR primer set and sequences for 16S rRNA amplification.

Table 3.2: PCR programme for 16S rRNA amplification.

Table 3.3: Sequencing PCR programme.

Table 3.4: Media compositions of ASRM and PSGM.

Table 3.5: Designated names of the enrichment samples.

Table 3.6: Sequences of *dsrAB* gene fragments primer set

Table 3.7: PCR programme for the amplification of *dsrAB* gene fragments.

Table 3.8: Physicochemical characteristics of mine drainages.

Table 3.9: The hydro-geochemical data of the three water samples.

Table 3.10: Microbial cell count estimations by DAPI staining technique.

Table 3.11: Concentrations and purity rations of the extracted gDNA from raw samples.

Table 3.12: Sequencing results obtained from BLAST analysis for AMD water samples and the sludge sample

Table 3.13: Concentrations of extracted gDNA from the tertiary cultures.

Table 3.14: Sequencing results obtained from BLAST algorithm for tertiary enrichment samples from DGGE analysis.

Table 4.1: Metal (Fe^{2+} and Zn^{2+}) concentrations in the batch cultures.

Table 4.2: Sulfate reduction efficacy of SRB consortium.

Table 4.3: Sequencing results obtained from the BLAST analysis for samples obtained from bioreactors with metals (R1 and R2).

Table 4.4: Sequencing results obtained from the BLAST analysis for samples obtained from bioreactors with and without pH control (R3 and R4).

Table 4.5: SEM-EDS results showing elemental composition of the precipitates in the Zn^{2+} sample (R1).

Table 4.6: SEM-EDS results showing elemental composition of the precipitates in the Fe^{2+} sample (R2).

Table 4.7: TEM-EDS results showing elemental composition of the precipitates in the Zn^{2+} containing sample analysed on spectrum.

CHAPTER 1

LITERATURE REVIEW

1. LITERATURE REVIEW

1.1. Introduction

Water is an essential element of life and all organisms are dependent on it to exist. It is the most abundant natural resource on earth, however, only 0.016% is liquid fresh water readily available for human consumption and domestic use (Derakhshani and Alipour, 2010; Meyer and Casey, 2004). Pollution of water is a global challenge and most human activities and industries contribute largely to the pollution (Mačingová and Luptáková, 2010). The most dominant water pollutant faced globally is Acid Mine Drainage (AMD) from the active and or abandoned mines which are continuously degrading the quality of groundwater, streams, rivers and complete river basins in mining practising countries (Nieto *et al.,* 2007).

AMD contaminated water is toxic due to the dissolved heavy metals making it domestically un-usable even for irrigation or feedstock consumption. Approximately one ton of water is used for one ton of rock to be crushed and processed to extract valuable minerals making water demands high for large scale mineral mines (White, 1985). The wastewater from the mines affects the groundwater systems and is released on to the surface which tends to flow into streams and rivers (McCarthy, 2011). If the AMD contaminated water persists on infiltrating the fresh streams without any treatment, water demands will continue rising leading to the economical imbalance as more money will be required in future to treat AMD contaminated water in the rivers.

1.2. Acid Mine Drainage

1.2.1. Background of Acid Mine Drainage

Acid mine drainage (AMD) or acid rock drainage (ARD) is a consequence of most industrial activities, principally mining. It is mostly characterized by a low pH, high concentrations of sulfate and heavy metals (Moosa *et al.,* 2005). AMD mostly occurs as runoff or seepage from waste mineral stockpiles or tailings from the mines. The source of AMD is the host rock which contains metal sulfides like pyrite (marcasite,

FeS_2), sphalerite (ZnS), galena (PbS), chalcocite (Cu_2S), millerite (NiS), cinnabar (HgS), arsenopyrite (FeAsS) and chalcopyrite ($CuFeS_2$) that are often mined for extraction of precious metals such as gold (Au), silver (Ag), lead (Pb), iron (Fe), zinc (Zn) and copper (Cu) to be used commercially (Baker and Banfield, 2003; Baker *et al.,* 2003; Kalin *et al.,* 2006). During mining or any other anthropogenic activity that involve the excavation of rocks, the host rocks exposes metal sulfides which react with air and water forming AMD (Kalin *et al.,* 200). The fragmented rocks, typically still containing metal sulfides are disposed around the mining area or completed construction sites which are referred to as tailings (Doepker and Drake, 1991). In AMD polluted streams, the water tends to have a pH less than 3.5 and dissolved metals which are harmful to most of the aquatic life (Henry *et al*., 1999). Not only active mines serve as major sources of AMD but abandoned surface and underground mines also produce AMD that can pollute hundreds kilometres of streams in a decade after mining has stopped (Hedin *et al.,* 2005; Hoffert, 1947). AMD can also form naturally through the weathering process where the host rock is exposed. During rainy seasons, AMD form at a slow pace with low toxicity that might continue for years without recognition as it gets diluted (Gray, 1997).

1.2.2. Acid Mine Drainage formation

AMD formation is a well-studied and understood process (McCarthy, 2011) that involves a series of chemical and biochemical reactions that takes place when pyrite (FeS_2, fool's gold or iron di-sulfide) and other metal sulfide minerals are exposed to water and oxygen (in the air), normally during mining (Nieto *et al.,* 2007). When metal sulfides are oxidised, metals leach into the drainage resulting in high dissolved metal concentrations which makes the drainage toxic. As the sulfur from the metal sulfide minerals gets oxidised, high sulfate concentrations are formed which react with released hydrogen to form sulphuric acid that makes the drainage acidic and further promoting dissolution of heavy metals (Akcil and Koldas, 2006; Moosa *et al*., 2005).

Oxidation of pyrite or any other metal sulfide by atmospheric oxygen and water takes place according to Equation 1.1, a so-called "initiator reaction" which releases

ferrous iron, sulfate and hydrogen ions in the drainage (Kalin *et al.,* 2006; Küsel, 2003; Nieto *et al.,* 2007). The reaction is slow due to the insolubility nature of pyrite and most metal sulfides associated with the host rock.

Equation 1.1: $2FeS_2 + 7O_2 + 2H_2O \rightarrow 2Fe^{2+} + 4SO_4^{2-} + 4H^+$

Further oxidation of ferrous iron to ferric iron takes place in the environment according to Equation 1.2 but the oxidation process is not always spontaneous as the conversion of iron species in AMD partially depends on the pH of the environment. However, the presence of various iron oxidizing bacteria in the AMD catalyse the oxidation process of ferric iron (Akcil and Koldas, 2006; Marini *et al.,* 2003). At pH conditions below 4 which are typical for most AMD, ferrous iron is relatively stable especially in the presence of oxygen (Kalin *et al.,* 2006). The presence of acidophilic bacteria such as *Acidithiobacillus ferrooxidans* and *Leptospirillum ferrooxidans,* catalyses and enhances the oxidation process of ferrous iron to ferric iron by 10^4 to 10^6 times compared to the reaction rate in their absence (Doepker and Drake, 1991; Taylor *et al*., 1984). In contrast, at pH values above 4, ferric iron is biologically oxidized by iron oxidizing bacteria such as *Gallionella ferruginea* which are present in AMD with low acidic conditions (Johnson and Hallberg, 2005).

Equation 1.2: $Fe^{2+} + O_2 + 4H^+ \rightarrow Fe^{3+} + 2H_2O$

In pH conditions above 4, exposure of ferric iron to fresh water results in the precipitation of ferric hydroxide ($Fe(OH)_3$) so-called “Yellow Boy” while releasing protons in the drainage according to Equation 1.3. Yellow Boy is visually detected by an ochre deposit at the bottom of the streams (Atkins and Pooley, 1982; Kakooei *et al.,* 2012; Kalin *et al.,* 2006).

Equation 1.3: $Fe^{3+} + 2H_2O \rightarrow Fe(OH)_3 + 3H^+$

In highly acidic environments (pH < 4), ferric iron is highly soluble and serves as an oxidizing agent with greater affinity for pyrite (Marini *et al.,* 2003). In these conditions, ferric iron reacts spontaneously with pyrite releasing more ferrous iron, sulfate and protons in the drainage according to Equation 1.4. The oxidation process of pyrite by ferric iron is known as the “ferric shunt” which results in more acid production in

AMD. The net chemically and biologically mediated AMD formation reaction outlined in Equation 1.5 summarises the series of equations that takes place resulting in a highly acidic drainage with high sulfate concentrations (Johnson and Hallberg, 2005; Marini *et al.,* 2003). The oxidation process of metal sulfide minerals by ferric ir

.on can be induced directly by *A. ferrooxidans* biofilm that form extracellular polymeric substances (EPS) which allow attachment of cells to the metal sulfide to allow ferric iron attack of the mineral sulfide to catalyse the oxidation process (Kakooei *et al.,* 2012; Küsel, 2003; Nieto *et al.,* 2007).

Equation 1.4: $$FeS_2 + 14Fe^{3+} + 8H_2O \rightarrow 15Fe^{2+} + 2SO_4^{2-} + 16H^+$$

Equation 1.5: $$4FeS_2 + 15O_2 + 14H_2O \rightarrow 4Fe(OH)_3 + 8H_2SO_4$$

The accelerated rate of pyrite oxidation by bacterial activity leads to the rapid decrease of pH in the drainage which in return induces dissolution of metals like Cd^{2+}, Co^{2+}, Cr^{3+}, Cu^{+}, Fe^{2+}, Mn^{2+}, Pb^{2+} and Zn^{2+} (Henry *et al*., 1999; Nieto *et al.,* 2007). The flow rate of water over the host rock, contact time of water on rock and temperature plays important roles in the rate and toxicity of AMD during its formation (Mačingová and Luptáková, 2010). In South Africa, the biggest AMD sources in the environment are the gold, iron and coal mining due to the methods used during their extraction while diamond, magnesium, chrome and vanadium mines produces less to non-significant volumes of AMD (McCarthy, 2011).

1.2.3. Properties of Acid Mine Drainage

Mine drainages differ in characteristics based on the composition of their water source and post formation contaminants (metals) associated with ore minerals that leach in the water during mining. Typical drainages from mostly gold mines can have very low pH values (below 4) hence called acid mine drainages (AMD). Mine drainages with higher pH (above 4 to 9) are called alkaline mine drainages (AMD) also referred to as non-acid mine drainage (NMD). The drainage contain neutralizing minerals which reverse the acidity of AMD that resulted from pyrite oxidation and this drainage is often observed in coal mine (Akcil and Koldas, 2006).

Stagnant or stored AMD in oxic dams with high iron concentrations have stabilized acidic conditions due to the cycling of iron species (Fe^{2+}/Fe^{3+}) mediated by acidophilic bacteria, which prevents methanogenic or sulfate reducing activities to occur as they require anoxic environment to take place (Kalin *et al.,* 2006; Küsel, 2003). However, biofilm of sulfate-reducing bacteria (SRB) and methanogens colonise at the base of the catchment within the sediments where minimal sulfate reduction takes place. Such environments has served as a source of most isolated SRB from AMD such as *Desulfovibrio* sp., *Desulfomonas* sp., *Desulfobacter* sp., *Desulfococcus* sp., *Desulfotomaculum* sp. and *Desulfobulbus* sp. (Rzeczycka and Blaszczyk, 2005; Wargin, 2007). The diversity found in AMD includes bacterial groups that are divisions of *Proteobacteria*, *Firmicutes* and Acidobacteria. Within the *Proteobcteria* group which is the widest studied group of microbial SRB, there are: α-proteobacteria (*Acidiphilum* sp.), β-proteobacteria (*Thiomonas* sp.), ϒ-proteobacteria (*Acidithiobacillu* sp. and *Thiobacillus* sp.) and δ-proteobacteria (*Desulfovibrio* sp.). From the Archaeal lineage, *Thermoplasmatales* and *Sulfolobales* were reported to form part of the microbial diversity in AMD and from the Eucarya lineage, Ciliates (*Cinetochilium* genus) and amoeba (*Vahlkampfi* sp.) are the most isolated eukaryotes from AMD (Baker and Banfield, 2003; Kalin *et al.,* 2006; Pini *et al.,* 2011; Quaiser *et al.,* 2003; Sharmin *et al.,* 2013).

NMD is common in most coal mining drainages and formed similar to AMD which result in high sulfate but low metals concentrations due to higher pH values (4 – 9 (Akcil and Koldas, 2006; Marini *et al.,* 2003). NMD also occur in flowing streams contaminated with AMD in which the pH of the water rises as the AMD gets diluted by fresh flowing water but the sulfate concentrations remain relatively high because of the continuous oxidation of tailing while ferric hydroxide precipitates to the bottom of the stream with other metals discolouring the water (Akcil and Koldas, 2006). The water mostly appears blue due to the precipitated metals which discolour the bottom of the streams (Marini *et al.,* 2003). In most coal associated rocks, neutralizing chemicals like sodium carbonate or bicarbonate (Na_2CO_3 or Na_2HCO_3) and calcium carbonate ($CaCO_3$) also known as calcite are present and serve as a buffering agents by raising the pH of AMD to over 6.5 which is a typical pH for NDM (Akcil and Koldas, 2006; Foti *et al.,* 2007). Due to the higher pH conditions, some metals like Cd^{2+}, Ni^{2+}, Fe^{2+}, Zn^{2+}, Cu^{2+} and Pb^{2+} precipitate to the bottom of the streams like

Fe(OH) (Rose *et al.,* 1998; Zagury *et al.,* 2006). However, high concentrations of Ca^{2+}, Mg^{2+}, Na^{+}, SO_4^{2-} and NO_3^{-} remain dissolved in the drainage because the high pH (> 6.5) conditions do not induce their precipitation. Lower diversity of SRB species and other extremophiles have been detected in NMD with dominant species being *Acidiphilium* sp. and *Gallionella* sp. (Atkins and Pooley, 1982; Johnson and Hallberg, 2005; Lin *et al.,* 2012).

1.3. Acid Mine Drainage treatment options

In order to treat mine drainage (AMD or NMD) from any mine, first the process of mobilization, transportation and sequestration of relevant chemical components must be understood and characterized to apply relevant treatment option for the drainage (Marini *et al.,* 2003).

1.3.1. Overall Acid Mine Drainage treatment options

Treating AMD from its source is considered the best way to prevent AMD from reaching the fresh flowing water but this is not always possible for most impacted areas (Johnson and Hallberg, 2005). There are two options of remediating AMD which are chemical and biological systems that employ abiotic and biotic strategies respectively (Sierra-Alvarez *et al*., 2006). Both strategies have been applied widely to raise the pH and to mitigate heavy metals from the drainages without any further environmental pollution especially by the disposal of the by-products of the treatment option. Further classification of the treatment options was developed and the chemical and biological systems were separately classified into both active and passive treatments according to Figure 1.1 (Johnson and Hallberg, 2005). Passive treatment requires less resources to operate and mostly utilizes natural resources which do not need constant monitoring once in operation whereas active treatment requires constant monitoring and continuous input of not necessarily natural resources once in operation to sustain the process (Johnson and Hallberg, 2005; van Eeden *et al.,* 2009).

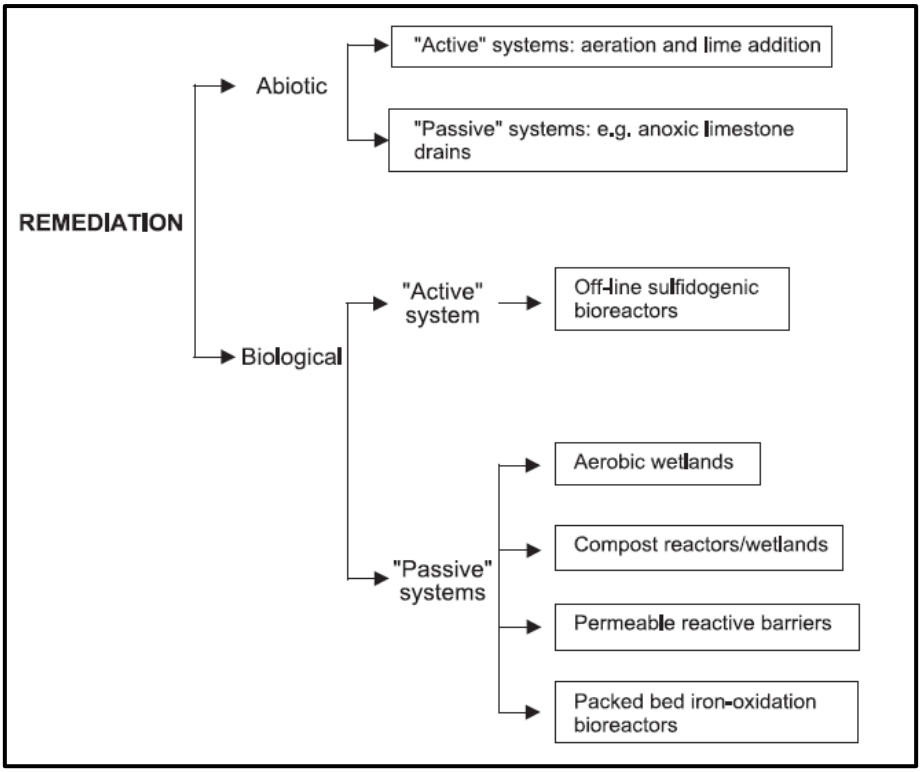

Figure 1.1: Biological (biotic) and chemical (abiotic) strategies for acid mine drainage remediation. (Taken from Johnson and Hallberg, 2005).

1.3.2. Chemical Acid Mine Drainage treatment

Chemical treatments involve addition of alkaline material like limestone (calcium oxide, CaO) directly into the AMD to raise the pH. However, the method results in the formation of slurry metals precipitate which are also toxic (Kalin *et al.,* 2006). Passive systems of abiotic treatment option have always been the first preference for most industries with the aim of cutting maintenance cost of the systems. In passive systems, limestone is added in anoxic environment to avoid ferric iron oxidative reactivity to be activated hence increasing the pH of the drainage. Although passive anoxic treatment is effective to certain extend, it is not suitable to treat all kinds of AMD and the volumes of AMD required to be treated daily (Rose *et al.,* 1998; Kalin *et al.,* 2006).

Active abiotic systems complement most of the remediation activities unachieved by the passive abiotic system. This employs aeration of the system with simultaneous addition of a chemical-neutralizing agent such as: lime, calcium carbonate ($CaCO_3$),

sodium carbonate ($NaCO_3$), sodium hydroxide (NaOH) and magnesium oxide (MgOH) (Neculita *et al.,* 2007). The neutralizing agent increases the pH of the AMD which will directly induce a rapid oxidation of ferrous iron that in return precipitate with dissolved metals forming a slurry by-product with high concentrations of metals which will require pre-treatment before disposal (Johnson and Hallberg, 2005; Zagury *et al.,* 2006).

1.3.3. Biological Acid Mine Drainage treatment

Biological systems employ biotic entities such as plants, algae, fungi and bacteria to treat AMD normally in bioreactors or wetlands and the process is called “Bioremediation” (Derakhshani and Alipour, 2010; Rose *et al.,* 1998). Passive biological treatments are carried out in both aerobic and anaerobic wetlands where AMD is channelled through a treatment system containing reactive barriers with biological entities like bacteria, algae and plants that assist in precipitating dissolved metals. Aerobic wetlands are normally used for the mildly acidic or net-alkaline water with elevated iron concentrations. The aeration of the wetland is necessary for dissolved iron to oxidize and precipitate with other metals hence remediating the drainage during the flow (Al-Zuhair *et al.,* 2008). The anoxic passive biological systems require construction of reactors which include the addition of lime stone beneath or mixed with organic substrate to be utilized by supplied inoculum of bacteria like SRB to remediate AMD. This option has been widely used to treat highly acidic AMD with elevated sulfate concentrations (Neculita *et al.,* 2007). The system aims at reducing sulfate by SRB while oxidizing the organic matter to carbonates that generate alkalinity in the drainage according to Equation 1.6 (Neculita *et al.,* 2007). Sulfate-reduction process occurs in anoxic environments with low to no oxygen mediated by SRB. The SRB utilize SO_4^{2-} as an electron acceptor converting it into hydrogen sulphide (H_2S) that react with metals (Me^{2+}) to form metal sulfide precipitates ($MeS_{\downarrow}$) according to Equation 1.7 (Luptakova *et al.,* 2012; Neculita *et al.,* 2007; Zagury *et al.,* 2006). During this process, sulfate concentrations are reduced and metals are mitigated from the drainage through precipitation (Zagury *et al.,* 2006). One of the advantages of using this method is that the

precipitated metals can be retrieved from the by-products and used for commercial purposes.

Equation 1.6: $SO_4^{2-} + 2CH_2O \rightarrow H_2S + 2HCO_3^-$

Equation 1.7: $H_2S + Me^{2+} \rightarrow MeS_{\downarrow} + 2H^+$

Active biological systems rely entirely on bioremediation to reduce sulfate concentrations and increase the pH of mostly acidic AMD. Microorganisms capable of metals immobilization like SRB are employed in anoxic sulfidogenic bioreactors to remediate AMD (Johnson and Hallberg, 2005). The anaerobic bioreactors constructed for this type of treatment act as reversal chambers of AMD formation process that takes place when alkalinity is generated in the environment with subsequent metals and sulfate reduction (Sierra-Alvarez *et al*., 2006). In the bioreactors with bacterial consortia aimed at remediating AMD, processes such as methanogenesis, fermentation, denitrification, iron reduction, manganese reduction, ammonification and sulfate reduction takes place depending on the chemical composition of the drainage (van Eeden *et al.,* 2009). Organic substrate is required in the bioreactor operations to serve as the carbon source and electron donor needed for bacterial activities that reverse the AMD acidity and toxicity by immobilizing metals. To acquire best remediation results from severe cases of AMD contamination, both passive and active biological treatments are applied respectively but require constant monitoring and maintenance (Sierra-Alvarez *et al*., 2006; Zagury *et al.,* 2006).

1.4. Role of Sulfate-reducing bacteria in Acid Mine Drainage

SRB are commonly employed in AMD treatments where they utilize the sulfate as their terminal electron acceptor reducing it to hydrogen sulfide according to Equation 1.6 while oxidizing the organic matter (Al-Zuhair *et al.,* 2008; Sierra-Alvarez *et al*., 2006). The produced H_2S during sulfate reduction reacts with dissolved metals according to Equation 1.7 precipitating them out of the solution.

1.4.1. Characteristics and diversity of sulfate-reducing bacteria

SRB are a diverse group of bacteria which are abundant in some extreme natural environments and have been isolated from various environments including soil, sediments and non-polluted water (Kakooei *et al.,* 2012; Wargin, 2007). They are considered to be some of the oldest and mostly studied bacterial groups (Wargin, 2007). Their interesting functions in the ecosystem makes them to be widely studied and classified under a number of groups based on their complex characteristics (Castro *et al.,* 2000; Kakooei *et al.,* 2012). They are detected by H_2S production in the environment which has an unpleasant smell and result in black precipitates of ferrous sulfide in the presence of iron minerals (Wargin, 2007). Majority of known cultivable SRB belong to a group of bacteria known as the delta proteobacteria (Baumgartner *et al*., 2006), which two families of SRB were proposed: the Desulfovibrionaceae and the Desulfobacteriacea. Most abundant SRB isolated from various environments belong to the genera *Desulfovibrio* and *Desulfomicrobium* which are mostly the key sulfate reducers in natural anaerobic sediments (Castro *et al.,* 2000). Castro and co-workers classified SRB into four groups: Gram-negative mesophilic SRB, Gram-positive spore-forming SRB, bacterial thermophilic SRB and archael thermophilic SRB shown on Table 1.1 (Castro *et al.,* 2000). The SRB classification and representative specie selection was mainly based on their rRNA sequence analysis which provides information about the evolution of the SRB and their distantly related species. The groups were further characterized according to their morphology, nature of motility, GC contend of their DNA%, presence of the Desulfovibrin pigment and cytochromes, complete or incomplete oxidation of acetate and their optimum growth temperatures (Castro *et al.,* 2000). The characterization of SRB based on growth temperature was limited between 25 and 70ºC (Castro *et al.,* 2000; Karr *et al*., 2005) but some were isolated in temperatures as high as 130ºC in hydrothermal vents (Christophersen *et al.,* 2011; Kallmeyer and Boetius, 2004).

Table 1.1: Classification of representative sulfate-reducing bacteria (Taken from Castro *et al.,* 2000).

	Shape	Motility	GC content of DNA (%)	Desulfo-vibrin	Cytochr-omes	Oxidation of acetate	Growth temp (^{0}C)
Gram-negative mesophilic SRB							
Desulfobulbus	lemon to rod	-/+	59-60	-	b, c, c^3	**I**[a]	25-40
Desulfomicrobium	ovoid to rod	+/-	52-67	-	b, c	**I**	25-40
Desulfomonas	rod	-	66	+	c	**I**	30-40
Desulfovibrio	spiral to vibrioid	+	49-66	+/-	c^3, b, c	**I**	25-40
Desulfobacter	oval to rod	+/-	44-46	-		**C**[b]	20-33
Desulfobacterium	oval to rod	+/-	41-52	-	b, c	**C**	20-35
Desulfococcus	spherical or lemon	-/+	46-57	+/-	b, c	**C**	28-35
Desulfomonile	rod	-	49	+	c^3	**C**	37
Desulfonema	filaments	Gliding	35-42	+/-	b, c	**C**	28-32
Desulfosarcina	oval rods to coccoid packages	+/-	51	-	b, c	**C**	33
Gram-positive spore-forming SRB							
Desulfotomaculum	straight to curved rods	+	48-52	-	b, c	**I/C**	most 25-40, some 40-65
Bacterial thermophilic SRB							
Thermodesulfobacterium	vibrioid to rod	-/+	30-38	-	c^3, c	**I**	65-70
Archaeal thermophilic SRB							
Archaeoglobus	coccoid	+/-	30-38	-	n.r.[c]	**I**	64-92

[a]I, incomplete.

[b]C, complete.

[c]n.r., not reported.

SRB are known to regulate the sulfur cycle in the natural environments and are involved in the organic matter turnover in anaerobic soils and sediments (Castro *et al.,* 2000; Sánchez-Adrea *et al.,* 2014). Sulfur is one of the most abundant elements on earth concentrated in the earth's crust associated with metals occurring as metal sulfides. Sulfur can occur in nine different oxidation states as shown in Figure 1.2 and every oxidation state of sulfur can be acted on by microorganism to change its state of oxidation (Sánchez-Adrea *et al.,* 2014). The final oxidation state of sulfur is sulfate (SO_4^{2-}) which is the highly reactive with most elements forming compounds like $CaSO_4$, $CuSO_4$ and most dangerously sulfuric acid (H_2SO_4) which is the most

role player in the acidity and toxicity of mine drainages since SO_4^{2-} concentrations are elevated (Al-Zuhair *et al.,* 2008; Sánchez-Adrea *et al.,* 2014).

Oxidation and reduction of sulfur and its compounds can be chemically or biologically mediated. Figure 1.2 shows three transformation processes (oxidation, reduction and disproportionation) undertaken by microorganisms in sulfur cycling of the environment. Dissimilatory sulfate reduction which is mediated by SRB in anaerobic conditions where sulfate is reduced to sulfide according to Equation 1.6 (Luptakova *et al.,* 2012; Sánchez-Adrea *et al.,* 2014). Dissimilatory sulfate reduction is mediated by some SRB where they convert the elemental sulfur into hydrogen sulfide. Assimilatory sulfate reduction which all SRB are capable of is one of the sulfate reduction strategies since the reduced sulfide is assimilated in the bacterial biomass, proteins and amino acids (Christophersen *et al.,* 2011). Sulfide oxidation of reduced sulfur species back to sulfate by sulfide-oxidizing bacteria (SOB) such as methanogenic, lithotrohic and phototrophic bacteria which uses mostly ferric iron and oxygen as their electron acceptors. To continue the cycle from sulfate to sulfide, sulfate reduction by SRB is required to transform sulfur species (Dahl *et al.,* 2005; Foti *et al.,* 2007). Lastly, disproportionation of sulfur species where coupled oxidation and reduction of sulfur compounds such as thiosulfide ($S_2O_3^{2-}$), sulfite (SO_3^{2-}) and elemental sulfur (S_8^0) which are mostly present as intermediate compounds during sulfate reduction to hydrogen sulfide (Sánchez-Adrea *et al.,* 2014).

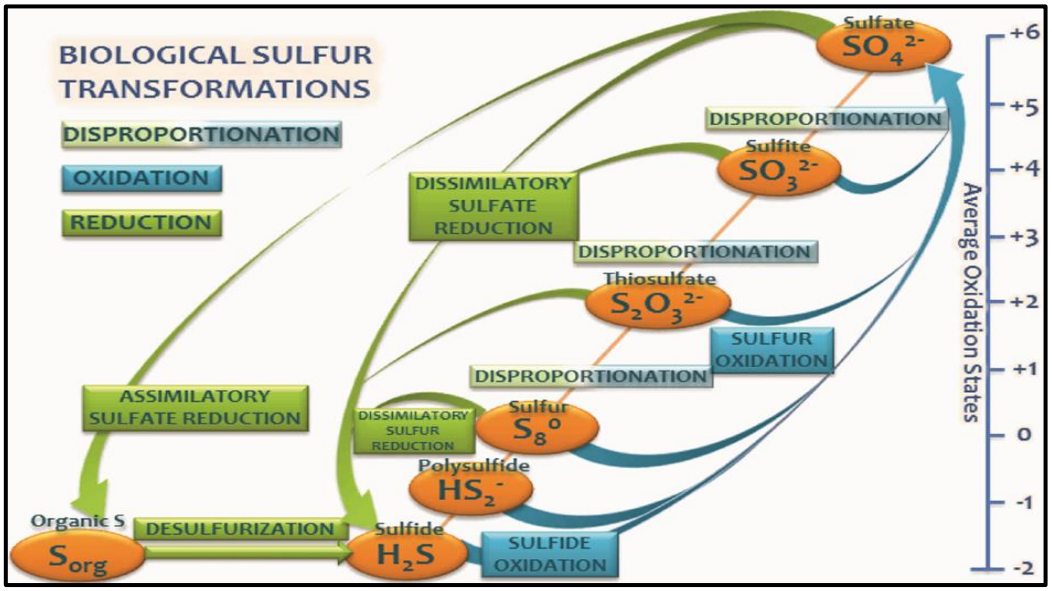

Figure 1.2: Biological sulfur transformations in natural and artificial environments. (Taken from Sánchez-Adrea *et al.,* 2014).

1.4.2. Factors affecting biological sulfate reduction in AMD

Function of SRB in AMD remediation is simply to convert sulfate into sulfide reducing the SO_4^{2-} concentrations in the drainage simultaneously utilizing protons hence neutralizing the drainage. The biogenic sulfide (S^{2-}) reacts with dissolved metals such as Fe^{2+}, Pb^{2+}, Cu^{+}, Cd^{2+}, Ni^{4+} and Zn^{2+} forming insoluble precipitates which is an indirect metals removal from the drainage by SRB (Sánchez-Adrea *et al.,* 2014). This reversal process of AMD formation is largely dependent on the environmental conditions which SRB operates in. The first priority for a successful AMD remediation by SRB is an anoxic to anaerobic condition which will allow maximum sulfate reduction to take place with less to no sulfide oxidation. Then the process should be optimized with a suitable carbon source and electron donor selection. Other non-compulsory requirements for successful sulfate reduction are optimum pH and temperature which differs according to various SRB groups (Castro *et al.,* 2000; Kakooei *et al.,* 2012). Concentrations of sulfate, sulfide and different metals can also negatively affect the sulfate-reduction capacity of SRB (Russel *et al.,* 2003).

1.4.2.1. Electron donor and carbon source selected for SRB growth

Due to low concentrations of organic matter especially carbon based minerals in the AMD, additional carbon source and electron donor are required when growing SRB. SRB obtain their energy through the oxidation of organic compounds according to Equation 1.6 (Rzeczycka and Blaszczyk, 2005). One factor that limits the microbial sulfate reduction and metals removal from AMD is the supply of energy and carbon source used by the SRB (Russel *et al.,* 2003). Various carbon sources had been used in the isolation and growth of SRB and sodium lactate was reported to be more preferred donor by SRB (Wargin, 2007). Variety of electron donors such as alcohols, aromatic compounds, fatty acids and hydrogen are usable by SRB to reduce sulfate but utilization of these various donor sources by microorganisms does not yield similar energy levels seen by growth rates and biomass production of the SRB (Karr *et al*., 2005). Utilization of organic acids (lactic, pyruvic, formic and acetic) and alcohols (ethanol and propanol) by SRB as electron donors have been studied widely and used as a classification scheme dividing SRB based on type of organic

substrate used and if the substrate is completely or incompletely oxidized and degraded (Castro *et al.,* 2000; Rzeczycka and Blaszczyk, 2005). The most important factors to consider when choosing the suitable carbon source and electron donor for a specific group of SRB are the ability of SRB to utilize the substrate, the suitability of the substrate for the treatment system. This is coupled to the amount of sulfate to be reduced through the use of the selected substrate (Kaksonen and Puhukka, 2007). Wide range of electron donor options for SRB reveals the less fastidious requirements of nutrients to grow SRB but definitely a suitable one is required to obtain desired sulfate reduction results using SRB (Rzeczycka and Blaszczyk, 2005; Zagury *et al.,* 2006).

1.4.2.2. The effect of temperature on SRB

SRB can be classified into three groups based on the temperature at which they optimally reduce sulfate. First being the mesophiles which grow at temperatures less than 40ºC such as *Desulfovibrio* sp. which is known to optimally grow at temperatures between 25 and 40ºC (Sawicka *et al.,* 2012). Secondly are the moderate thermophiles which are SRB growing optimally at temperatures between 40 and 60ºC such as *Desulfotomaculum* sp. (Castro *et al.,* 2000; Fichtel *et al.,* 2012). The last group are the thermophilic SRB which can grow at temperatures from 60 till 110ºC such as *Archaeoglobus* sp. which was reported to have been isolated from hydrothermal vent chimney and can grow at 88ºC (Belkin *et al.,* 1985). Although these groups have been studied, the detection and successful isolation of SRB from extreme conditions like frozen lakes in the Arctic where the temperature ranges between -1 to 8ºC has been reported and the isolated SRB are called psychrotolerant SRB. The highest sulfate reduction percentages obtained by the psychrotolerant/mesophilic SRB was reported to be between 20 to 50% at temperature ranges of 0 to 40ºC (Moosa *et al*., 2005; Sawicka *et al.,* 2012). SRB successfully used to reduce sulfate at 102ºC was isolated from a thermal vent with the highest recorded temperature of 130ºC. These bacteria showed typical characteristics of archaea growing in extremely hot conditions (Fichtel *et al.,* 2012; Kallmeyer and Boetius, 2004). Even though SRB have been isolated from various habitats with extreme temperatures, that does not mean they can optimally reduce

sulfate completely to sulfide in these environmental conditions similar to those of their isolation habitats hence application of SRB in bioremediation require optimization. Biological sulfate reduction is possible and efficient at temperatures above 30ºC but the SRB activity slows down at low temperatures below 10ºC (Kakooei *et al.,* 2012).

1.4.2.3. The effect of pH on sulfate reduction

Most of the known SRB have been isolated from AMD with pH values lower than 4 indicating their tolerance to acidic conditions and most likely high metals concentrations (Hard *et al.,* 1997). The presence of SRB in acidic environments does not mean their condition of origin is their optimum for sulfate reduction. Most of the studied SRB have been reported to grow optimally at pH between 6 and 8 which is the desired pH level when treating acidic drainages (Sánchez-Adrea *et al.,* 2014). SRB that are susceptible to low pH tends to result in minimal sulfate reduction and low biomass yields in these unfavourable conditions. Acidic environments affect SRB negatively compared to neutral and slightly alkaline environments because most of organic acids do not dissociate in low pH environments hence limiting carbon supply to the SRB for growth (Hard *et al.,* 1997; Kaksonen and Puhakka, 2007). Resistance of acidophilic SRB to low pH conditions is due to the fatty acids contained in their cell walls which are not vulnerable to the acidic medium and hence they thrive in these harsh conditions. This is in relation to the neutrophilic SRB with mostly acid permeable cell walls that allow acids to diffuse through the membrane resulting in the acidification of the cytoplasm which could be lethal to microbial cells. This could all lead to low sulfate reduction in the acidic environments. To avoid such toxicity, consortia containing both acidophilic and neutrophilic SRB can be used or the AMD being treated could be pre-treated with neutralizing agents to raise the pH prior to introduction to the SRB inoculum (Fortin *et al.,* 1996; Postgate, 1984). The other vital purpose of keeping pH above 5 is to keep the hydrogen sulfide (HS^-) in the solution form for the reaction with dissolved metals that enhances metals sulfide precipitation which is slowed down at low pH because of the sulfide being in a gas form (H_2S) hence unavailable to dissolved metals (Fortin *et al.,* 1996; Kaksonen and Puhukka, 2007).

1.4.2.4. Sulfate and sulfide concentrations affecting sulfate reduction

Presence and activity of SRB in the environment is detected by sulfide production which is noted by a pungent odour similar to that of rotten eggs. Biogenic hydrogen sulfide which forms according to Equation 1.7 can be present in three different forms (H_2S, HS^- and S^{2-}) in either liquid or gaseous phase (Kaksonen and Puhukka, 2007). The concentration of each form depends on the reversible chemical equilibria represented by Equation 1.8 and 1.9 at temperatures between 25ºC and 30ºC (Kaksonen and Puhukka, 2007).

Equation 1.8: $H_2S \leftrightarrow HS^- + H^+$

Equation 1.9: $HS^- \leftrightarrow S^{2-} + H^+$

The form at which sulfide occur depends on the pH of its environment. At pH values below 6, hydrogen sulfide is mostly in an undissociated gaseous form which is toxic to most SRB at high concentrations. The undissociated H_2S affect the metabolic coenzymes and denature proteins by precipitating metal ions in the active sites within the bacterial cells. In terms of metals precipitation by the biogenic sulfide, the gaseous form easily diffuses out of the solution without much interaction with dissolved metals in cases where opened systems like wetlands are employed. In closed anaerobic systems, the gaseous hydrogen sulfide creates pressure which leads to partial dissociation and dissolves in the medium which will later negatively affect the bacterial cells (Kaksonen and Puhukka, 2007; Postgate, 1984).

At pH values between 6 and 8, the H_2S dissociates according to Equation 1.8 to yield hydrogen sulfide (HS^-) which is mostly in a liquid form available to dissolved metals. The dark grey shaded portion of the graph in Figure 1.3 highlights the pH range where the dissociation of H_2S to HS^- takes place and shows dominance beyond that point. The higher pH induces metals precipitation as they react with sulfides present in the medium. The sulfide in a form HS^- is not directly toxic to SRB but indirectly affect their metabolisms by precipitating metals like iron which are needed by some groups of SRB. The biologically induced metal sulfide precipitates

are a positive sign of successful sulfate reduction and metals removal from the medium which are part of the remediation strategies by SRB.

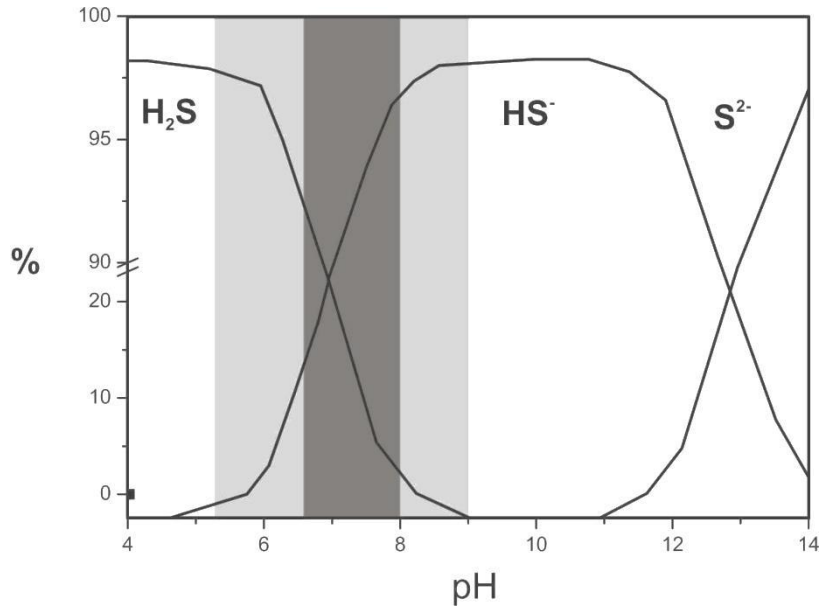

Figure 1.3: Sulfide speciation as a function of pH at 25ºC. (Taken from Kaksonen and Puhukka, 2007).

1.4.2.5. Effect of high metals concentrations on sulfate-reduction

Metals such as iron, zinc, copper and lead are toxic to SRB at high concentrations. Metal sulfide precipitates that form during sulfate reduction are not directly toxic to SRB but can block access of substrates and nutrients to SRB as they accumulate around cells in the biofilm. Some of the metals contained in AMD can pass through the cell wall and membranes of the cells and precipitate with the intra-generated H_2S resulting in precipitates within the cell which become toxic as they accumulate within the cells (Utgikar *et al.,* 2002).

Metals can affect SRB by exerting their toxicity on the biological systems of the cells by altering multiple biochemical pathways simultaneously. According to Harrison and co-workers (2007), metals can affect SRB biochemically by substitutive metal-ligand binding where one metal ion replaces another at the binding site of a specific biomolecule which destroys the biological function of the target molecule. The second metal effect mechanisms is the covalent or ionic redox (reduction-oxidation) reactions of metal ions with cellular thiols (R-SH) such oxyanions which liberate

reactive oxygen species like superoxide ($O_2^{\cdot -}$) as by-products which are toxic to growing bacteria. Some metals affect the membrane transport process where the toxic metals occupy the binding sites inhibiting biochemical reactions in the cell to proceed normally (Harrison *et al.,* 2007). Most of the bacteria isolated from streams and sediments with toxic metals have thrived through the conditions by making biofilms which protect most of the inter biofilm bacterial cell which tends to develop resistance against the toxic metals (Harrison *et al.,* 2007; Teitzel and Parsek, 2003).

1.5. Conclusions

Acid mine drainage is generated by oxidation of metal sulfide minerals like pyrite, galena, sphalerite and chalcopyrite contained in the earth's crust referred to as minerals host rock. Oxidation of these minerals takes place during anthropogenic activities, principally mining. The oxidation process of these minerals results in low pH conditions with high concentrations of dissolved sulfate and metals. Microorganisms such as *Acidithiobacillus ferrooxidans* catalyses the AMD generation rates up to 10^4 to 10^6 times. Depending of the chemical contents of the drainage, high pH conditions of some drainages are possible with low metals concentrations but high sulfate concentrations and this drainage is called non-acid mine drainage (NMD) or alkaline mine drainage.

Biological and chemical treatment options are available to aid in AMD remediation but most of the systems are expensive to implement and maintain. AMD treatment, especially aided by biological sulfate reduction can be enhanced if SRB are characterized. A cost effective, efficient and reliable system is required for both active and abandoned mines generating million litres of AMD contaminated water. Due to the high cost demands of neutralizing chemicals like calcium carbonate, sodium carbonate and bicarbonate to treat AMD, various passive biological systems have also been developed to treat AMD with lower costs. The reversal process of AMD formation can be mediated by application of microorganisms such as sulfate reducing bacteria (SRB).

SRB are anaerobic bacteria that utilizes sulfate as their terminal electron acceptor to oxidize the organic matter while releasing hydrogen sulfide. The biogenic hydrogen sulfide will react with dissolved metals and precipitate them which will lead into the elevation of pH as sulfate concentrations gets reduced. The use of SRB in AMD or NMD interaction requires background knowledge of the SRB and factors that affect sulfate reduction like carbon source, temperature, pH changes and metals concentration require constant monitoring to obtain best remediation results. The SRB mediated metal precipitation as part of mitigating AMD or NMD also require attention to evaluate the limitations metal concentrations exert on the bacteria. The identity and characterization of phase minerals present in biogenic precipitates still require further exploration which is the partial focus in this study.

1.6. References

- **Akcil, A. and Koldas, S.** (2006) Acid mine drainage (AMD): causes, treatment and case studies. *Journal of Cleaner Production* **14:** 1139 – 1145.
- **Al-Zuhair, S., El-Naas, M. and Al-Hassani, H.** (2008) Sulfate inhibition effect on sulfate reducing bacteria. *Journal of Biochemical Technology* **1(2):** 39 – 44.
- **Atkins, A. S. and Pooley, F. D.** (1982) The effect of Bio-mechanism on acidic mine drainage in coal mining. *International Journal of Mine Water* **1:** 31 – 44.
- **Baker, B. J. and Banfield, J. F.** (2003) Microbial communities in acid mine drainage. *Federation of European Microbiological Societies* **44:** 139 – 152.
- **Baker, B.J., Moser, D.P., MacGregor, B.J., Fishbain, S., Wagner, M., Fry, N.K., Jackson, B., Speolstra, N., Loos, S., takai, K., Lollar, B.S., Fredrickson, J., Balkwill, D., Onstoff, T.C., Wimpee, C.F. and Stahl, D.A.** (2003) Related assemblages of sulphate-reducing bacteria associated with ultra-deep gold mines of South Africa and deep basalt aquifers of Washington State. *Environmental Microbiology*. **5:** 267-277.
- **Baumgartner, L. K., Reid, R. P., Dupraz, C., Decgo, A. W., Buckley, D. H., Spear, J. R., Przekop, K. M. and Visscher, P. T.** (2006) Sulfate reducing bacteria in microbial mats: Changing paradigms, new discoveries. *Sedimentary geology* **185:** 131 – 145.
- **Belkin, S., Wirsen, C. O. and Jannasch, H. W.** (1985) Biological and abiological sulfur reduction at high temperatures. *Applied and Environmental Microbiology* **49(5):** 1057 – 1061.
- **Castro, H. F., Williams, N. H. and Ogram, A.** (2000) Phylogeny of sulfate-reducing bacteria. *Federation of European Microbiological Societies* **31:** 1 – 9.
- **Christophersen, C. T., Morrison, M. and Conlon, M. A.** (2011) Overestimation of the abundance sulfate-reducing bacteria in human feces by Quantitative PCR targeting the *Desulfovibrio* 16S rRNA gene. *Applied and Environmental Microbiology* **77(10):** 3544 – 3546.
- **Dahl, C., Engels, S., Pott-Sperling, A. S., Schulte, A., Sander, J., Lübbe, Y., Deustre, O. and Brune, D.** (2005) Novel genes of the *dsr* gene cluster and evidence for close interaction of Dsr protein during sulfur oxidation in the

phototropic sulfur bacterium *Allochromatium vinosum. Journal of Bacteriology* **187(4):** 1392 – 1404.

- **Derakhshani, R. and Alipour, M.** (2010) Remediation of acid mine drainage by using tailings decant water as a neutralization agent in Sarcheshmeh copper mine. *Research Journal of Environmental Sciences* **4:** 250 – 260.
- **Doepker, R. D. and Drake, P. L.** (1991) Laboratory stud of submerged metal-mine tailings 1: Effect of solid-liquid contact time and aeration on contaminant concentrations. *Mine Water and The Environment* **10:** 29 – 42.
- **Fichtel, K., Mathes, F., Könneke, M., Cypionka, H. and Engelen, B.** (2012) Isolation of sulfate-reducing bacteria from sediments above the deep-subseafloor acquifer. *Frontiers in microbiology* **3(5):** 1 – 12.
- **Fortin, D., Davis, B. and Beveridge, T. J.** (1996) Role of *Thiobacillus* and sulfate-reducing bacteria in iron biocycling in oxic and acidic mine tailings. *Federation of European Microbiological Societies* **21:** 11 – 24.
- **Foti, M., Sorokin, D. Y., Lomans, B., Mussman, M., Zacharova, E. E., Pimenov, N. V., Kuenen, J. G. and Muyzer, G.** (2007) Diversity, activity, and abundance of sulfate-reducing bacteria in saline and hypersaline soda lakes. *Applied and Environmental Microbiology* **73(7):** 2093 – 2100.
- **Gray, N. F.** (1997) Environmental impact and remediation of acid mine drainage: a management problem. *Environmental Geology* **30:** 62 – 71.
- **Hard, B. C., Friedrich, S. and Babel, W.** (1997) Bioremediation of acid mine drainage water using facultatively methylotrophic metal-tolerant sulphate-reducing bacteria. *Microbiology Research* **152:** 65 – 73.
- **Harrison, J. J., Ceri, H. and Turner, R. J.** (2007) Multimetal resistance and tolerance in microbial biofilms. *Nature* **5:** 929 – 938.
- **Hedin, R. S., Stafford, S. L. and Wells, A. G.** (2005) Acid mine drainage from abandoned gas wells. *Mine Water and Environment* **24:** 104 – 106.
- **Henry, T. B., Irwin, E. R., Grizzle, J. M., Wildhaber, M. L. and Brumbaugh, W. G.** (1999) Acute toxicity of an acid mine drainage mixing zone to Juvenile Bluegill and Largemouth Bass. *Transactions of the American Fisheries Society* **128:** 919 – 928.
- **Johnson, D. B. and Hallberg, K. B.** (2005) Acid mine drainage remediation options: a review. *Science of the Total Environment* **338:** 3 – 14.

- **Kakooei, S., Ismail, M. C. and Ariwahjoedi, B.** (2012) Mechanisms of microbiologically influenced corrosion: A review. *World Applied Science Journal* **17(4):** 524 – 531.
- **Kaksonen, A. H. and Puhakka, J. A.** (2007) Sulfate reduction based bioprocesses for the treatment of acid mine drainage and the recovery of metals. *Engineering in Life Sciences* **7(6):** 541 – 564.
- **Kalin, M., Fyson, A. and Wheeler, W. N.** (2006) The chemistry of conventional and alternative treatment systems for the neutralization of acid mine drainage. *Science of the Total Environment* **366:** 395 – 408.
- **Kallmeyer, J. and Boetius, A.** (2004) Effects of temperature and pressure on sulfate reduction and anaerobic oxidation of methane in hydrothermal sediments of Guaymas Basin. *Applied and Environmental Microbiology* **70(2):** 1231 – 1233.
- **Karr, E. A., Sattley, W. M., Rice, M. R., Jung, D. O., Madigan, M. T. and Achenbach, L. A.** (2005) Diversity and distribution of sulfate-reducing bacteria in permanently frozen lake Fryxell, McMurdo Dry Valleys, Antarctica. *Applied and Environmental Microbiology* **71(10):** 6353 – 6359.
- **Küsel, K.** (2003) Microbial cycling of iron and sulfur in acidic coal mining lake sediments. *Water, Air, and Soil Pollution* **3:** 67 – 90.
- **Luptakova, A., Ubaldini, S., Fornari, P. and Macingova, E.** (2012) Physical-chemical and biological-chemical methods for treatment of acid mine drainage. *Chemical Engineering Transactions* **28:** 115 – 120.
- **Mačingová, E. and Luptáková, A.** (2010) Removal of sulphates from mining waste waters using the sulphate-reducing bacteria. *MineraliaSlovaca.***42:** 333-336.
- **Marini, L., Saldi, G., Cipolli, F., Ottenello, G. and Zuccolini, M. V.** (2003) Geochemistry of water discharges from the Libiola mine, Italy. *Geochemical Journal* **37:** 199 – 216.
- **McCathy, S.** (2011) The impact of acid mine drainage in South Africa. *South African Journal of Science* 107(5/6), Art. #712, 7 pages. Doi:10.4102/sajs.v107i5/6.712.
- **Meyer, J. A. and Casey, N. H.** (2004) Exposure of potentially toxic trace elements in indigenous goats in the natural communal production system of

the northern region of South Africa. *South African Journal of Animal Science* **34:** 219 -222.

- **Moosa, S., Nemati, M. and Harrison, S. T. L.** (2005) A kinetic study on anaerobic reduction of sulphate, part II: incorporation of temperature effects in the kinetic model. *Chemical Engineering Science* **60:** 3517 – 3524.
- **Murr, L. E.** (1980) Theory and practice of copper sulphide leaching in dumps and in-situ. *Minerals Science Engineering* **12(3):** 121 – 189.
- **N Nercessian, O., Bienvenu, N., Moreira, D., Prieur, D. and Jeanthon, C.** (2005) Diversity of functional genes of methanogens, methanotrophs and sulfate reducers in deep-sea hydrothermal environments. *Environmental Microbiology* **7(1):** 118 – 132.
- **Neculita, C. M., Zagury, G. J. and Kulnieks, V.** (2007) Short-term and long-term bioreactors for acid mine drainage treatment. *Proceedings of the Annual International Conference on Soils, Sediments, Water and Energy* **12:** Article 2.
- **Nieto, J. M., Sarmiento, A. M., Olias, M., Canovas, C. R., Riba, I., Kalman, J. and Delvalls, T. A.** (2007) Acid mine drainage pollution in the Tinto and Odiel rivers (Iberian Pyrite Belt, SW Spain) and bioavailability of the transported metals to the Huelva Estuary. *Environment International* **33:** 445 – 455.
- **Pini, F., Galardinin, M., Bazzicalupo, M. and Mengoni, A.** (2011) Plant-bacteria association and symbiosis: Are there common genomic traits in *Alphaproteobacteria? Genes* **2:** 1017 – 1032.
- **Postgate, J. R.** (1984) The sulphate reducing bacteria. *2nd Edition. University press, Cambridge*, UK.
- **Quaiser, A., Ochsenreiter, T., Lanz, C., Schuster, S. C. Treusch, A. H., Eck, J. and Schleper, C.** (2003) Acidobacteria form a coherent but highly diverse group within the bacterial domain: evidence from environmental genomics. *Molecular Microbiology* **50(2):** 563 – 575.
- **Rose, P. D., Boshoff, G. A., van Hille, R. P., Wallace, L. C. M., Dunn, K. M. and Duncan, J. R.** (1998) An integrated algal sulphate reducing high rate ponding process for the treatment of acid mine drainage wastewaters. *Biodegradation* **9:** 247 – 257.

- **Russell, R. A., Holden, P. J. Wilde, K. L. and Neilan, B. A.** (2003) Demonstration of the use of *Scenedesmus* and *Carteria* biomass to drive bacterial sulfate reduction by *Desulfovibrio alcoholovorans* isolated from an artificial wetland. *Hydrometallurgy* **71:** 227 – 234.
- **Rzeczycka, M. and Blaszcyzyk, M.** (2005) Growth and activity of sulphate-reducing bacteria in media containing phosphogypsum and different sources of carbon. *Polish Journal of Environmental Studies* **14(6):** 891 – 895.
- **Sánchez-Andrea, I., Sanz, J. L., Bijmans, M. F. M. and Stams, A. J. M.** (2014) Sulfate reduction at low pH to remediate acid mine drainage. *Journal of Hazardous Materials* **269:** 98 – 109.
- **Sawicka, J. E., Jørgensen, B. B. and Brüchert, V.** (2012) Temperature characteristics of bacterial sulfate reduction in continental shelf and slope sediments. *Biogeosciences* **9:** 3425 – 3435.
- **Sharmin, F., Akelin, S., Huygens, F. and Hargreaves, M.** (2013) Firmicutes dominate the bacterial taxa within sugar-cane processing plants. *Scientific Reports* **3(3107):** 1 – 7.
- **Sierra-Alvarez, R., Karri, S., Freeman, S. and Field, J. A.** (2006) Biological treatment of heavy metals in acid mine drainage using sulfate reducing bacteria bioreactors. *Water Science and Technology* **54(2):** 179 – 185.
- **Taylor, B. E., Wheeler, M. C. and Nordstrom, D. K.** (1984). Stable isotope geochemistry of acid mine drainage: Experimental oxidation of pyrite. Geochemica et Cosmochimica Acta **48:** 2669 – 2678.
- **Teitzel, G. M. and Parsek, M. R.** (2003) Heavy metal resistance of biofilm and planktonic *Pseudomonas aeruginosa. Applied and Environmental Microbiology* **69:** 2313 – 2320.
- **Utgikar, V. P., Tabak, H. H., Haines, J. R. and Govind, R.** (2003) Quantification of toxic and inhibitory impact of copper and zinc on mixed cultures of sulfate-reducing bacteria. *Biotechnology and Bioengineering* **82(3):** 306 – 312.
- **van Eeden, E. S., Liefferink, M. and Durand, J. F.** (2009) Legal issues concerning mine closure and social responsibility in the West Rand. *TD: The journal for Transdisciplinary Research in Southern Africa* **5(1):** 51 – 71.

- **Wargin, A., Olańczuk-Neyman, K. and Skucha. M.** (2007) Sulphate-reducing bacteria, their properties and methods of elimination from groundwater. *Polish Journal of Environmental Studies* **16(4):** 693 – 644.
- **White, R. T.** (1985) Water-treatment practice in South African gold mines. *Journal of the South African Institute of mining and metallurgy.* **85:** 81 – 87.
- **Zagury, G. J., Kulnieks, V. I. and Neculita, C. M.** (2006) Characterization and reactivity of organic substrates for sulphate-reducing bacteria in acid mine drainage treatment. *Chemosphere* **64:** 944 – 954.

CHAPTER 2

INTRODUCTION TO THE PRESENT STUDY

2. INTRODUCTION TO THE PRESENT STUDY

2.1. Introduction

Akcil and Koldas (2006) stated that “South Africa is blessed with the occurrence of many minerals, often in large quantities and of strategic importance to it and to other nations. The country has one of the most sophisticated and developed mining industries in the world. The overall goal of managing environmental impacts in South Africa is to design and implement mitigating measures that minimize the residual impact of mining”. Acid mine drainage (AMD) is a global challenge polluting hundreds of kilometres of streams in most mining practicing countries (Baker and Banfield, 2003). The toxic water with high metals and sulfate concentrations affect both aquatic and terrestrial life (Al-Zuhair *et al.,* 2008; van Eeden *et al.,* 2009). Due to a large number of new, currently operating and abandoned mines in South Africa, many litres of fresh water gets contaminated daily by AMD which is mostly discarded without pre disposal treatment at the mining site hence affecting the water quality by lowering the pH and introducing various metals into the water. Both chemical and biological treatment options have been developed and applied to minimize AMD spread and effects in the environment but various challenges have been encountered in both treatment options (Kalin *et al.,* 2006; Sánchez-Adrea *et al.,* 2014).

Bacterial communities mainly sulfate-reducing bacteria (SRB) used in biological treatments (bioremediation), have been isolated and enriched from various mine drainages and other natural environments such as salt lakes, frozen lakes, hydrothermal vents and deep sub-surfaces where oxygen is minimal (Kakooei *et al.,* 2012). The SRB utilize (reduce) sulfate as their terminal electron acceptor while oxidizing the organic matter releasing H_2S which react with metals forming metal-sulfide precipitates (Al-Zuhair *et al.,* 2008; Castro *et al.,* 2000; Kakooei *et al.,* 2012; Sánchez-Andrea *et al.,* 2014; Zagury *et al.,* 2006).

There are both AMD and non-acid mine drainage (NMD) producing mines in South Africa which potentially contain different microbial communities including different SRB which can be used in studies that will contribute to the knowledge that might

lead to effective biological remediation processes. Due to the annual seasonal changes which result in water temperatures of less than 10ºC in winter and more than 30ºC in summer, such fluctuations affect the bacterial communities in water and mostly the sulfate reduction process by SRB. In acidic drainages with pH lower than 3.5, SRB activity is negatively impacted and also the dissolved metals have sulfate-reduction inhibition effects that makes treatments using these agents less effective for acidic mine drainages. High sulfate and sulfide concentrations associated with AMD or sulfate reduction process negatively affect some co-cultured bacteria such as fermentative and iron reducing bacteria that play important roles in biogeochemical reactions during biological sulfate reduction processes (Al-Zuhair *et al.,* 2008; Akcil and Koldas, 2006; van Eeden *et al.,* 2009).

In this study, SRB were enriched from three different mine drainages. The cultures were used to evaluate SRB tolerance to conditions known to affect biological sulfate reduction. The purpose of bacterial evaluation in AMD was to acquire knowledge that will extend the abilities to finally use bacteria in remediation processes by controlling their environmental conditions and adverse effects. Understanding biological sulfate reduction and aspects affecting the process is vital for optimization requirements for effective AMD bioremediation. Knowing the adaptability limits of SRB to high metals concentrations, varied pH and temperature could assist in the optimization strategies.

2.1.1. Study aims and objectives

The aim of this study was to respectively evaluate and study the biogeochemical processes and the sulfate reduction behaviour of SRB containing consortia enriched from three different mine drainage contaminated sites in South Africa.

The main objectives of this study were to first characterize the selected drainages into either AMD or NMD based on their geochemical characteristics. The second objective was to identify, characterize and enrich SRB contained in AMD and NMD. The third objective was to evaluate the sulfate reduction potential and behaviour of the enriched SRB when exposed to high metals and sulfate concentrations, low pH and temperatures in different batch experiments. This was coupled to kinetics

studies at respective varied pH and temperature conditions known to affect sulfate reduction according to literature. The last objective was to apply the optimum conditions according to the batch experiments in a bioreactor study to explore the metals-microbe interactions in a more controlled environment. All these aims and objectives could extend the knowledge of SRB processes during their interaction with AMD and or NMD.

2.2. References

- **Akcil, A. and Koldas, S.** (2006) Acid mine drainage (AMD): causes, treatment and case studies. *Journal of Cleaner Production* **14:** 1139 – 1145.
- **Al-Zuhair, S., El-Naas, M. and Al-Hassani, H.** (2008) Sulfate inhibion effect on sulfate reducing bacteria. *Journal of Biochemical Technology* **1(2):** 39 – 44.
- **Baker, B. J. and Banfield, J. F.** (2003) Microbial communities in acid mine drainage. *Federation of European Microbiological Societies* **44:** 139 – 152.
- **Kakooei, S., Ismail, M. C. and Ariwahjoedi, B.** (2012) Mechanisms of microbiologically influenced corrosion: A review. *World Applied Science Journal* **17(4):** 524 – 531.
- **Kalin, M., Fyson, A. and Wheeler, W. N.** (2006) The chemistry of conventional and alternative treatment systems for the neutralization of acid mine drainage. *Science of the Total Environment* **366:** 395 – 408.
- **Sánchez-Andrea, I., Sanz, J. L., Bijmans, M. F. M. and Stams, A. J. M.** (2014) Sulfate reduction at low pH to remediate acid mine drainage. *Journal of Hazardous Materials* **269:** 98 – 109.
- **van Eeden, E. S., Liefferink, M. and Durand, J. F.** (2009) Legal issues concerning mine closure and social responsibility in the West Rand. *TD: The journal for Transdisciplinary Research in Southern Africa* **5(1):** 51 – 71.
- **Zagury, G. J., Kulnieks, V. I. and Neculita, C. M.** (2006) Characterization and reactivity of organic substrates for sulphate-reducing bacteria in acid mine drainage treatment. *Chemosphere* **64:** 944 – 954.

CHAPTER 3

THE STUDY AND EVALUATION OF MICROBIAL COMMUNITIES FROM ACID MINE DRAINAGES AND NON ACID MINE DRAINAGE FOR THEIR SULFATE REDUCTION POTENTIAL

3. THE STUDY AND EVALUATION OF MICROBIAL COMMUNITIES FROM ACID MINE DRAINAGES AND NON ACID MINE DRAINAGES FOR THE SULFATE REDUCTION POTENTIAL

3.1. Abstract

Three mine drainages were collected from study sites: Site-Ex, Site-Ka and Site-Po which showed different hydro-geochemical characteristics and microbial diversities. The drainages from Site-Po and Site-Ka with characteristics typically of acid mine drainage had low cell counts (4.0×10^2 cells/mL and 5.7×10^2 cells/mL, respectively) indicating poor support of microbial existence. The sludge sample from Site-Po and Site-Ex drainage had higher cell counts (2.4×10^5 cells/mL and 5.0×10^3 cell/mL, respectively) indicating more favourable conditions for bacterial growth as the soil particles served as matrix for bacterial attachment enabling biofilm formation. The bacterial cells in each drainage sample were found to be viable and therefore, culturable. Molecular analysis revealed unique microbial diversities with dominant sulfate-reducing bacteria (SRB) species of *Desulfovibrio* sp., *Desulfosporosinus* sp. and *Desulforudis* sp.. The bacteria in the drainages and sludge were successfully enriched in two media: Anaerobic sulfate reducing medium (ASRM) and Postgate medium (PSGM) in which morphological, metabolic and molecular characterization confirmed the presence of SRB in the cultures. Biogenic precipitates were evaluated by the Scanning Electron Microscopy (SEM) and were visually identified as pyrite and sphalerite precursors. Finally, the confirmation of successful SRB enrichments was done by the amplification of the dissimilatory sulfite reductase (*dsrAB*) gene fragments using gene specific primers.

Keywords: Acid mine drainage; Non-acid mine drainage; Bacterial enrichment; Denaturation gradient gel electrophoresis; Scanning electron microscopy.

3.2. Introduction

Acid mine drainage (AMD) serve as source of some extremophiles, especially bacteria of which some of them are used in biotechnological applications like bioleaching of valuable minerals such as gold and copper (Atkins and Pooley, 1982). The study of the microbial communities in AMD is vital as the generation of AMD toxicity can be attributed to the microbial activities that enhance acid production in most metal leaching environments like oxidizing ferrous iron while replenishing ferric iron (Bond *et al.,* 2000). Majority of studies focusing on microbial communities in AMD are based on cultivation approaches (Baker *et al.,* 2003a) which can result in the alterations of the total microbial diversity in the wastewater, so this report employs both cultivation and molecular approaches to study the microbial communities in three AMD contaminated study sites.

Chemical composition of the drainages dictates the type of microorganisms found in it as not all bacteria can withstand high concentrations of metals. Highly acid or alkaline wastewaters contain different microbial communities and the pH of the water results from chemical reactions and bacterial activities in the water. Figure 3.1 depicts two mine drainages, one with low pH < 3.5 termed acid mine drainage (AMD) and the other with high pH > 5.5 to 7.5 termed non-acid mine drainage (NMD).

AMD, chemically described on the left side of Figure 3.1, results from mainly gold mining and it is formed when metal sulfide minerals like pyrite (FeS_2) gets exposed to oxygen and water during mining resulting in ferrous iron, sulfate and hydrogen ions (H^+) that induces acidity in the water (Hazen *et al.,* 2002; Küsel, 2003). The generated acidity enhances the dissolution of heavy metals such as aluminium (Al^{3+}), ferrous iron (Fe^2), zinc (Zn^{2+}), manganese (Mn^{2+}) and copper (Cu^{2+}) as well as high sulfate concentrations while keeping the pH low. The ferrous iron, further gets oxidised to ferric iron by oxygen and in the presence of bacteria like *Acidithiobacillus ferroxidans,* the oxidation process gets catalysed 10^4 to 10^6 times faster than in their absence (Küsel, 2003; Murr, 1980; Taylor *et al*., 1984). Continuous introduction of water onto the ferric iron results in the precipitation of iron hydroxide ($Fe(OH)_3$) identified by a red 'ochre' deposit which is known as "Yellow Boy" because of its colour at the bottom of mostly AMD contaminated streams (Atkins and Pooley,

1982). Microbial groups normally dominant in AMD and previously isolated are shown under the chemical description of AMD formation process in Figure 3.1.

NMD is common in coal mining drainages and its chemical formation process is outlined on the right side of Figure 3.1. Similarly with AMD formation, metal sulfide are exposed to oxygen and water till the formation of “Yellow boy” but in NMD, there are neutralizing chemicals like calcium carbonate ($CaCO_3$) present in the coal associated rocks also referred to as “host rocks”. The $CaCO_3$ act as a buffering agent by raising the pH of AMD to over 6.5 converting the water to be NMD hence low metal concentrations due to the high pH that results which does not support the metals dissolution process. However, high concentrations of calcium (Ca^{2+}), magnesium (Mg^{2+}), sodium (Na^{+}), SO_4^{2-} and nitrate (NO_3^{-}) remain dissolved in the drainage because the high pH (> 6.5) conditions do not induce their precipitation. Acidophilic and iron oxidising bacterial species (*Acidiphilium* sp. and *Gaallionella* sp. respectively) outlined under the chemical formation process of NMD are some of the dominant microbial groups detected thus far (Atkins and Pooley, 1982; Lin *et al.,* 2012). Low diversity of methanogenic bacteria and SRB has been characterized to be associated with NMD. Most SRB are unable to grow at high pH where iron cycling mediated by iron reducing and iron oxidizing bacteria is stabilized except those that can form spores like *Desulfosporosinus* sp. which tend to withstand the NMD conditions and only becomes active when anaerobic conditions are attainable (Küsel, 2003).

SRB are a diverse group of microorganisms which play a vital role in natural sulfur cycle and often used in bioremediation processes of AMD. They utilize SO_4^{2-} as their terminal electron acceptor while oxidizing the organic matter with a release of H_2S which reacts with dissolved metals forming metal sulfide precipitates. During this process, pH of the water is raised hence the toxicity of the drainage is reduced (Winch *et al.,* 2009). All known SRB synthesize the dissimilatory sulfite reductase enzyme (DSR), encoded by the *dsrAB* gene fragments which is responsible for catalysing the final steps in sulfate reduction after SRB gets exposed to SO_4^{2-} (Karr *et al.,* 2005). The *dsrAB* gene fragments encompass *α* (*dsrA*) and *β* (*dsrB*) subunits with combined size of approximately 1900 base pairs (bp) combined (Nercessian *et al*., 2005). The *dsrA* subunit with a size of approximately 1000 to 1100 bp and *dsrB*

subunit with a size of approximately 800 to 900 bp are situated at the 3'-end and the 5'-end of the *dsrAB* gene respectively. The *dsrAB* gene which is targetable with DSR1F and DSR4R primer set can be used to detect the presence of SRB in the environment. The amplification and sequencing of the *dsrAB* gene fragments have been employed widely in most environmental studies to profile SRB communities (Karr *et al*., 2005).

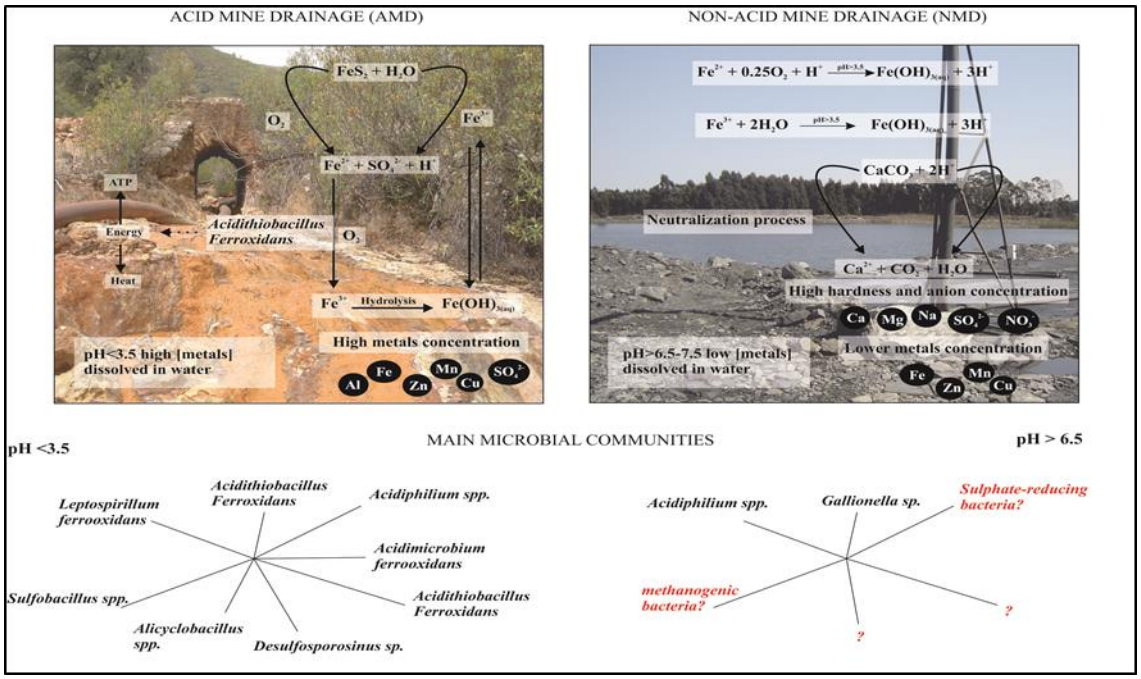

Figure 3.1: AMD and NMD chemical formation process and the microbial diversities dominant in them. (Generic Figure).

3.2.1. Aims and objectives of the chapter

The first aim of the study was to evaluate the physicochemical properties of acid or non-acid mine drainages from the three selected mine wastewaters. The second aim was to characterize the microbial communities associated with the AMD and NMD contaminated water.

The first objective was to chemically and biologically analyse and characterize the drainages. The second objective was to select suitable medium to enrich a consortium containing SRB to be evaluated for sulfate reduction potential at varied environmental conditions. The last objective was to confirm the presence of SRB in the enrichments using molecular and microscopic techniques.

3.3. Materials and methods

3.3.1. Localization and environmental settings

South Africa is one of the most intense mining practicing countries in the world with an increasing number of new and abandoned mines. Figure 3.2 depicts a South African map with highlighted areas of precious geological minerals that result in high mining activities in the country (McCarthy, 2011). The yellow shaded area represents the Witwatersrand basin which is the geologically underground gold concentration. Over the basin, there are several gold mining activities taking place especially in Gauteng, Mpumalanga and Free State provinces. The basin is known as the largest gold reserve in the world and has contributed approximately half of the world's mined gold used commercially (van Eeden *et al.*, 2009). The area shaded in black represent the coalfields which are concentrated with underground coal mostly extracted through open pit mining. The map also shows rivers that flow over the gold and coal fields that are at risk of being contaminated by mine drainages. The circled areas on the map were selected for the study and water samples were collected from the mine drainage contaminated water around these mining areas.

Site-Ex is a coal mining company situated in the Mpumalanga province and was selected as one of the study sites due to the challenge of water storage. The drainage from the mine exceeds the storage capacity of the built dams resulting in the spillage of the drainage around the dams. The company is one of the biggest coal producers in South African and the biggest coal supplier to the main South African electricity provider "ESKOM". The waste water pumped from the mines is stored in dams, some of the water is reused for mining process but most of it is not re-usable and therefore require treatment (McCarthy, 2011). From this site, only water was collected from the dams and used for the experiments as described in this chapter.

Site-Ka is an abandoned coal mine located approximately 130 km North East of Johannesburg in Gauteng province. The area where the site is situated spans approximately 220 ha. The mine belongs to a holding company that supplies bricks and mining equipment to active mines around the country. Due to the abandonment of the mine, rain and groundwater flooded the pits resulting in various sinkholes

around the area. The company has estimated approximately 5 to 10 billion litres of water that seeped from the mining area and requires treatment as it has typical characteristics of NMD with high pH, elevated concentrations of dissolved metals and sulfate making the drainage suitable for the study.

Site-Po is a drainage catchment dam hosting water from various gold mines around the West Rand area which is part of the Witwatersrand gold basin. The site is located towards the far east of Johannesburg and gold mining around this catchment started around late 1880s. The catchment area extends over 1600 square kilometres with minimal treatment from the drainage sources. The water has been reported to contain various metal contaminants with different pH ranges at different sites because of the different sources of water (Maleke *et al.,* 2014). From this site, water and sludge samples were collected and used for the study.

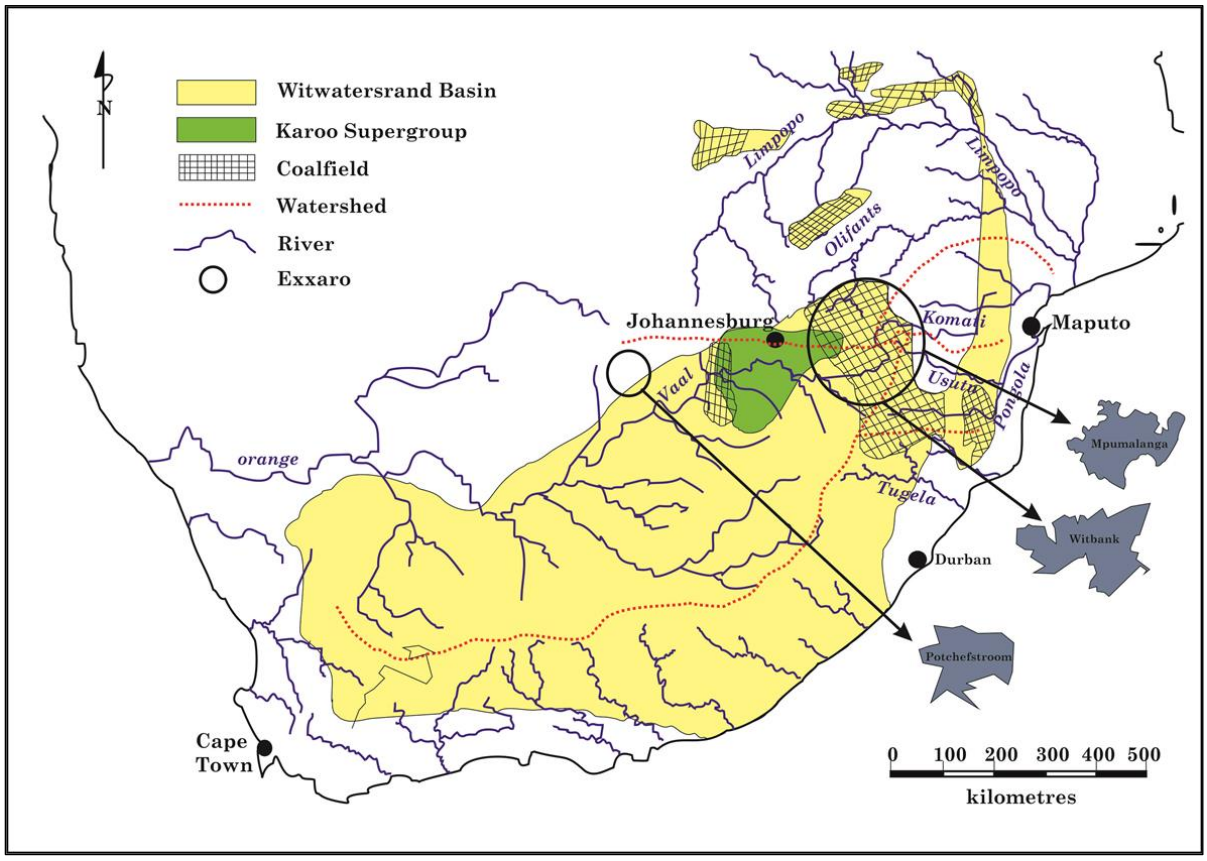

Figure 3.2: South African map indicating selected study sites. Location 1: Site-Ex, Location 2: Site-Ka and Location 3: Site-Po (Taken from McCarthy, 2011).

3.3.2. Samples collection

Sampling of AMD from the three sites (Site-Ex, Site-Ka and Site-Po) was performed by collecting mine wastewaters from the respective drainages depicted in Figure 3.3 using 25 L polyethylene drums (filled to the brim). From Site-Po catchment, black upper layered sludge was collected from the floor of the dam using a clean water washed shovel into an air tight zip-lock bag. The samples were transported within 24 hours from their respective sites to the laboratory at the University of the Free State (UFS) with care to avoid any biological or chemical changes in the samples.

Figure 3.3: Sampling sites selected for the study. A: Site-Ex, B: Site-Ka and C: Site-Po.

3.3.3. Chemical analysis

3.3.3.1. Physicochemical parameters

Upon arrival at the laboratory, some analytical parameters were measured immediately before storage (Marini *et al*., 2003). The pH, Oxidation Reduction Potential (ORP), Total Dissolved Solids (TDS) and Electrical Conductivity (EC) were analysed with portable probes (ORP probe model ExStik®II – RE300 and a multi-probe model ExStik® – EC500 was used for pH, ORP, TDS and EC measurements) in the laboratory. A 20 mL beaker was used to collect 5 mL of each sample from the 25 L drums and the tip of the probe was rinsed and inserted into the sample. Parafilm “M” (Bemis Flexible packaging, Neenah, WI 54956) was used to seal the opening between the brim of the beaker and the upper tip of the probe before recoding any results. For pH, TDS and EC, readings were recorded from the probe after the values were stable for more than 10 seconds while for ORP readings, the lowest values attained were considered.

Thereafter, samples were stored at 4°C to slow down the metabolic activity of the microorganisms and also to preserve any organic or decaying materials in the samples during storage. To avoid frequent opening and closing of the 25 L drums which may induce contamination and aeration, the samples were dispensed into sterile Schott bottles (500 mL) to be used as working samples.

3.3.3.2. Sulfate concentrations

Sulfate concentrations were determined using a HACH spectrophotometer, model DR900 according to method "8051 (USEPA[1] SulfaVer 4 Method[2])" described in the HACH procedure manual. Dilutions were made when the readings did not fit within the range of the spectrophotometric detection limits of 2 to 70 mg/L of SO_4^{2-}. This method was also benchmarked in our laboratory and approved by the SABS water analysis proficiency scheme for water analysis with a satisfactory Z score.

3.3.3.3. Sulfide concentrations

Sulfide concentrations were determined according to the methylene blue method adapted from Fonselius *et al*., 1999. The "Methylene blue" method refers to the blue colour product that forms when sulfide react with N, N- dimethyl-*p*-phenylene diamine hydrochloride (methylene blue dye) and ferric iron (Fe^{3+}) in the presence of an acidic medium (Fraçkowiak and Rabinowitch, 1996; Sakamoto-Arnold *et al*., 1986). A standard curve was constructed from the sulfide assay using sodium sulfide (Na_2S) titrated and standardised with potassium iodide (KI) and potassium hypoiodite (KIO).

All solutions for the assay were prepared from reagents of analytical grade obtained from Merck (Merck (Pty) Ltd South Africa) or Sigma (Sigma-Aldrich® South Africa) and used without further purification. Double distilled water (ddH_2O) was used in all cases, except for analytical methods where the ddH_20 was further purified using a Millipore water purification system to remove metal ions and the water is referred to as Milli-Q water. A 0.1 N Na_2S standard stock solution was prepared by dissolving

2.402 g of $Na_2S.9H_2O$ into 100 mL of de-oxygenated Milli-Q water (prepared by bubbling N_2 gas in the vial for 1 hour). The Na_2S crystals were dissolved under the N_2 gas to avoid additional O_2 contamination. The vial containing the standard Na_2S solution was protected from light by wrapping the vial with aluminium foil. In another vial containing 99 mL de-oxygenated Milli-Q water, 1 mL of the prepared stock solution was added to make a Sulfide solution with final concentration of 0.001 N (1000 µmol/L) to be used for the standard curve. Amine solution was prepared by dissolving 2 g of Dimethyl-*p* -Phenylene diamine hydrochloride in 200 mL Milli-Q water and finally, 200 mL concentrated H_2SO_4 (37%, v/v) was added in the solution. The volume of the amine solution was adjusted to 1 L by adding Milli-Q water and mixed well before storage. Iron solution was prepared by dissolving 10 g of $NH_4Fe(SO_4)_{2.}12H_2O$ and 2 mL concentrated H_2SO_4 adjusted to a final volume of 100 mL by Milli-Q water. Lastly, Zinc acetate solution was prepared by dissolving 2 g of $Zn(O_2CCH_3)_2$ in 100 mL Milli-Q water and all solutions were stored at 4°C.

A standard curve was constructed with 0.001 N (1000 µM/L) Na_2S dilutions ranging from 1 to 100 µmol/L prepared in triplicates. Dilutions were prepared to a final volume of 1000 µL in transparent cuvettes. The standard dilution analysis was done by first adding the zinc acetate solution (375 µL) into 2 mL cuvette followed by 1000 µL of the standard solution, 200 µL of the Amine reagent and finally 25 µL of the iron solution. The solutions were mixed by inverting the cuvettes twice and then incubated in the dark for 1 hour. Absorbance of the samples was read using a spectrophotometer (Spectronic® GENESYS™ 5) at 670 nm. The standard curve on Figure 3.4 was constructed using the obtained results. For the analysis of the AMD samples, the same analysis method was followed without diluting the AMD water. The straight line equation ($y = 0.0201x+0.03$ with R^2 value of 0.9967) obtained from the graph was used to calculate the exact sulfide concentrations in the AMD samples from the acquired absorbance values.

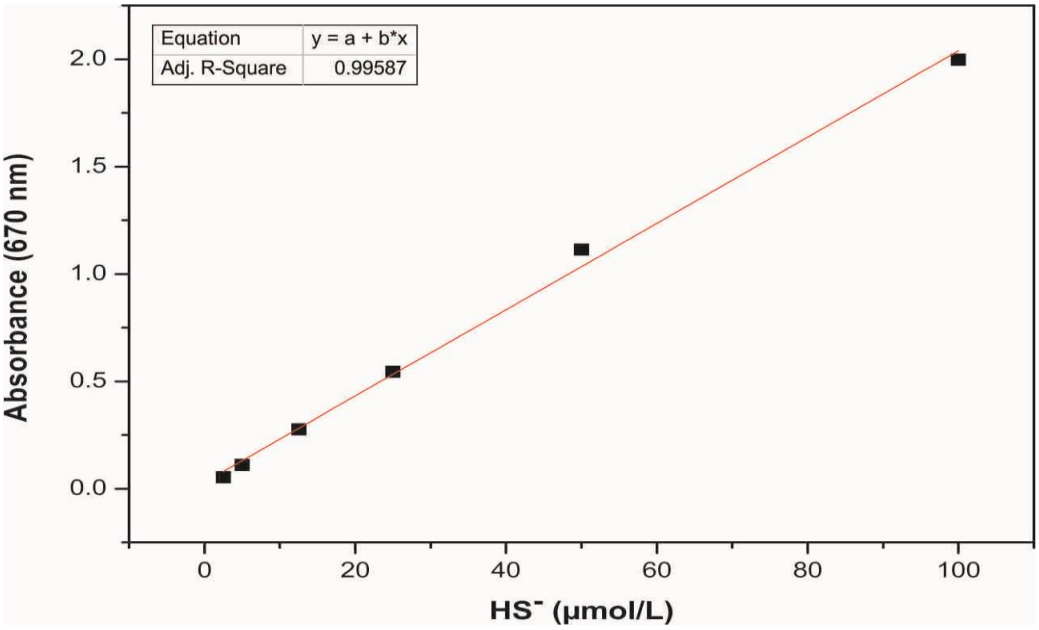

Figure 3.4: Standard curve relating sulfide concentrations to absorbance (670 nm).

3.3.3.4. Other chemical analysis

For further geochemical analysis, 250 mL of each of the water samples were sent to the Institute of Groundwater Studies (IGS) at the University of the Free State (UFS) for analysis by equipment such as Inductively Coupled Plasma Mass Spectrometry (ICP-MS) which detects metals and non-metals at very low concentrations such as 1 ng/L (Ammann, 2007).

3.3.4. Microbial characterization

3.3.4.1. DAPI staining

Microscopic techniques were performed to detect, enumerate, visualize and determine the viability of the bacteria present in the samples. Microbial detection and enumeration were done according to the 4',6-diamidino-2-phenylindole (DAPI) Nucleic Acid Staining technique for total (both dead and viable) microorganisms in the environmental samples as described by Kepner and Pratt (1994). The DAPI staining reagent stains the DNA in microbial cells with intact cell walls which will appear light blue against a dark blue background irrespective of their viability state (Suzuki *et al*., 1997).

From each of the three AMD water samples, 1.78 mL volumes were subjected to DAPI staining analysis. From the sludge sample, 2 g was weighed and suspended in 100 mL of ddH_2O and the liquid portion of the sample was used for DAPI analysis. These samples were fixed with 0.22 mL of 37% (v/v) Formaldehyde added to a final concentration of 4% (v/v) and incubated for 20 minutes at room temperature. The fixed samples were filtered through a 0.22 µM pore sized Millipore filter (GTBT-type) in the sterile glass filtration system (Milli-pore). A sterile blade was used to excise a quarter of the filter and transferred into a sterile petri dish using a sterile pair of tweezers. The piece of filter was stained with 10 µL of DAPI staining solution (10 µg/mL) and incubated in the dark for 2 minutes at room temperature. Distilled water was used to rinse the stain from the filter before it was mounted to a glass slide and covered with a thin glass coverslip by 10 µL of citifluor. A camera incorporated epifluorescence microscope (Axioski light and epifluorescent microscope (Zeiss, Germany)) with a grid intact ocular was used to enumerate the stained cells that fluoresced light blue under 100x magnification when using the blue field mercury lamp. Stained cells were counted from 3 different fixed fields on the slide and the mean number of cells was calculated using equation 3.1 and used in equation 3.3 to give a final estimated number of cells in each sample.

Equation 3.1: $$Mean\ No\ of\ cells = \frac{Total\ No\ of\ counted\ cells}{No\ of\ fields\ counted}$$

Equation 3.2: $$Filter\ Area\ = \pi r^2$$

$$Filter\ Area\ = \pi\ x\ 8000^2 (radius\ of the\ filter = 8000)$$

$$Filter\ Area\ = 2.10\ x\ 10^8\ \mu m^2$$

Equation 3.3: $$No\ of\ cells/mL = \frac{(Mean\ No\ of\ cells)\ x\ (Filter\ area)\ x\ (Dilution\ Factor)}{(Reticule\ area)\ x\ (Sample\ Volume\ used\ in\ mL)}$$

$$No\ of\ cells/mL = \frac{(Mean\ No\ of\ cells)\ x\ (2.10\ x\ 10^8\ \mu m^2)\ x\ (1)}{(10^5\ \mu m^2)\ x\ (Sample\ Volume\ used\ in\ mL)}$$

3.3.4.2. Live/Dead staining

A commercial LIVE/DEAD® BacLight™ Bacterial viability kit (Molecular Probes – Invitrogen detection technologies) was used to show the viability of the cells in the samples. The kit is convenient for monitoring the viability of bacterial populations as a function of the membrane integrity of the cells. The technique's fluorescent reagents stain the cell membranes (Berney *et al*., 2007) enabling them to fluoresce under the epifluorescence microscope where the viable cells with intact membranes stain green and those with compromised or damaged membranes (considered to be dead) stain red (Boulos *et al*., 1999).

Bacterial cells from the samples were concentrated by centrifuging 2 mL from each drainage in a 2 mL Eppendorf tube at 6 000 *x g* for 15 minutes. The supernatants from centrifuged samples were discarded and the pellets were re-suspended with 1 mL of 0.85% (w/v) NaCl each and incubated for 1 hour at room temperature with gentle yet thorough mixing every 15 minutes. The samples were again centrifuged for 15 minutes at 10 000 *x g* and the supernatants were discarded with the subsequent pellet re-suspension with 100 µL of 0.85% NaCl. The centrifugation and pellet re-suspension step was repeated three times before the staining step was initiated which is the modified step from the provided protocol with kit (LIVE/DEAD® BacLight™ Bacterial viability kit). The rest of the staining process was done according to the manufacturer's instructions. The stained cells were visualized under the epifluorescence microscope using the green field mercury lamp (filter 0.9, Excitation BP 450-490).

3.3.4.3. Gram staining

A Gram staining technique used for microscopic examination of bacteria was employed to visualize the morphological characteristics of bacteria and also to classify the enumerated cells into two groups of either gram negative or positive for bacteria with a thin or a thick peptidoglycan layer in their cell walls respectively (Chandra and Mani, 2011). This technique is a four step procedure that involves staining with different reagents and rinsing of the cells mounted to a glass slide to make cells stand out against their background appearing either being pink or purple

(Davies *et al*., 1983). Prior to Gram staining procedure, 2 mL of each water samples were added in separate 2 mL Eppendorf tubes and centrifuged at 6 000 *x g* for 5 minutes. From the centrifuged samples, 1.5 mL was discarded from the top of the sample and the remaining sample (0.5 mL) was then subjected to Gram staining. The samples were fixed and mounted on a glass slide by gentle heating over a gas flame. The fixed samples were then flooded with crystal violet and allowed to stand for 1 minute which was rinsed off with distilled water (dH_2O). The iodine solution was then flooded over the sample and also allowed to incubate for 1 minute and rinsed with dH_2O. Ethanol (95% v/v) was used to decolorize the previously added solutions till their blue-violet colour was not emitted and then rinsed with dH_2O as previously done. The last solution flooded on the slides was the counter stain safranin which was also allowed to stand for 1 minute before being rinsed with dH_2O. The glass slides were blotted with a paper towel and the stained cells were visualized using the camera incorporated epifluorescence microscope (on light microscope mode) under 1 000 x magnification.

3.3.5. Molecular characterization

3.3.5.1. Genomic DNA extraction

Identification of bacterial communities in the AMD was done by molecular analysis. All primers used in this study were obtained from Integrated DNA Technologies (IDT) or Inqaba Biotech™ unless otherwise stated. The bacterial genomic DNA was extracted using a NucleoSpin soil kit (NucleosSpin® Soil Kit" - Macherey-Nagel) according to the manufacturer instructions. From each AMD sample, 250 mL was filtered through a sterilized 0.20 µm pore sized membrane filter (PALL-Pall Corporation) to concentrate the cells. Sterile blades were used to carefully and finely cut the filters into small pieces with less destruction to the trapped cells on the filter. The liquid portion of the sludge sample was used for gDNA extraction process commercial kit. The gDNA extracts were visualized on a 0.8% (w/v) agarose gel stained with ethidium bromide (2.5 mg/µL). The gel was resolved at 90 volts for 1 hour and visualized under UV illumination with a Chem-Doc XRS (Bio-Rad Laboratories) gel documentation system. The purity and concentrations of the gDNA

was determined by the NanoDrop spectrophotometer ND-1000 (NanoDrop Technologies, Wilmington, DE).

3.3.5.2. Amplification of the partial 16S rRNA gene fragment

From the gDNA extracts, a conserved portion of 16S ribosomal RNA (rRNA) fragment in all bacteria was amplified using the Polymerase Chain Reaction (PCR) technique with a set of primers one containing a GC clamp (40 nucleotides GC rich sequence) suitable for the Denaturation Gradient Gel Electrophoresis (DGGE) preparatory step. The partial bacterial 16S rRNA fragments were amplified using 341F-GC and 907R primer set with sequences outlined in Table 3.1 adapted from Muyzer *et al*., 1993. The GC clamp attached to the 5' end of 341F primer and the M nucleotide in the 907R serving as a degenerate base representing either A or C, are characteristics enabling the primers to anneal to the specific gene target fragments (Dar *et al*., 2005; Karr *et al*., 2005; Muyzer *et al*., 1993; Rozak and Rozak, 2008).

Table 3.1: PCR primer set and sequences for 16S rRNA amplification.

Primer	Sequence
*341F	5'-CCT ACG GGA GGC AGC A -3'
*907R	5'- CCG TCA ATT CMT TTG AGT TT -3'
**GC-clamp	5'-CGCGCGCCGCGCCCCGCGCCCGTCCCGCCGCCCCCGCCCG-3'

*Muyzer *et al*., 1993; **Karr *et al*., 2005

PCR mixture containing: 5 µL of Buffer (10x), 1 µL of dNTPs mix (10 mM), 1 µL of BSA (10 µg/µL, 1 µL of forward primer 341F-GC (10 µ M), 1 µL of reverse primer 907R (10 µg/µL), 0.25 µL of Taq DNA polymerase, 1 µL of template DNA extracts (50 to 100 ng/µL – adjusted according to the NanoDrop results) and the volumes were adjusted to 50 µL by adding autoclaved Milli-Q water. The amplification was performed by the use of a PCR machine "Thermal Cycler (PxE 0.2, Thermo Electron Corporation)" according to the programme in Table 3.2 modified from the original programme by Muyzer *et al*., 1993.

Table 3.2: PCR programme for 16S rRNA amplification.

Step	Temperature	Duration	Number of cycles
Initial denaturation	95°C	5 minutes	1
Denaturation	95°C	40 seconds	
Annealing	55°C	45 seconds	25
Extension	70°C	2 minutes	
Final extension and elongation	72°C	10 minutes	1
Holding	4°C	Holding step	1

The PCR products (amplicons) were visualized on a 1% (w/v) agarose gel stained with ethidium bromide (EtBr) (2.5 mg/µL). A DNA standard marker (O'GeneRuler^{TM} Ladder Mix, 0.1 µg/µL) marker was loaded on the first lane of the gel to serve as the reference point for band size estimation followed by the samples (5 µL amplicon and 2 µL loading dye). The gel was ran at 90 volts for 1 hour and visualized under the UV illumination with a Chem-Doc XRS (Bio-Rad Laboratories) gel documentation system. All PCR products (amplicons) with an expected band size of 566 to 600 bp, were subjected to DGGE.

3.3.5.3. Denaturation Gradient Gel Electrophoresis (DGGE)

DGGE was selected for microbial diversity studies as it is routinely used and known to help avoid large scale sequencing efforts (Mühling *et al*., 2008). Samples represented by defined and intense bands on the 1% (w/v) agarose gel were subjected to DGGE processing while those with faint or multiple bands were repeated with a modified annealing temperature on the PCR programme. A Bio-Rad DCodeTM Universal Mutation Detection System was used for casting the DGGE gel prepared as follows: All system components were washed with tap water and blotted with a paper towel before use. A 1x TAE (Tris Acetate EDTA) buffer was prepared to a final volume of 7 L by diluting 140 mL of the TAE buffer (50x TAE) in 680 mL distilled water. The buffer was added into the gel casting tank and the lid was placed over the tank to reduce evaporation of the buffer. Two stock denaturants solutions (0% (w/v) and 80% (w/v) Urea and Formamide (UF)) were prepared in 50 mL falcon

tubes. For 0% (w/v) UF, the following reagents were added into a sterile falcon tube: 8.75 mL of 40% bis-acrylamide, 1 mL of 50x TAE (242 g/L of Tris-HCl, 18.6 g/L of EDTA (Ethylene-Diamine-Tetra acetic Acid) and 57.1 mL of Glacial Acetic Acid into 1 L) buffer and the volume of the mixture was adjusted to 50 mL by adding 40.25 mL of milli-Q water. For 80% (w/v) UF, 16.8 g of Urea was weighed into the sterile falcon tube and dissolved with 8.75 mL of 40% (w/v) bis-acrylamide, 1 mL of 50x TAE buffer, 16 mL of deionized Formamide and the volume was adjusted to 50 mL with Milli-Q water. The falcon tube containing 80% (w/v) UF solution was vigorously vortexed till all the Urea was dissolved. Both the falcon tubes containing 0 and 80% (w/v) UF solutions were wrapped with aluminium foil and stored at 4°C to protect the denaturants from direct light as they lose their reactivity in light.

Two glass plates were prepared for casting 30 mL of the gradient gel separated by spacers with the thickness of 1 mm and held stable and firm by sandwich clamp on a casting stand. From the stock solutions (0 and 80% (w/v) UF), working solutions with high (60% (w/v) UF) and low (40% (w/v) UF) densities were prepared in 20 mL volumes by mixing 10 mL of each 0 and 80% (w/v) UF for 40% (w/v) UF while for 60% (w/v) UF density solution, 5 mL of 0% (w/v) UF and 15 mL of 80% (w/v) were mixed. Polymerization of the separation gels (40 and 60% (w/v) UF) was activated and catalysed by the addition of 130 µL of 12.5% (w/v) Ammonium Persulfate (APS) and 14.7 µL of N,N,N',N'-tetramethyl-ethylene-diamine (TEMED) into each solution and mixed thoroughly before being casted between the glass plates using the bio-rad gradient gel casting system.

A delivery wheel was used to deliver the gels between the plates starting with the high density gel (60% (w/v) UF) followed by low density gel (40% (w/v) UF) in a gradient manner to allow gradient separation from low density gel through to the high density gel at the bottom. A comb was inserted when the glass plates were almost filled and then filled to the brim with gentle addition of the gel to avoid spillage of the gel and the destruction of the gradient in the gel. The gel was covered with aluminium foil and left to stand for an hour at room temperature before it was moved into a dark cupboard for two hours. The TAE buffer in the tank was warmed to 60°C before inserting the gel into the tank. The comb was removed and the wells were flushed with the buffer in the tank using 1 mL pipette.

The amplicons obtained from the 16S rRNA PCR were prepared for DGGE analysis by mixing 15 µL of the amplicons and 5 µL of the loading dye. The samples were loaded on the DGGE gel towards the centre and the power source was turned on. The buffer temperature was once again allowed to reach 60°C before the DGGE pump was activated and the gel was ran at 100 volts and 50 ramps for 16 hours. The gel was stained in 400 mL of ethidium bromide (2.5 mg/µL), prepared in 1x TAE buffer for 1 hour and rinsed three times with distilled water and visualized with a gel documentation system Chem-Doc XRS (Biorad Laboratories) under a UV illumination. Visible bands were marked and excised using a sterile blade and incubated overnight immersed in 50 µL of autoclaved Milli-Q water at 55°C.

The eluted DGGE bands were used as templates for the re-amplification of the DNA fragments using the same PCR programme and conditions used in the amplification of 16S rRNA describe in section 3.3.5.2 but the template volume was increased to 5 µL, the forward primer (341F) used did not contain a GC clamp and the annealing temperature was reduced by two units from 55 to 53°C. The re-amplified amplicons were examined on a 1% agarose gel as done for the 16S rRNA PCR to confirm if there was amplification of the DNA fragments.

The amplified samples were subjected for amplicon purification step as follows: 35 µL of each amplicon was mixed with 5 µL of the loading dye before loading 20 µL of the samples per well (2 wells for one sample). The gel was ran as previously done for 16S rRNA gene amplicons, bands were excised and subjected to gel extraction step using a commercial Bio-Flux Gel extraction kit (Bio-Technology Co.Ltd) according to the manufacture's instruction. The extracted DNA fragments were then subjected to sequencing PCR.

A DNA sequencing BigDye terminator v. 3.1 kit, was used to process the extracted DNA for sequencing using the PCR technique. A total sequencing PCR reaction volume of 10 µL containing the following reagents was prepared for each sample: 2 µL of 1x Sequencing Dilution buffer, 0.5 µL of Sequencing Premix, 1 µL of reverse primer 907R (3.2 pmol Primer) and 6.5 µL template (purified DNA fragments from DGGE (re-amplified bands)). The PCR tubes were clearly marked and placed in a PCR machine "Thermal Cycler (PxE 0.2, Thermo Electron Corporation)" and the sequencing PCR was performed according to the programme shown in Table 3.3.

Table 3.3: Sequencing PCR programme.

Step	Temperature	Duration	Number of cycles
Initial denaturation	96°C	1 minute	1
Denaturation	96°C	10 seconds	
Annealing	50°C	5 seconds	25
Extension	60°C	4 minutes	
Holding step	4°C	Till stopped	1

The volumes of the sequencing PCR products were adjusted to 20 µL by the addition of 10 µL of autoclaved Milli-Q water before the purification step. EDTA/ethanol precipitation method was selected for the purification of the sequencing PCR products. To the 20 µL solutions, 5 µL of EDTA (125 mM with a pH of 8.5) was added and the solutions were transferred into 1.5 mL Eppendorf tubes in which, 60 µL of absolute ethanol was added per tube and the tubes were vortexed for 5 seconds then incubated at room temperature for 15 minutes. The tubes were centrifuged for 20 minutes at 20 000 *x g* and 4°C. The supernatant was discarded from the tubes and 60 µL of 70% (v/v) Ethanol was immediately added into the tubes. The tubes were again centrifuged for 10 minutes at 20 000 *x g* and 4°C. The supernatant was discarded and the pellet was dried in the speed-vac (Eppendorf Concentrator, 5301) for 10 minutes at 30°C. The dry pellets containing purified DNA were sent for sequencing by the Capillary Sequence 3120x1 ABI Genetic Analyzer (Applied Biosystems) at the department of Microbial, Biochemical and Food Biotechnology, University of the Free State. The resulting sequences were converted from the ABI format to the Microsoft word format using Finch-TV software (Version 1.4.0) and the sequences representing bacterial groups were compared with the DNA sequences data deposited in the gene bank database through National Centre for Biotechnology Information (NCBI) to identify the bacteria present in AMD samples by names.

3.3.6. Microbial enrichments

One of the oldest techniques used in bacterial studies is cultivation, even though it has its own limitations, it has been used successfully to study novel and well known or established microorganisms (Muyzer and Stams, 2008; Park, 2004). Enriching the microbial consortium from a natural source is always a challenge as a specific medium is required to enrich a desired group of microorganisms and also keeping in mind that only less than 1% of the bacteria in nature can be cultured (Muyzer and Stams, 2008). The targeted microbial consortium or isolates from the collected samples had to display sulfate reduction. To enrich such a bacterial community, two media compositions were selected: anaerobic sulfate reducing medium (ASRM) and Postgate medium B (PSGM) were used to grow the microorganisms in anaerobic vials.

ASRM was adopted from studies done by Botes and Kieft to grow SRB in medium containing carbon sources like acetate, lactate or glycerol while the PSGM contained sodium lactate as the main carbon source as outlined in Table 3.4 (media defined in our laboratory by visiting Prof Tom Kieft). PSGM was adopted with modifications from studies done by Ghazy and co-workers in 2011. The medium has been widely used with modifications from the original recipe by Postgate (1984) to study SRB. PSGM recipe contains two vital acids (thioglycolic and ascorbic) known to enhance anaerobic conditions and reducing power of the medium during SRB growth (Ghazy *et al.,* 2011) and the medium is known to be suitable for isolating, enriching and maintaining SRB (Kaksonen *et al*., 2003; Postgate, 1984). The media components were weighed and diluted up to 800 mL with distilled water and up to 1 L of 50:50% of distilled: tap water for ASRM and PSGM respectively into two separate 2 L Schott bottles. The pH of the media was adjusted to 6.2 with 0.05 M NaOH and 0.05 M HCl using the electronic pH probe. For ASRM, 1 g of yeast extract was diluted separately into 100 mL distilled water and filter-sterilized into an autoclaved 150 mL vial before the degassing process.

Table 3.4: Media compositions of ASRM and PSGM.

	PSGM-B	**ASRM**
Chemical reagents	**Amount in g/L**	**Amount in g/L**
KH_2PO_4	0.5	-
NH_4Cl	1	1
Na_2SO_4	1	1
$CaCl_2.2H_2O$	-	0.1
$CaCl_2.6H_2O$	0.1	-
$MgSO_4.7H_2O$	2	2
Sodium lactate (60-70%, w/w)	5 mL*	7.48
Sodium Acetate	-	3.28
Yeast extract	1	1**
K_2HPO_4	-	0.5
Ascorbic acid	0.1	-
Thioglycolic acid	0.1	-
Tap/Sea water	500 mL	-
Distilled water	500 mL	800 mL
pH adjustments	6 – 7.5	6 – 7.5

(* = replaceable by 3.48 mL glycerol)

(** = prepared separately)

3.3.6.1. Anaerobic media preparations

ASRM (70 mL) was added into each of the six 150 mL sterile sealed serum vials. Resazurin which serves as a redox indicator was added to detect if oxygen gets introduced into the vials after degassing or during the incubation period. From the stock solution of PSGM (80 mL) was also added into another six 150 mL sterile and sealed serum vials. Serum vials containing ASRM, PSGM and yeast extracts depicted in Figure 3.5 were secured on a shaker and connected to tubes from the degassing system with the aim to eliminate all the air containing oxygen from the vials replacing it with nitrogen. The pink colour in the ASRM vials indicates the presence of oxygen in the medium. The degasser was set to operate for 30 cycles for an hour while shaking the vials with approximately 100 kPa of nitrogen purged into the vials.

After degassing, all the media in the vials were then sterilized by autoclaving for 20 minutes at 120°C. The vials were allowed to cool and 10 mL of degassed, filter sterilized yeast extracts was added into each serum vial containing ASRM. To get rid of the oxygen that might have entered the vials during addition of yeast extracts, 100 µL of filter sterilized and degassed, 2.5% (m/v) cysteine-Hydrochloric acid (Cyc-HCl) was added in the vials containing ASRM. The cys-HCl is known to react with oxygen resulting in disulphide and water. One vial containing ASRM was opened and the pH was re-adjusted to 6.5 while taking note of the amount of NaOH (0.05 M) added to raise the pH. The noted amount was then added to the other five vials containing 80 mL of ASRM.

Figure 3.5: Anaerobic serum vials containing enrichment media. Left: PSGM, Middle: two vials containing yeast extract and Right: ASRM.

3.3.6.2. Media inoculation and incubation

The acclimation process for the adaptability of SRB from the collected wastewaters was done by growing the bacteria in the media representing synthetic AMD. The media were inoculated as follows: the vials, sludge and water samples were placed in the anaerobic chamber (COY- Laboratory Product INC. 14500 COY DR. Grass Lake, MI49240) and AMD water was used as 20% (v/v) inoculum in vials designated for Site-Ex, Site-Ka and Site-Po. Using sterile syringes, 20 mL of each AMD sample from the three sites were aseptically added into the six vials, three containing ASRM and the other thee containing PSGM according to Table 3.5. For sludge samples, 10 grams was diluted in degassed 100 mL autoclaved Milli-Q water and used as inoculum. For negative controls, autoclaved Milli-Q water was added as inocula and all samples were incubated at 30^0C for 20 days.

Table 3.5: Designated names of the enrichment samples.

Vial No	Sample description
1	Negative control in PSGM
2	Negative control in ASRM
3	Primary culture of Sludge in PSGM
4	Primary culture of Sludge in ASRM
5	Primary culture of Site-Ex AMD in PSGM
6	Primary culture of Site-Ex AMD in ASRM
7	Primary culture of Site-Ka AMD in PSGM
8	Primary culture of Site-Ka AMD in ASRM
9	Primary culture of Site-Po AMD in PSGM
10	Primary culture of Site-Po AMD in ASRM

3.3.6.3. Secondary inoculation into fresh media

After 20 days of the primary culture incubation period, the cultures were used as inocula for the secondary cultures acclimation. For the secondary cultures, PSGM and ASRM were prepared as described in section 3.3.6.1 and using sterile syringes, (20 mL) primary cultures were inoculated into the vials (with 80 mL of either ASRM or PSGM) in the anaerobic chamber. The passaging was done aseptically to avoid contamination and oxygen intrusion during inoculation process. The vials were incubated for another 20 days at 30^0C.

3.3.6.4. Tertiary inoculation into the fresh media

As done for the secondary cultures, the ASRM and PSGM were prepared as described in section 3.3.6.2 and the 20 mL inocula from the secondary cultures were introduced into 10 vials of 150 mL capacity (with 80 mL of ASRM in 5 and PSGM in

another 5). The tertiary cultures were also incubated for 20 days at 30^0C. After the last day of incubation, the samples were subjected to microbial and molecular analysis to identify the enriched bacteria according to techniques described under sections 3.3.4 and 3.3.5 respectively.

3.3.6.5. Microbial characterization of enriched cultures

The tertiary cultures were subjected to microbial characterization by the use of microscopy techniques. DAPI staining, Live/Dead cell staining and Gram staining techniques were applied according sections 3.3.4.1, 3.3.4.2 and 3.3.4.3 respectively.

3.3.6.6. Molecular analysis of the enriched tertiary cultures

Genomic DNA was extracted from the tertiary cultures as described in section 3.3.5.1. The extracted gDNA was used as templates for the amplification of 16S rRNA gene according to the method described in section 3.3.5.2. The PCR products were subjected to DGGE and bands sequencing analysis as described in section 3.3.5.3.

3.3.6.7. Amplification of the *dsrAB* gene fragments from gDNA

From the remaining gDNA extracted from the tertiary cultures described in section 3.3.5.6, 1 µL gDNA from each of the selected samples with higher DNA concentrations were used as templates to amplify the dissimilatory sulfite reductase AB (*dsrAB*) gene fragments conserved in all known SRB (Karr *et al.,* 2005). Sample selection was done based on the NanoDrop results. From the drainage samples enrichments in ASRM and PSGM, one gDNA sample with high concentration was used whereas both sludge gDNA samples were subjected to PCR amplification of *dsrAB* gene fragments. The PCR mixture similar to the one described under section 3.3.5.2 but with different primer set was made up with respective reagents up to a volume of 50 µL. Gene specific primer set, DSR1F and DSR4R with sequences showed in Table 3.6, previously used by Karr and co-workers (Karr *et al.,* 2005; Nakagawa *et al.,* 2004; Dar *et al.,* 2006), were employed to amplify the *dsrAB* gene

fragments according to the adopted protocol. The PCR programme summarized in Table 3.7 was followed with modifications to optimize the amplification reaction (Leloup *et al.,* 2006; Nakagawa *et al.,* 2004; Nercessian *et al*., 2005).

Table 3.6: Sequences of *dsrAB* gene fragments primer set.

Primer	Sequence
*DSR1F	5'-ACSCACTGGAAGCACG-3'
*DSR4R	5'-GTGTAGCAGTTACCGCA-3'

*Karr *et al.,* 2005

Table 3.7: PCR programme for the amplification of *dsrAB* gene fragments.

Step	Temperature	Duration	Number of cycles
Denaturation	94°C	1 minute	
Annealing	54°C	1 minute	20
Extension	72°C	3 minutes	
Final extension and elongation	72°C	10 minutes	1
Holding	4°C	Holding step	1

The PCR reaction resulted in multiple bands when visualized on the 1% (w/v) agarose gel. For the specificity of this reaction, the annealing temperature was crucial hence needed optimization. Gradient PCR was performed on both high concentrations sludge gDNA of samples enriched in PSGM and ASRM with annealing temperatures ranging between 50^0C and 60^0C (50.0^0C, 50.8^0C, 52.1^0C, 54.0^0C, 56.2^0C, 58.0^0C, 59.3^0C and 60.0^0C). The gradient PCR was ran for 29 cycles rather than the 20 cycles used previously. The PCR products were again visualized on the 1% (w/v) of agarose gel.

3.3.6.8. Cryopreservation of the enriched cultures

During the acclimation process, cultures were preserved and stored at -80^{0}C in 40% (v/v) glycerol. Before the passaging process of inoculating the fresh medium with the 20 days cultures (primary, secondary to tertiary), 2 mL from each culture was aseptically harvested and added into 2 mL of sterile 40% (v/v) glycerol to make a 1:1 (v/v) of culture : glycerol solution and stored in the -80^{0}C (Perry, 1995).

3.3.6.9. Scanning Electron Microscopy

The tertiary cultures were subjected to Scanning Electron Microscopy (SEM) analysis to visualize the metal-microbe interactions in the cultures. The samples preparation involved drying of the culture components by lyophilisation. From each vial, 20 mL was aseptically harvested using sterile needles in the anaerobic chamber into 50 mL falcon tubes and centrifuged for 15 minutes at 4 000 g. The tubes were returned back in the anaerobic chamber without disturbing the pellet and the supernatant was discarded. The pellets were then immersed in liquid nitrogen for 20 minutes followed by overnight lyophilisation. The resulting powder samples were sent to the Centre of Microscopy at the University of the Free State to be analysed by SEM (Joel JSM-7800F Field Emission SEM) with high resolution equipped with Oxford Aztec EDS and Gatan Mono CL4. The samples were mounted and coated with gold and carbon on separate plates to analyse the metal-microbe interactions. The backscattering mode was also applied to visualize the morphology of metals contained in the samples.

3.4. Results and discussions

3.4.1. Samples description and analysis

Samples were collected as described in section 3.3.2 and upon arrival at the laboratory, 500 mL samples volumes were stored to serve as working volumes and the physicochemical characteristics were analysed. The samples were also visually analysed to compare the colour characteristics. It was noted that sample from Site-Po had a rusty colour whereas the other two were clear. Table 3.8 displays results of the initial analysis as described in section 3.3.3.1. The data shows that Site-Ka and Site-Po samples had low pH values of 3.40 and 2.90 respectively which are the characteristics of a typical acid mine drainage (Jong and Parry, 2006). In contrast, the Site-Ex sample had a pH of 7.28 indicating mere alkaline or non-acid mine drainage as described by Johnson and Hallberg (2005). Site-Po water sample had the highest EC of 422 mS/m which correlated with its high TDS value of 2940 mg/L. The same correlation was observed in Site-Ex and Site-Ka water samples and was also described by Hedin (2008). Sulfide concentrations were low in all samples. Site-Po had the highest sulfate concentrations followed by Site-Ex and Site-Ka respectively. The sulfate concentrations showed close relation with EC and TDS as they were both high for Site-Po water sample compared to the other two samples. This means that the drainages might contain high metals concentrations from the dissolution of metal sulfide minerals (ZnS, FeS_2, $CuFeS_2$ and PbS) caused by mining activities or from mining waste such as tailings. The oxidative process of metal sulfide minerals could have also been catalysed by the presence of acidophilic oxidative bacteria in the environment (Baker *et al,.* 2003b; Johnson and Hallberg, 2005). The ORP values in all samples were high (<100 mV), showing that the redox reactions at the sampling sites do not support SO_4^{2-} reduction. Furthermore, high SO_4^{2-} and low S^{2-} concentrations in the drainages representing redox couple (SO_4^{2-} /S^{2-}) indicate that the environmental conditions at the sampling sites were not supportive (oxic) to achieve low ORP values (-200 mV to -300 mV) necessary to promote bacterial sulfate reduction (Barton and Fauque, 2009).

Table 3.8: Physicochemical characteristics of mine drainages.

Parameter	Site-Ex	Site-Ka	Site-Po
pH	7.82	3.40	2.90
EC(mS/m)	169	170	422
TDS(mg/L)	1180	1190	2940
ORP(mV)	187	406	428
S^{2-}(mg/L)	0.0433	0.0433	0.0435
SO_4^{2-}(mg/L)	1050	975	3700

Further analysis of the water samples was done as described in section 3.3.3.4 to quantify selected metals of interest shown in Table 3.9. The pH values of Site-Ka and Site-Po samples still showed that the water was acidic with confirmed high sulfate concentrations whereas Site-Ex water sample showed similar pH value but lower sulfate concentration compared to the colorimetric data. The latter sulfate concentrations are different with respect to the results obtained by colorimetric methods, although the differences were not significant. According to the hydro-geochemical data, highest metals concentrations were detected in Site-Po sample as it was expected because of the high EC and TDS values previously obtained. The most dominant metals (highlighted in red on Table 3.9) were Ca, Fe, Mg, Mn and Na with concentrations of 544,5 mg/L, 464,79 mg/L, 167,6 mg/L, 40.232 mg/L and 104.1 mg/L respectively in Site-Po sample which is believably the reason for high EC and TDS. The rusty brown colour in Site-Po sample was then confirmed to be due to high iron concentrations as it is known to result in yellow to orange colour when it precipitates in water (Sánchez España *et al*., 2005). In general, gold mines are associated with pyrite (FeS_2) which is stable underground but produces iron hydroxide ($Fe(OH)_2$) and sulphuric acid (H_2SO_4) when exposed to water and oxygen which is possibly the reason why there are high concentrations of iron and sulfate concentrations in AMD resulting from gold mines Site-Ka and Site-Po samples (Naicker *et al.,* 2003). Metals that were detected in Site-Ka sample were: Al, Ni and Zn (highlighted in blue) with concentrations of 40.528 mg/L, 1.1115 mg/L and 3.5265

mg/L respectively. The high dissolved concentrations of metals in Site-Ka and Site-Po releases high concentrations of H^+ in the drainages which are the evidence of oxidative processes that resulted in low pH. The non-acid mine drainage water (Site-Ex) did not contain high metals concentrations due to its alkaline state which allowed metal hydroxide precipitation. The alkaline state of Site-Ex water was possibly due to the presence of calcite or dolomite at the sampling site which their presence are detected by high Ca and Mg concentrations in water. There were metal concentrations which is a typical characteristic of most coal mine drainages characterized by high pH (Banks *et al*., 2002).

The characteristics of each water sample could sustain diverse SRB species. The next milestone that was embarked on after the water characterization was the one to determine the presence of microorganisms in the samples and to investigate their sulfate reduction potential.

Table 3.9: The hydro-geochemical data of the three water samples.

Parameter	Site-Ex	Site-Ka	Site-Po
pH	7.9	2.98	4.75
EC (mS/m)	166	301.5	433
Ca (mg/L)	240.3	190.73	544.5
Mg (mg/L)	129.3	59.415	167.6
K (mg/L)	8.267	6.63	10.5
P (mg/L)	<1	<1	<1
Na (mg/L)	16.77	31.54	104.1
Fe (mg/L)	0.05	85.04	464.79
Al (mg/L)	0.0163	40.528	0.004
Mn (mg/L)	0.0377	10.5705	40.232
Ni (mg/L)	0.0023	1.1115	0.365
Zn (mg/L)	0.027	3.5265	0.049
SO_4^{2-} (mg/L)	941.67	1206.5	2933

3.4.2. Microbial characterization results

3.4.2.1. Microbial cell counts by DAPI staining

The first microscopic technique applied was based on staining reagent DAPI and was performed as described in section 3.3.4.1. The sludge and the three water samples were subjected to the analysis and the microorganisms were counted using equations 3.1, 3.2 and 3.3. The numbers of cells are recorded in Table 3.10 with some of the correlating images depicted in Figure 3.6.

The DAPI staining images showed the presence of bacterial cells in all water samples. Care had to be taken as turbid or sludge samples had material that was misleading during counting. The sludge sample contained the highest estimated number of cells (2.4×10^5 cells /mL) as was expected because biofilm usually forms at the bottom of the dam since the soil serves as the source of attachment for microbial colonization. Furthermore, there was low concentrations of planktonic cells in the water samples compared to the sludge as the cells tends to fix themselves to the sediments to form biofilm that serves as their protection to the extreme conditions of the AMD (Nies, 1999; Nies, 1995). Site-Ex water sample had more bacterial cells (5×10^3) compared to Site-Ka (5.7×10^2) and Site-Po (4×10^2) which the estimated amounts can be attributed to the pH and metals concentrations previously analysed. In addition to the cell counts, the DAPI stain is also informative with respect to the various morphologies of the microbial diversity as it can be seen in Figure 3.6.

Table 3.10: Microbial cell count estimations by DAPI staining technique.

Sample	Number of cells/mL
Sludge	2.4×10^5
Site-Ex	5.0×10^3
Site-Ka	5.7×10^2
Site-Po	4.0×10^2

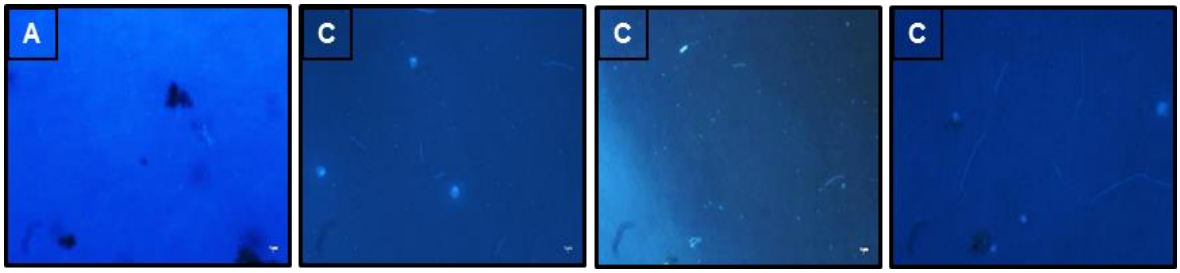

Figure 3.6: DAPI staining images. A: Sludge sample, B: Site-Ex, C: Site-Ka and D: Site-Po. Scale bar = 1 µm.

3.4.2.2. Bacterial viability test by Live/Dead staining

The three water samples were further analysed with the Live/Dead cell staining technique to determine the viability of the cells contained. The Live/Dead staining technique was applied according to the procedure explained in section 3.3.4.2. Images of the respective samples depicted in Figure 3.7, showed both viable cells appearing as green spots (indicated by a blue arrows) and dead cells appearing as orange to red spots (indicated by red arrows) in all samples. The microscopic results confirmed that there are viable bacteria in the water samples and have a potential to be cultured.

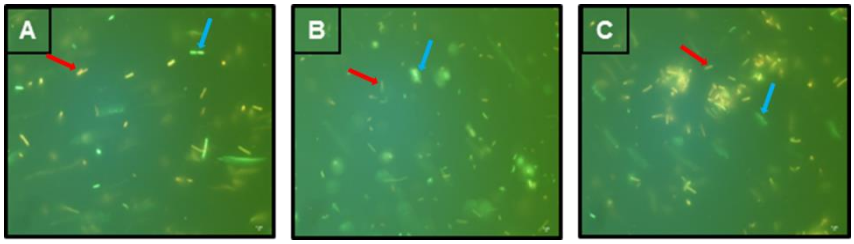

Figure 3.7: Live/Dead staining images from the three water samples. A: Site-Ex, B: Site-Ka and C: Site-Po.

3.4.2.3. Morphological characterization of bacteria by gram staining

Gram staining technique was applied to characterize microbial morphologies according to the procedure described in section 3.3.4.3. Based on the captured Gram staining images depicted in Figure 3.8, various morphologies of microorganisms were observed in all samples. The Gram negative bacteria, appearing as pink to red spots were more dominant than the Gram positive bacteria.

From the images, rod, cocci and filamentous shaped microorganisms were observed in the samples indicating the morphological diversities in the water samples. The filamentous microorganisms observed in Figure 3.8 C, appeared in Live/Dead staining image Figure 3.7 C of the same sample (Site-Po) which shows a direct correlation of the obtained microscopic results.

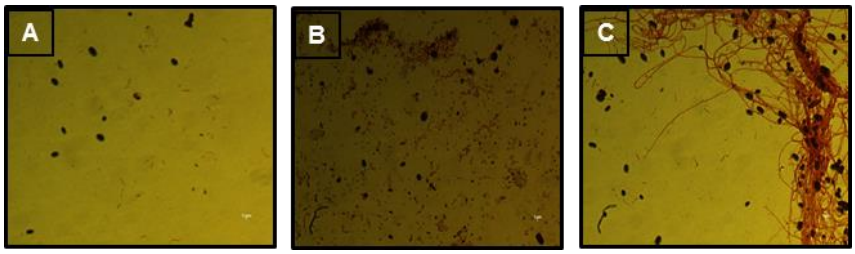

Figure 3.8: Gram stained bacterial cells from the three water samples. A: Site-Ex, B: Site-Ka and C: Site-Po.

3.4.3. Molecular characterization results

3.4.3.1. Genomic DNA extraction

The samples were concentrated as one considered the low cell numbers in the samples prior to gDNA extraction. A 250 mL volume of each sample was filtered through a 0.2 µm pore sized membrane filter. gDNA was extracted from the membrane filter using the NucleosSpin® Soil Kit according to the manufacturer's instructions as described in section 3.3.5.1. The extracted gDNA were visualized on a 0.8% (w/v) agarose gel depicted in Figure 3.9 A for water samples and the sludge sample was divided into two and the results obtained are depicted on Figure 3.9 B. Figures showed successful extraction of gDNA from the samples as the bands appear above the 10 000 bp mark in relation to the gene ruler. The bands are faint with smears below them, indicating low concentrations, shearing and the low integrity of the DNA.

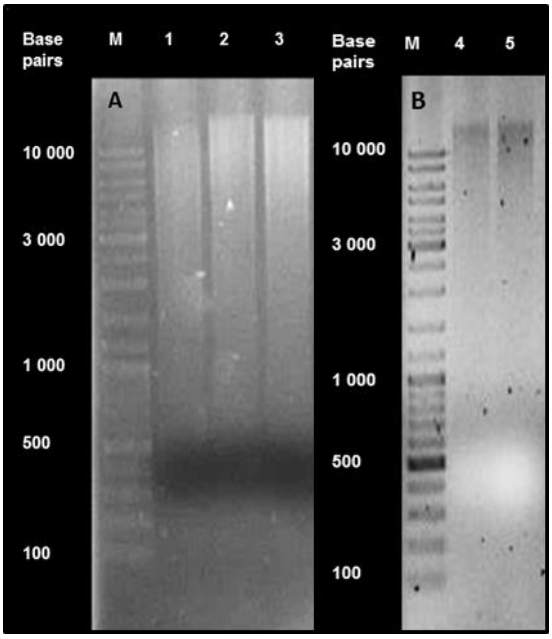

Figure 3.9: Genomic DNA extracts visualized on a 0.8% (w/v) agarose gel. A: representing the water samples and B: representing the two sludge samples.

C. Lane M: DNA standard Marker (O'GeneRuler^{TM} Ladder Mix), Lane 1: Site-Ex, Lane 2: Site-Ka and Lane 3: Site-Po.
D. Lane M: DNA standard Marker (O'GeneRuler^{TM} Ladder Mix), Lane 4: Sludge 1 and Lane 5: Sludge 2.

The extracted gDNA were further analysed to confirm the concentrations and to give indications of the purity using the NanoDrop spectrophotometer ND-1000 (NanoDrop Technologies, Wilmington, DE) and the obtained data is shown in Table 3.11. AMD water samples yielded low concentrations of the extracted gDNA possibly due to the low cellular concentrations in the samples compared to the sludge samples. The A_{260}/A_{280} absorbance ratio around 1.8 indicates low protein or RNA contamination and thus further processing could be done.

Table 3.11: Concentrations and purity rations of the extracted gDNA from raw samples.

Sample	[ng/µL]	A_{260}/A_{280}
Site-Ex	12.27	1.77
Site-Ka	38.61	1.43
Site-Po	100	1.86
Sludge 1	150	1.81
Sludge 2	142	1.91

3.4.3.2. Amplification of the partial 16S rRNA gene fragments

The amplification of the 16S rRNA fragment using 341F-GC and 907R primers with sequences outlined in Table 3.1 was performed according to the described method summarised in section 3.3.5.2. Already extracted gDNA of *Escherichia coli* culture was used as positive control. The samples were visualized on a 1% (w/v) agarose gel and results are shown in Figure 3.10. As expected, bacterial amplicons with band sizes of around 600 bp were obtained in all the samples irrespective of the low concentrations of gDNA extracted from the AMD samples.

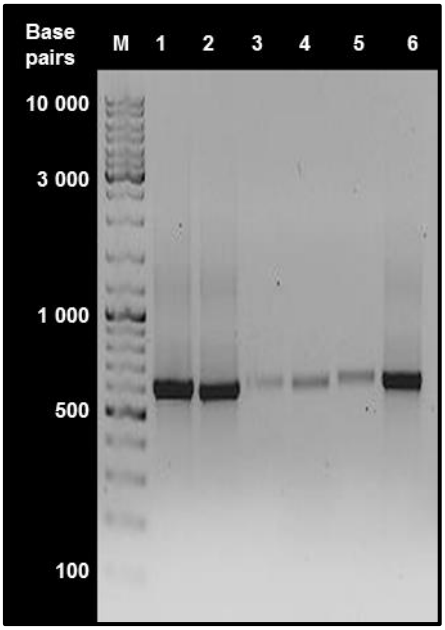

Figure 3.10: Amplification results of the partial 16S rRNA fragments from the extracted gDNA on a 1% (w/v) agarose gel. Lane M: DNA standard Marker (O'GeneRuler^{TM} Ladder Mix), Lane 1: Sludge 1, Lane 2: Sludge 2, Lane 3: Site-Ex, Lane 4: Site-Ka, Lane 5: Site-Po and Lane 6: Positive control.

3.4.3.3. Denaturation Gradient Gel Electrophoresis (DGGE) analysis

The microbial diversity in the samples were determined by the use of DGGE whereby the bacterial PCR products were loaded on to the DGGE gel prepared and resolved according to the procedure discussed in section 3.3.5.3. The DGGE gel was visualized under the Chem-Doc XRS (Biorad Laboratories) and the DGGE profiles are shown below in Figure 3.11.

Adrade and co-workers (2012) showed that each band resolved on a lane of DGGE represents a portion of the bacterial population (Adrade *et al*., 2012) thus displaying the diversity of the sample. From the profiles shown in Figure 3.11, it seems that the sludge, Site-Ex and Site-Po samples had diverse bacterial communities than in the Site-Ka water. It is also notable that the microbial diversity in the Site-Po water appears to be more similar to the microbial diversity in the Sludge sample from the same sampling location. The lower diversity in Site-Ka AMD could be due to the low pH and high Aluminium concentrations in the drainage. Most microorganisms are dictated by the environmental conditions for their survival while few adapt and thrive to grow and convert their metabolic activities to suit their survival strategies in the foreign habitats (Bond *et al*., 2000; Maleke *et al*., 2014). Thus, sequencing would reveal if the microbial communities in the samples are populations that can tolerate extremely low pH conditions and high metals concentrations.

The identification of the bacterial communities in the samples was done by excising the bands and processing them for sequencing as described in section 3.3.5.3 which involved the amplification of the DNA contained in each band and the amplified DNA were sequenced. The obtained sequences were subjected to BLAST analysis against the NCBI database to find the closest homologs similar to the microorganisms to identify the ones found in the respective samples under analysis. The BLAST results are shown in Table 3.12 with accession numbers (NO), descriptions of sequences and relational data of the obtained sequences and the hits from NCBI database (E-Value and Max ID %). The microbial identification indicated that there are bacteria capable of sulfate reduction in all samples, for example, the *Desulfovibrio* sp. known for their role in sulfate reduction and sulphide formation in most anaerobic environments.

Site-Ex defined to be a non-acid mine drainage, contained mainly two bacterial phylum: *Beta-Proteobacteria* and *Actinobacteria* from which the genes for *Acidovorax* sp. and *Rhodoluna* sp. respectively were detected. The two bacterial groups are mostly abundant in water and soil depending on organic matter for survival. Site-Ka contained *Clostridium* sp. as the most dominant bacteria that belong to the *Firmicutes* phylum and it has been reported to play a significant role in sulfate reduction and survive the harsh conditions like low pH and high metals

concentrations by making endospores which become active when environmental conditions are favourable for their growth. Site-Po revealed a more diverse bacterial community seen by more bands than the other two water samples. Interestingly, phylum *delta-Proteobacteria* genes were detected and represented by the *Desulfovibrio* sp. and *Desulfosporosinus* sp. which are well known sulfate-reducing bacteria. Additionally, phylum *Firmicutes* were also detected in Site-Po drainage displaying a wide range of diversity in the presence of high concentrations of heavy metals and low pH. The sludge sample revealed similar but less microbial diversity compared to the drainage from Site-Po even though the samples were collected from one site. In the sludge, genes representing one of the novel SRB, *Desulforudis* sp. together with other bacteria (*Thioalkalimicrobium* sp., *Bacillus* sp. and *Methanobrevibacter* sp) that can withstand extreme conditions were detected (Musingarimi *et al.,* 2010).

The difference in microbial communities in AMD and NMD showed that drainage characteristics affect the microbial existence in the water. The presence of SRB in the samples gives the microbial consortium in the wastewaters potential to be studied and used in bioremediation technologies to reduce sulfate and precipitate potential toxic metals in the mine waste waters as they have been previously used to treat toxic waste waters (Bond *et al.,* 2000). Since the microbial diversity studies confirmed the presence of SRB, enrichments was commenced in selected media.

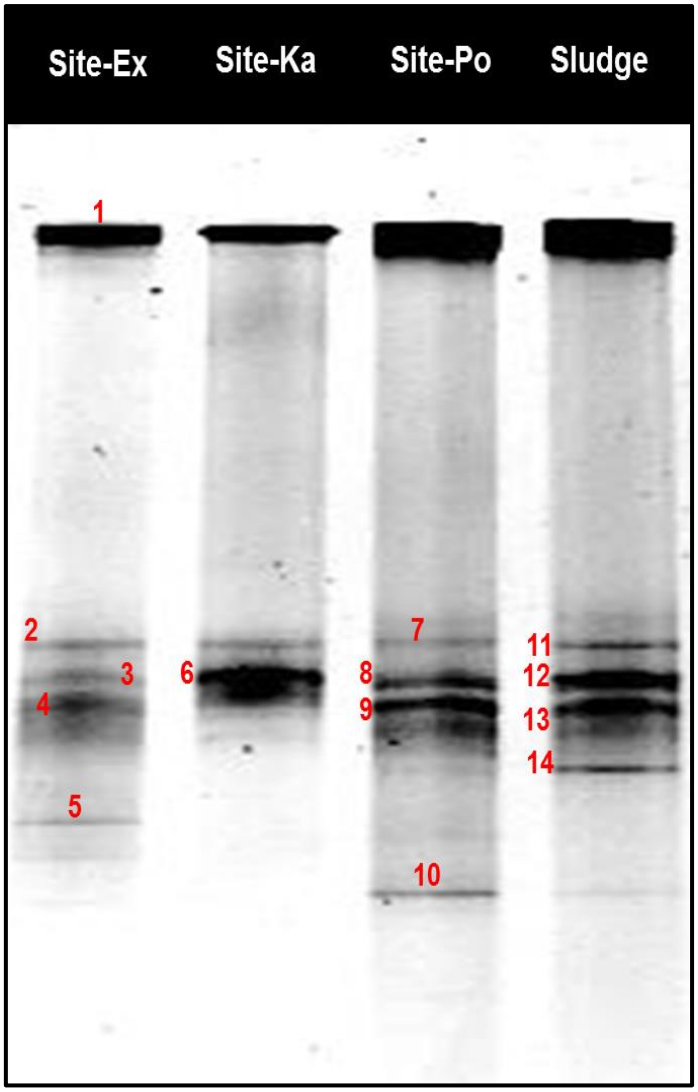

Figure 3.11: DGGE profile of the sludge and AMD water samples. Lane 1: Site-Ex, Lane 2: Site-Ka, Lane 3: Site-Po and Lane 4: Sludge sample.

Table 3.12: Sequencing results obtained from BLAST analysis for AMD water samples and the sludge sample

Band No	Accession No	Description	E-Value	Max ID %
1	FM992007.1	Uncultured *beta proteobacterium* partial 16S rRNA gene isolate DGGE band WETLE-3R	1.00E-85	78%
2	HE573224.1	Uncultured *beta proteobacterium* partial 16S rRNA gene, clone EJIR08 42	4.00E-65	73%
3	KF931153.1	*Acidovorax valerianelle* strain KACC 16998 16S ribosomal RNA gene, partial sequence	2.00E-64	72%
4	FR648015.1	Uncultured *actinobacterium* partial 16S rRNA gene, clone 4508-27F	0.00E+00	96%
5	CP007490.1	*Candidatus Rhodoluna lacicola* strain MWH-Ta8, complete genome	0.00E+00	98%
6	KJ957172.1	*Clostridium beijerinckii* strain NCP270 16S ribosomal RNA gene, partial sequence	3.00E-155	86%
7	GQ406188.1	Uncultured Firmicutes bacterium clone TS-42-4 16S ribosomal RNA gen, partial sequence	0	97%
8	EF520531.1	Uncultured *delta proteobacterium* clone ADK-BTh02-84 16S ribosomal RNA gene, partial sequence	6.00E-26	88%
9	AB908747.1	Uncultured *Desulfovibrio* sp. Gene for 16S ribosomal RNA, partial sequence, clone: 3CP(+)2_56	3.00E-24	87%
10	CP003108.1	*Desulfosporosinus orientis* DSM 765, complete genome	7.00E-24	79%
11	CP000002.3	*Bacillus licheniformis* ATCC 14580, complete genome	1	88%
12	CP001719.1	*Methanobrevibacter ruminantium* M1, complete genome	1.3	96%
13	CP002776.1	*Thioalkalimicrobium cyclinum* ALM1, complete genome	5.2	88%
14	NR_075067.1	*Candidatus Desulforudis audaxviator* MP104C strain MP104C 16S ribosomal RNA, complete sequence	3.00E-07	78%

3.4.4. Microbial enrichments results

3.4.4.1. Results analysis of the anaerobic enrichments

Enrichments for SRB were done as discussed in section 3.3.6. The Postgate medium (PSGM) and the Anaerobic Sulfate-Reducing Medium (ASRM) were successfully used to enrich SRB. Both media were used anaerobically for the acclimation process of SRB containing consortia in three phases as described in sections 3.3.6.2; 3.3.6.3 and 3.3.6.4. The anaerobic cultures were enriched and the third generation cultures were subjected to microscopic, molecular and chemical analysis. The media changed colour in the vials as observed in Figure 3.12 due to the growing bacteria on the supplied carbon source in the media and also indicating the sulfate reduction process identified by a black colour (Jenčárová and Luptáková, 2011). The black colour was described as a chemical product of biogenic hydrogen sulfide (H_2S) and dissolved metals (Me^{2+}) like iron, zinc, copper and lead as summarised in equation 3.4 and 3.5 (Jenčárová and Luptáková, 2011).

Equation 3.4: $2CH_2O + SO_4^{2-} \leftrightarrow 2H_2CO_3 + H_2S$

Equation 3.5: $H_2S + Me^{2+} \rightarrow MeS_{\downarrow} + 2H^+$

The gas emitted from all the closed vials had characteristics of a rotten egg smell indicating the production of the hydrogen sulfide gas as another confirmation sign of sulfate reduction (Abd-El-Malek and Rizk, 1958; Ghazy *et al.,* 2011; Al Tamimi, 2011). After 20 days of incubation period, from the tertiary cultures, 2 mL was harvested from each culture and cryopreserved in 40% sterile glycerol as described under section 3.3.6.8 and the remaining samples were subjected to microscopic, molecular and further downstream studies.

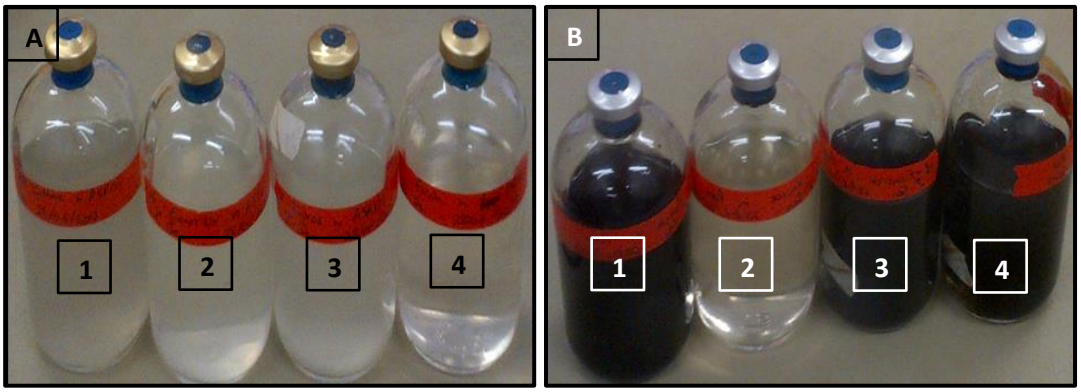

Figure 3.12: Tertiary anaerobic enrichment cultures in both ASRM and PSGM. A1: Sludge in ASRM, A2: Site-Ex in ASRM, A3: Site-Ka in ASRM and A4: Site-Po in ASRM. B1: Sludge in PSGM, B2: Site-Ex in PSGM, B3: Site-Ka in PSGM and B4: Site-Po in PSGM.

3.4.4.2. Microbial characterization of tertiary enrichment cultures

Microscopic analysis was done on the tertiary cultures as described in section 3.3.6.5 for gram staining, DAPI staining and Live/Dead staining. Figure 3.13 depicts gram staining results (A – H), DAPI staining (I – L) and Live/Dead staining (M – P). The cultures enriched from the AMD water samples, seemed to have adapted well as most of the microorganisms were still viable after the 20 days of incubation period. Microbial cells enumeration could not be done due to the precipitates that had formed in the media and their interaction with the cells.

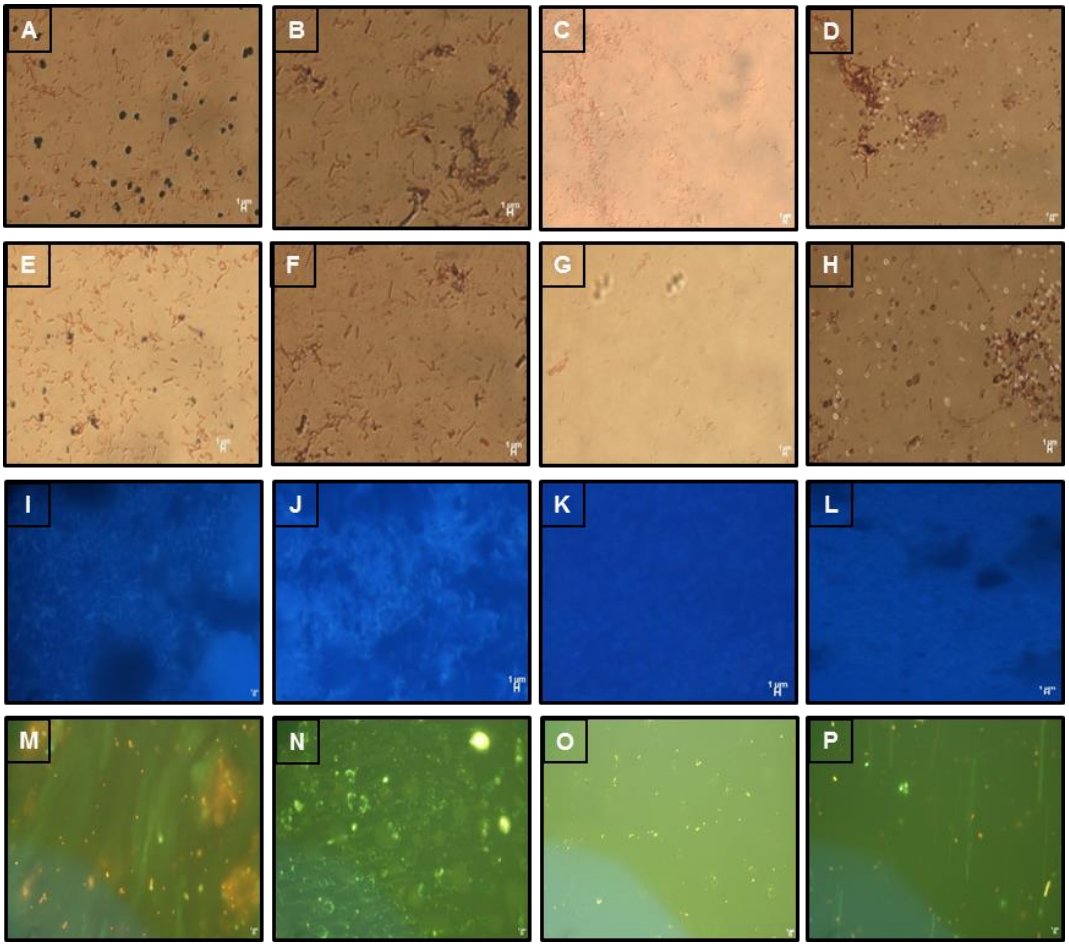

Figure 3.13: Microscopic analysis results of tertiary enrichment cultures. A-D: Gram staining (PSGM). A: Sludge in PSGM, B: Site-Ex in PSGM, C: Site-Ka in PSGM and D: Site-Po in PSGM.
E-H: Gram staining (ASRM). E: Sludge in ASRM, F: Site-Ex in ASRM, G: Site-Ka in ASRM and H: Site-Po in ASRM.
I-L: DAPI staining. I: Sludge in PSGM, J: Site-Ex in PSGM, K: Site-Ka in PSGM and L: Site-Po in PSGM.
M-P: Live/Dead staining. M: Sludge in PSGM, N: Site-Ex in PSGM, O: Site-Ka in PSGM and P: Site-Po in PSGM. Scale bar = 1 µm.

3.4.5. Molecular analysis of the enriched tertiary cultures

3.4.5.1. Genomic DNA extraction of the tertiary enrichment cultures

The genomic DNA was extracted as described in section 3.3.6.6 from the tertiary cultures. The concentrations and purity of the gDNA were determined by the NanoDrop and the results obtained from the analysis are outlined in in Table 3.13

revealing average gDNA concentrations around 50 ng/µL and the A_{260}/A_{280} absorbance ratios were mostly around 1.8. The Site-Po (sludge and AMD) samples, Site-Ka sample enriched in PSGM and Site-Ex sample enriched in ASRM resulted in low gDNA concentrations and the absorbance A_{260}/A_{280} rations in these samples were also lower than 1.8. That could be an indication of minimal protein and or RNA in the samples.

Table 3.13: Concentrations of extracted gDNA from the tertiary cultures.

Sample	**[ng/µL]**	**A_{260}/A_{280}**
Sludge in PSGM	56.4	1.87
Sludge in ASRM	97.44	1.88
Site-Ex in PSGM	82.65	1.96
Site-Ex in ASRM	28.31	1.75
Site-Ka in PSGM	6.05	1.28
Site-Ka in ASRM	53.78	1.89
Site-Po in PSGM	3.66	1.38
Site-Po in ASRM	3.92	1.56

3.4.5.2. Amplification results of the partial 16S rRNA fragments from the enrichments gDNA

The gDNA extracts were subjected to 16S rRNA fragment amplification as described in section 3.3.6.6 and the resulting PCR products were visualized on a 1% (w/v) agarose gel stained with ethidium bromide (Figure 4.14). The expected band sizes of approximately 600 bp were obtained in all the samples which showed the successful partial amplification of the 16S rRNA fragments. The faint bands above the bands of interest may be due to non-specific binding.

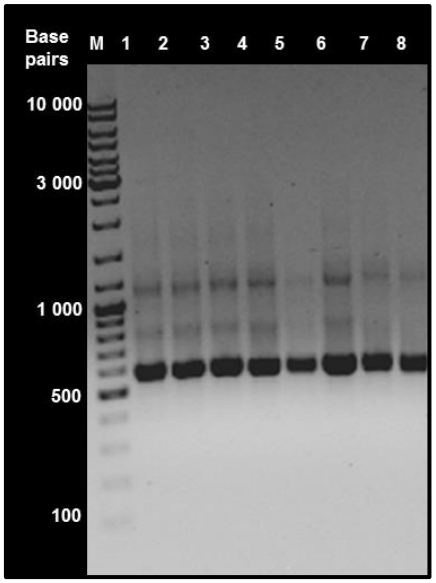

Figure 3.14: Amplification results of the partial 16S rRNA fragments from the extracted gDNA of tertiary cultures on a 1% (w/v) agarose gel. Lane M: DNA standard Marker (O'GeneRuler^{TM} Ladder Mix), Lane 1: Sludge in PSGM, Lane 2: Sludge in ASRM, Lane 3: Site-Ex in PSGM, Lane 4: Site-Ex in ASRM, Lane 5: Site-Ka in PSGM, Lane 6: Site-Ka in ASRM, Lane 7: Site-Po in PSGM and Lane 8: Site-Po in ASRM.

3.4.5.3. Denaturation Gradient Gel Electrophoresis (DGGE) analysis of the enriched cultures

The positive amplicons of the 16S rRNA fragments were subjected to DGGE analysis to study the diversity of the enriched cultures according to the procedure described in section 3.3.6.6. The DGGE profiles depicted in Figure 3.15 revealed a distinct microbial diversity enriched in the tertiary cultures which appeared to be more complex diversity with higher number of bands compared to DGGE profile for the raw AMD and sludge samples discussed in section 3.4.3.3. To identify the microbial communities in the enriched cultures, the visible (numbered) bands were excised and processed for sequencing as discussed under section 3.3.6.6. The sequences acquired were blasted against NCBI database and the results of the microbial groups were listed on Table 3.14. The data revealed high maximum identity percentages with low e-values confirming the presence of detected SRB in the enriched cultures. This served as a confirmation that the enrichment and acclimation processes were successful.

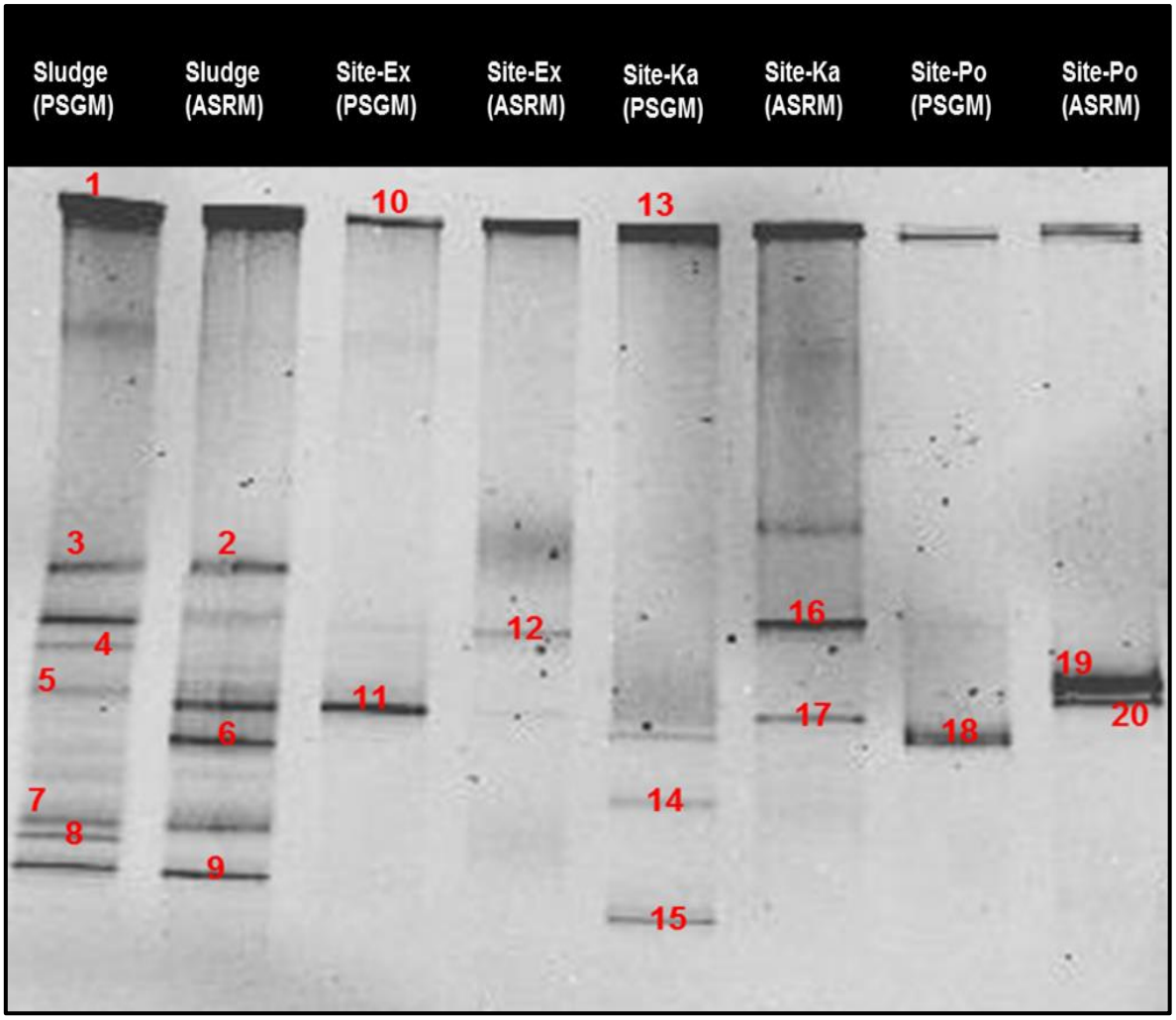

Figure 3.15: DGGE profile of tertiary cultures enriched in ASRM and PSGM. Lane 1: Sludge in PSGM, Lane 2: Sludge in ASRM, Lane 3: Site-Ex in PSGM, Lane 4: Site-Ex in ASRM, Lane 5: Site-Ka in PSGM, Lane 6: Site-Ka in ASRM, Lane 7: Site-Po in PSGM and Lane 8: Site-Po in ASRM.

Table 3.14: Sequencing results obtained from BLAST algorithm for tertiary enrichment samples from DGGE analysis.

Band No	Accession No	Description	E-Value	Max ID %
1	DQ677015.1	Iron-Reducing enrichment clone CL-W2 clone Cl-W2 16S ribosomal gene, partial sequence	1.00E-164	85%
2	X97852.1	*Anerofilum pentosovorans* strain Fae 16S ribosomal RNA gene, partial sequence	0	99%
3	NR_029315.1	*Anaerofilum agile* strain F 16S ribosomal RNA, partial sequence	0	99%
4	DQ852338.1	*Clostridium* sp. D3RC-2 16S ribosaml RNA gene, partial sequence	0	99%
5	NR_116427.1	*Desulfitobacterium aromaticivorans* strain UKTL 16S ribosomal RNA gene sequence	0	82%
6	NR_075068.1	*Desulfotomaculum kuznetsovii* strain DSM 6115 16S ribosomal RNA gene, complete sequence	0	88%
7	HM043272.1	Uncultured *Desulfovibrio* sp. clone MFC-19 16S ribosomal RNA gene, partial sequence.	2.00E-44	85%
8	NR_114608.1	*Sphaerochaeta globalas* strain Buddy 16S ribosomal RNA, partial sequence.	0	100 %
9	NR_026480.1	*Desulfovibrio sulfodismutans* strain ThAcO1 16S ribosomal RNA gene, partial sequence.	0	100 %
10	NR_044640.1	*Desulfiacinum infernum* strain BalphaG1 16S ribosomal RNA gene, complete sequence.	1.00E-26	73%
11	HE856418.1	Uncultured *Firmicutes* bacterium partial 16S rRNA gene, clone 2012NU-1-20	6.00E-06	95%
12	GU370098.1	*Clostridium* sp. P530(3) 16S ribosomal RNAgene, partial sequence.	0.00E+00	98%
13	JN038619.1	Uncultured Firmicutes bacterium clone MA-R45	3.00E-	71%

		16S ribosomal RNA gene, partial sequence	58	
14	CP000943.1	*Methylobacterium* sp. 4-46, complete genome	2.20E+00	91%
15	AJ229241.1	*Actinobacteria* from anoxic bulk soil 16S rRNA gene(strain PB90-5)	0.00E+00	99%
16	KC821442.1	*Methanogenic* prokaryote enrichment culture B31_3_86 16S ribosomal RNA gene, partial sequence	0.00E+00	95%
17	FN669637.1	Uncultured Firmicutes bacterium partial 16S rRNA gene, isolate DGGE band SP_MBR3	0.00E+00	98%
18	JX473121.1	Uncultured *Sphingobacteria* bacterium clone URO92.C09 16S ribosomal RNA gene, partial sequence	0	86%
19	AF361187.1	*Flexibacter* sp. CF 1 16S ribosomal RNA gene, partial sequence	5.00E-63	97%
20	JN656858.1	Uncultured *Bacteroidetes* bacterium clone KWK12S.25 16S ribosomal RNA gene, partial sequence	4.00E-14	81%

3.4.5.4. Amplification results of the *dsr* gene fragments from the extracted gDNA

From the genomic DNA extracted from the tertiary cultures, *dsr* gene fragment which is conserved in SRB was amplified using gene specific primers (DSR1F and DSFR4R) as described in section 3.3.6.7. Samples selected for PCR amplification were based on the higher concentrations of gDNA according to the NanoDrop results. From the drainage samples enrichments in ASRM and PSGM, one gDNA sample with high concentration was used whereas both sludge gDNA samples were subjected to PCR amplification of *dsrAB* gene fragments. Five gDNA samples were selected for PCR amplification, three drainage samples (Site-Ex in PSGM, Site-Ka in PSGM and Site-Po in ASRM) were selected and both sludge enrichments samples

(Sludge in PSGM and Sludge in ASRM). The PCR products were loaded on to a 1% (w/v) agarose gel stained with ethidium bromide. The PCR products depicted in Figure 3.16 A, showed multiple bands rather than a single band with expected size of 1900 base pairs. Gradient PCR was done on the sludge enrichments gDNA to optimize the annealing temperature for the primers to amplify the gene of interest. Gradient PCR results depicted in Figure 3.16 B, revealed the optimum annealing temperature to be towards 60ºC as seen by intense single bands of the expected band size. The intense bands where observed under the sludge sample enriched in PSGM suggesting the optimum expression of the target gene. Faint bands were observed for the sludge sample enriched in ASRM showing the possibility of low *dsr* gene expression in ASRM. Successful amplification of the *dsrAB* gene fragments confirmed the presence of SRB in the enriched consortium.

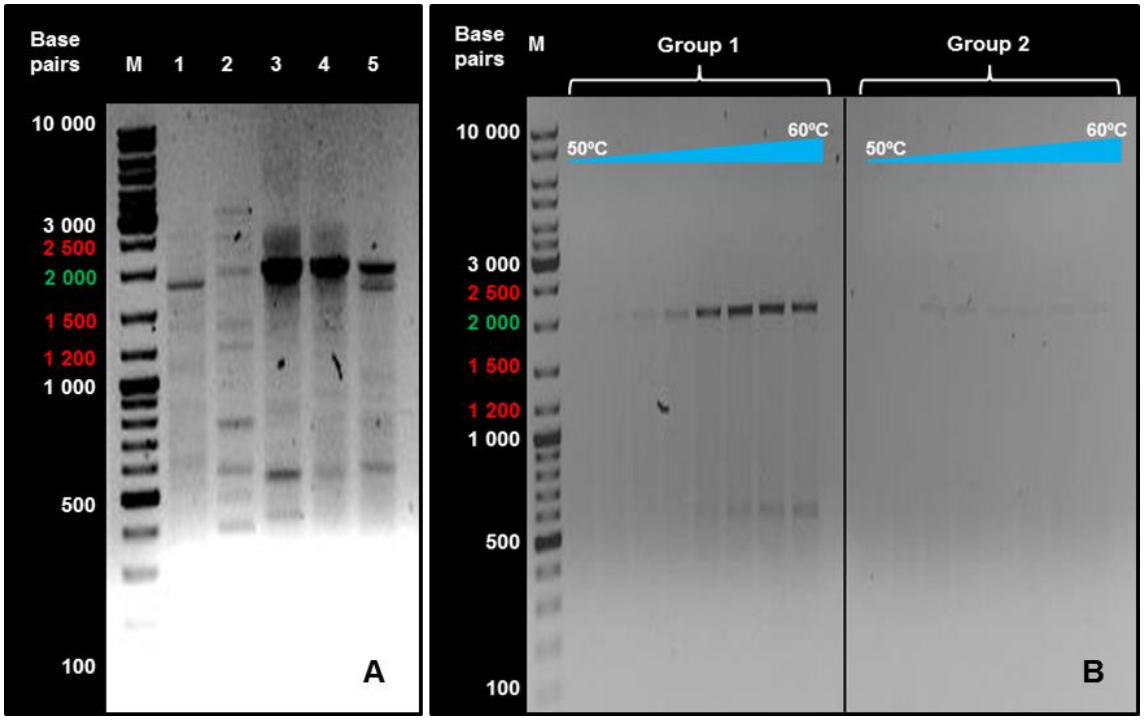

Figure 3.16: Amplification results of the *dsrAB* gene fragments on 1% agarose gels.
A: PCR products of the *dsrAB* gene fragments. Lane M: DNA standard Marker (O'GeneRuler™ Ladder Mix), Lane 1: Site-Ex in PSGM, Lane 2: Site-Ka in PSGM, Lane 3: Sludge in PSGM, Lane 4: Sludge in ASRM, Lane 5: Site-Po in ASRM.
B: Gradient PCR amplification of the *dsrAB* gene fragments from sludge samples. Lane M: DNA standard Marker (O'GeneRuler™ Ladder Mix), Group 1 Lanes: Sludge in PSGM and Group 2 Lanes: Sludge in ASRM.

3.4.5.5. Scanning Electron Microscopy analysis of the enriched cultures

The precipitates and associated biofilms were analysed by scanning electron microscopy to visualize the metal-microbe interactions. The sample preparations were done as described in section 3.3.6.9. The SEM micrographs shown in Figure 3.17 revealed that the biofilms of the enriched cultures were closely associated with the precipitates. The bacterial cells appeared to have various shapes and sizes. Figure 3.17 A, B and C shows the enriched microbial cells coated with gold enriched in PSGM and captured at high magnification ranging between 12 000 x to 20 000 x magnification. Figure 3.17 D was captured at 6 000 x magnification and shows clear bacterial cells enriched in ASRM displaying a biofilm surrounding particles like precipitates. These results are similar to what Gilmour and co-workers (2011) reported during their studies to isolate SRB. By visual observations, the circled bacterial cell on Figure 3.17 C looks similar in shape (vibrio) and size (approximately 2 µm) to the *Desulfovibrio* sp. depicted on Figure 3.17 I reported by Warthmann and co-workers (2005) and similarly by Gilmour and co-workers (2011). Figure 3.17 E, F and G shows the carbon coated samples viewed under the Secondary Back Scattering (SBSE) mode which allowed the release of high energy electrons to the surface of the sample and from the sample, the electrons were scattered to the detector for the generation of the micrograph. The images were captured at 50 000 Volts (50 kV) at the magnification ranging between 400 x to 5 000 x magnification and the captured images showed clear morphologies of the precipitates. Particles observed in Figures 3.17 E and F from the culture enriched in PSGM have been previously observed (depicted in Figure 3.17 H) and were identified as pyrite by Larrasoaña and co-workers (2014). Figure 3.17 G, captured at 5 400 x magnification from the culture enriched in ASRM, depicts white and smaller particles which are different compared to the ones observed in Figure 3.17 E and F. The white small particles were also observed by Wang and co-workers in 2014 and identified the particles as sphalerite (ZnS_2) precursors (Wang *et al*., 2014). The various precipitates observed during the SEM analysis suggest that the enriched bacteria might be able to precipitate the metals as the samples contained various metals

previously detected by ICP-MS analysis. The presence of SRB species identified by DGGE analysis confirmed the bio-mineralization processes and specifically the formation of metallic sulfide such as pyrite and sphalerite observed in our samples.

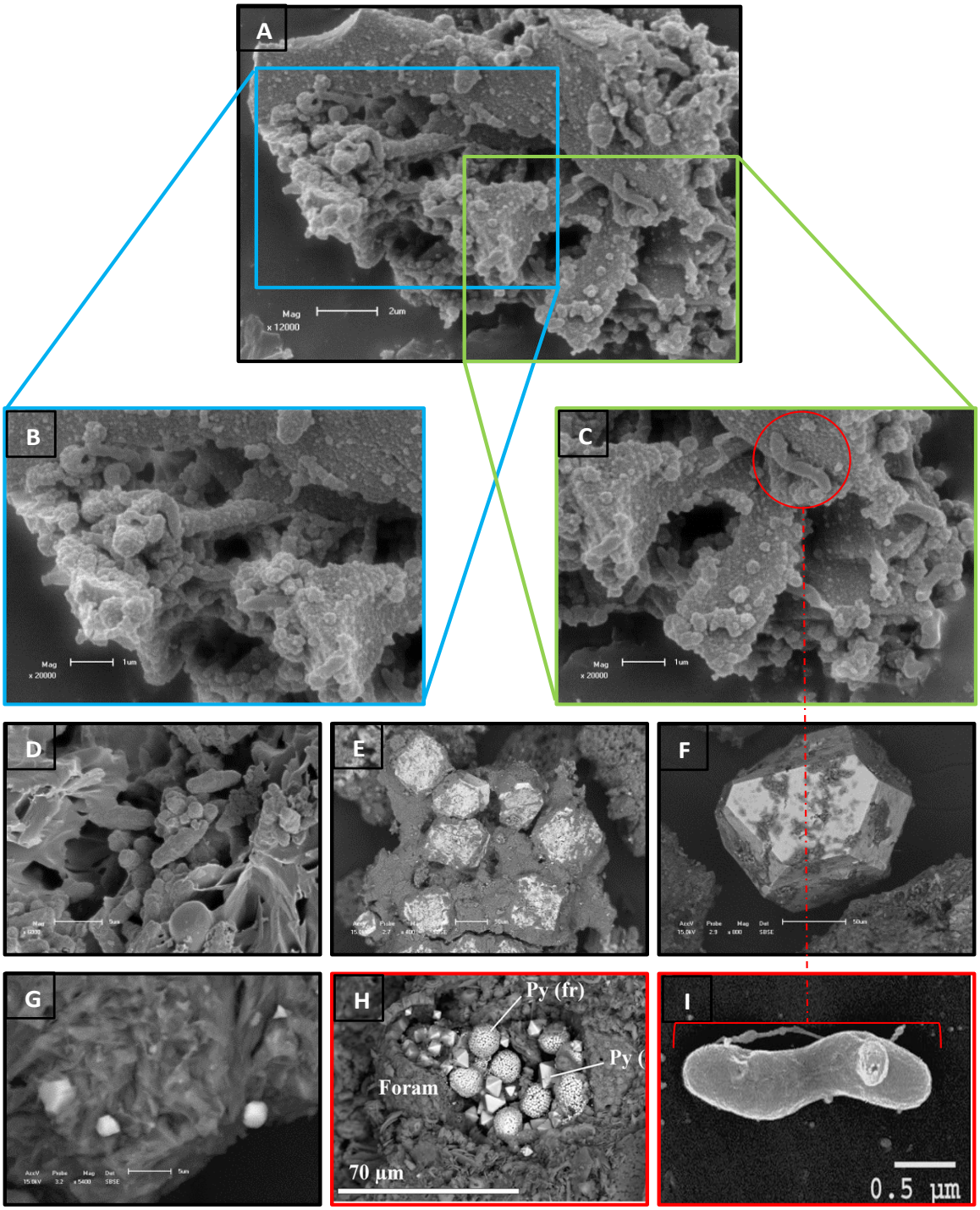

Figure 3.17: Scanning Electron Microscope image showing biofilm and precipitates formed in the tertiary enrichment cultures. A: Biofilm enriched in PSGM, B and C: Higher magnification of subsections of A, D: Biofilm enriched in ASRM, E and F: Back Scattering images of precipitates in culture enriched in PSGM, G: Back Scattering images of precipitates in culture enriched in ASRM, H: Reference image of Pyrite precipitates (Taken from Larrasoaña *et al*., 2014), I: Reference image of the *Desulfovibrio* sp. (Taken from Warthmann *et al.,* 2005).

3.5. Conclusions

The mine drainages collected from the three study sites: Site-Ex, Site-Ka and Site-Po showed different physiochemical characteristics including various metals concentrations and different microbial cells concentrations and diversities. The drainage from samples from Site-Ka and Site-Po with hydro-geochemical characteristics typically of AMD (high metals and sulfate concentrations and low pH) resulted in lower cell counts estimated to be 5.7 x 10^2 and 4.0 x 10^2 cells/mL, respectively. Under these conditions, bacterial cells form biofilms in the sediments which protects the existence of the bacteria in toxic environments. This was confirmed by the elevated number of cells in the sediment from Site-Po which had approximately 2.4 x 10^5 cells/mL. Site-Ex had the highest cell counts (5.0 x 10^3 cells/mL) compared to the other drainages and this was due to the hydro-chemical characteristics typically of NMD (alkaline pH, low metals and high sulfate concentrations). These conditions probably promoted bacterial growth including SRB. Bacterial cells in all sample were detected to be viable and therefore, culturable.

Two media compositions (ASRM and PSGM) were used for the enrichment of SRB and PSGM was found to be effective with easier detection of SRB growth. Bacteria growing in PSGM yielded a black colour due to the chemical reaction of iron and biogenic sulfide which also resulted in precipitates that were visually identified as pyrite and sphalerite precursors which are known to be biologically formed indirectly by the SRB activity. Molecular analysis of the enrichment cultures revealed unique microbial diversities from each drainage. All samples had dominant species of SRB such as *Desulfitobacterium* sp., *Desulfotomaculum* sp., and *Desulfovibrio* sp. as well as methanogenic bacteria, iron reducing bacteria and various firmicutes species.

The presence and successful enrichments of consortium containing SRB predicts that the cultures can be applied in bioremediation processes to reduce sulfate and indirectly precipitate metals by biogenic hydrogen sulfide. However, more tests are required to test the microbial activity and tolerance of SRB at different environmental conditions such as varied temperatures, pH ranges and metals concentrations. Even though the metal precipitates were visually identified, their chemical composition were required to accurately determine if the precipitates were biogenic as speculated

or phase minerals of chemical reactions of other metals besides metal sulfides. The subsequent chapter deals with mainly microbial sulfate reduction kinetics and application of the enriched consortia containing SRB in bioreactors containing varied growth conditions.

3.6. References

- **Abd-El-Malek, Y. and Rizk, S.G.** (1958) Counting of Sulphate-reducing Bacteria in Mixed Bacterial Populations. *Nature* **182:** 538
- **Adrade, L., Leite, D.C.A., Ferreira, L.G., Paula, G.R., Maguire, M.J., Hubert, C.R.J., Peixoto, R.S., Domingues, R.M.C.P. and Rosado, A.S.** (2012) Microbial diversity and anaerobic hydrocarbon degradation potential in an oil-contaminated mangrove sediment. *BioMedical Central Microbiology* **12:** 1 – 10.
- **Al Tamimi, W. H. A. S.** (2011) Activity of sulphate reducing bacteria isolated from Shatt Al Arab water on corrosion mild steel specimens *in vitro*. *Marsh Bulletin* **6(2):** 178 – 158.
- **Ammann, A.A.** (2007) Inductively coupled plasma spectrometry (ICP MS): a versatile tool. *Journal of Mass Spectrometry* **42:** 419 – 427.
- **Atkins, A. S. and Pooley, F. D.** (1982) The effect of bio-mechanism on acidic mine drainage in coal mining. *International Journal of Mine Water* **1:** 31 – 44.
- **Baker, B. J., Hugenholtz, P., Dawson, S. C. and Banfield, J. F.** (2003a) Extremely acidophilic protists from acid mine drainages host *Rickettsiales*-lineage endosymbionts that have intervening sequences in their 16S rRNA genes. *Applied and Environmental Microbiology* **69 (9):** 5512 – 5518.
- **Baker, B.J., Moser, D.P., MacGregor, B.J., Fishbain, S., Wagner, M., Fry, N.K., Jackson, B., Speolstra, N., Loos, S., takai, K., Lollar, B.S., Fredrickson, J., Balkwill, D., Onstoff, T.C., Wimpee, C.F. and Stahl,D.A.** (2003b) Related assemblages of sulphate-reducing bacteria associated with ultra-deep gold mines of South Africa and deep basalt aquifers of Washington State. *Environmental Microbiology*. **5:** 267-277.
- **Banks, D., Parnachev, V. P., Frengstad, B., Holden, W., Vedernikov, A. A. and Karnachuk, O. V.** (2002) Alkaline mine drainage from metal sulphide and coal mines: examples from Svalbard and Siberia. *Geological Society, London, Special Publications* **198:** 287 – 296.
- **Barton, L. L. and Fauque, G. D.** (2009) Chapter 2 Biochemistry, physiology and biotechnology of sulfate-reducing bacteria. *Advances in Applied Microbiology* **68:** 41 – 98.

- **Berney, M., Hammnes, F., Bosshard, F., Weilenmann, H.U. and Egli, T.** (2007) Assessing and interpreting bacterial viability using LIVE/DEAD® BacLight™ kit in combination with flow cytometry. *Applied and Environmental, Microbiology* **73(10):** 3283 – 3290.
- **Bond, P. L., Druschel, G. K. and Banfield, J. F.** (2000) Comparison of acid mine drainage microbial communities in physically and geochemically distinct ecosystems. *Applied and Environmental Microbiology* **66(11):** 4962 – 4971.
- **Boulos, L., Prèvost, M., Barbeau, B., Coallier, J. and Desjardins, R.** (1999) LIVE/DEAD® *Bac*Light™: application of a new rapid staining method for direct enumeration of viable and total bacteria in drinking water. *Journal of Microbiological Methods* **37:** 77 – 86.
- **Chandra, T. J. and Mani, P. S.** (2011) A study of 2 rapid tests to differentiate Gram positive and Gram negative aerobic bacteria. *Journal of Medical & Allied Science* **1(2):** 84 – 85.
- **Dar, S. A., Kuenen, J. G. and Muyzer, G.** (2005) Nested PCR-denaturing gel electrophoresis approach to determine the diversity of sulfate-reducing bacteria in complex microbial communities. *Applied and Environmental Microbiology* **71(5):** 2325 – 2330.
- **Dar, S. A., Yao, L., van Dogen, U., Kuenen, J. G. and Muyzer, G.** (2006) Analysis of diversity and activity of sulfate-reducing bacterial communities in sulfidogenic bioreactors using 16S rRNA and *dsrB* genes as molecular markers. *Applied and Environmental Microbiology* **73:** 594 – 604.
- **Davies, D. A., Anderson, G.K., Beveridge, T. J. and Clark, H. C.** (1983) Chemical mechanism of the Gram stain and synthesis of a new electron-opaque marker for electron microscopy which replaces the iodine mordant of the stain. *Journal of Bacteriology* **156(2):** 837 – 845.
- **Fonselius, S., Dyrssen, D. and Yhlen, B.** (1999) Determination of hydrogen sulphide. In Methods of Seawater Analysis. Eds: Grasshoff K, Kremling K, Ehrhardt M. Wiley-VCH, Weinheim, New York, Chichester, Brisbane, Singapore, Toronto. 1999; pp. 91-108.
- **Fraçkowiak, D. and Rabinowitch, E.** (1996) The methylene blue-ferrous iron reaction in a two-phase system[1]. *The Journal of Physical Chemistry* **70(9):** 3012 – 3014.

- **Ghazy, E. A., Mahmound, M. G., Asker, M. S., Mahmound, M. N., Abo Elsoud, M. M. and Abdel Sami, M. E.** (2011) Cultivation and detection of sulfate reducing bacteria (SRB) in sea water. *Journal of American Science* **7(2):** 604 – 608.
- **Gilmour, C. C., Elias, D. A., Kucken, A. M., Brown, S. D., Palumbo, A. V., Schadt, C. W. and Wall, J. D.** (2011) Sulfate-reducing bacterium *Desulfovibrio desulfuricans* ND132 as a model for understanding bacterial mercury methylation. *Applied and Environmental Microbiology* **77(12):** 3938 – 3951.
- **Hazen, J. M., Williams, M. W., Stover, B. and Wireman, M.** (2002) Characterization of acid mine drainage using a combination of hydrometric, chemical and isotopic analyses, Marry Murphy mine, Colorado. *Environmental Geochemistry and Health* **24:** 1 – 22.
- **Hedin, R.** (2008) Iron removal by a passive system treating alkaline coal Mine drainage. *Mine Water Environment Journal* **27:** 200 – 209.
- **Jenčárová, J. and Luptáková, A.** (2011) The effect of preparation of biogenic sorbent on zinc sorption.
- **Johnson, D. B. and Hallberg, K. B.** (2005) Acid mine drainage remediation options: a review. *Science of the Total Environment* **338:** 3 – 14.
- **Jong, T. and Parry, D. L.** (2006) Microbial sulfate reduction under sequentially acid conditions in an upflow anaerobic packed bed bioreactor. *Water Research* **40:** 2561 – 2571.
- **Kaksonen, A.H., Franzman, D.P. and Puhakka, J.A.** (2003) Performance and ethanol oxidation kinetics of a sulphate-reducing fluidized-bed reactor treating acidic metal-containing wastewater. *Biodegradation* **14:** 207 – 217.
- **Karr, E. A., Sattley, W. M., Rice, M. R., Jung, D. O., Madigan, M. T. and Achenbach, L. A.** (2005) Diversity and distribution of sulfate-reducing bacteria in permanently frozen lake Fryxell, McMurdo dry valleys, Antarctica. *Applied and Environmental Microbiology* **71(10):** 6353 – 6359.
- **Kepner, R. L. and Pratt, J. R.** (1994) Use of fluorochromes for direct enumeration of total bacteria in environmental samples: Past and present. *Microbiological Reviews* **58:** 603 – 615.

- **Küsel, K.** (2003) Microbial cycling of iron and sulfur in acidic coal mining lake sediments. *Water, Air, and Soil Pollution* **3:** 67 – 90.
- **Larrasoaña, J.C., Liu, Q., Hu, P., Roberts, A.P., Mata, P., Civis, J., Sierro, F.J. and Pérez-Asensio, J. N.** (2014) Paleomagnetic and paleoenvironmental implications of magnetofossil occurrences in late Miocene marine sediments from the Guadalquivir Basin, SW Spain. *Frontiers in Microbiology* **5(71):** 1 – 15.
- **Leloup, J., Quillet, L., Berthe, T. and Petit, F.** (2006) Diversity of the *dsrAB* (dissimilatory sulphite reductase) gene sequences retrieved from two contrasting mudflats of the Seine estuary, France. *Federation of European Microbiological Societies* **55:** 230 – 238.
- **Lin, C., Larsen, E. I., Nothdurft, L. D. and Smith, J. J.** (2012) Neutrophilic, Microaerophilic Fe(II)-Oxidizing bacteria are ubiquitous in aquatic habitats of a subtropica; Australian coastal catchment (ubiquitous FeOB in catchment aquatic habitats). *Geomicobiology Journal* **29:** 76 – 87.
- **Maleke, M., Williams, P., Castillo, J., Botes, E., Ojo, A., DeFlaun, M. and van Heerden, E.** (2014) Optimization of a bioremediation system of soluble uranium based on the biostimulation of an indigenous bacterial community. *Environmental Science and Pollution Research* (DOI 10.10017/s11356-014-3980-7).
- **Marinin, L., Saldi, G., Cipolli, F., Ottonello, C. and Zucconlini, V**. (2003). Geochemistry of water discharges from the Libiola mine, Italy. *Geochemical Journal.* **37:** 199-216.
- **McCarthy, S.** (2011) The impact of acid mine drainage in South Africa. *South African Journal of Science* 107(5/6), Art. #712, 7 pages. Doi:10.4102/sajs.v107i5/6.712.
- **Mühling, M., Woolven-Allen, J., Murrell, J. C. and Joint, I.** (2008) Improved group-specific PCR primers for denaturing gel electrophoresis analysis of the genetic diversity of complex microbial communities. *International Society for Microbial Ecology* **2:** 379 – 392.
- **Murr, L. E.** (1980) Theory and practice of copper sulphide leaching in dumps and in-situ. *Minerals Science Engineering* **12(3):** 121 – 189.

- **Musingarimi, W., Tuffin, M. and Cowan, D.** (2010) Characterisation of the arsenic resistance genes in *Bacillus* sp. UWC isolated from maturing fly ash acid mine drainage neutralised solids. *South African Journal of Science* **106(17):** 1 – 5.
- **Muyzer, G. and Stams, A. J.** (2008) The ecology and biotechnology of sulphate-reducing bacteria. *Nature reviews Microbiology* **6:** 441 – 454.
- **Muyzer, G., De Waal, E. C. and Uitterlinden, A. G.** (1993) Profiling of complex microbial populations by denaturing gradient gel electrophoresis analysis of polymerase chain reaction-amplified genes coding for 16S rRNA. *Applied and Environmental Microbiology* **59(3):** 695 – 700.
- **Naicker, K., Cukrowska, E. and McCarthy, T. S.** (2003) Acid mine drainage arising from gold mining activities in Johannesburg, South Africa and environs. *Environmental Pollution* **122(1):** 29 – 40.
- **Nakagawa, T., Ishibashi, J. I., Maruyama, A., Yamanaka, T., Morimoto, Y., Kimura, H., Urabe, T. and Fukai, M.** (2004) Analysis of dissimilatory sulfite reductase and 16S rRNA gene fragments from deep-sea hydrothermal sites of the Suiyo seamount, Izu-Bonin Arc, Western Pacific. *Applied and Environmental Microbiology* **70:** 393 – 403.
- **Nercessian, O., Bienvenu, N., Moreira, D., Prieur, D. and Jeanthon, C.** (2005) Diversity of functional genes of methanogens, methanotrophs and sulfate reducers in deep-sea hydrothermal environments. *Environmental Microbiology* **7(1):** 118 – 132.
- **Nies, D. H.** (1995) Iron efflux systems involved in bacterial metal resistance. *Journal of Industrial Microbiology and Biotechnology* **14(2):** 186 – 199.
- **Nies, D. H.** (1999) Microbial heavy-metal resistance. *Applied Microbiology* **51(6):** 730 – 750.
- **Park, E. Y.,** (2004) Recent progress in microbial cultivation techniques. *Advances in Biochemical Engineering* **90:** 1 – 33.
- **Perry, S. F.** (1995) Freeze-drying and cryopreservation of bacteria. *Methods in Molecular Biology* **38:** 21 – 30.
- **Postgate, J.R.** (1984) The sulphate-reducing bacteria, 2nd Edition. Cambridge University Press, UK.

- **Rozak, D. A. and Rozak, A. J.** (2008) Simplicity, function, and legibility in an enhanced ambigraphic nucleic acid notation. *Bio Techniques* **44:** 811 – 813.
- **Sakamoto-Arnold, C. M., Johnson, K. S. and Beehler, C. L.**(1986) Determination of hydrogen sulfide in seawater using injection analysis and flow analysis. *American Society of Limnology and Oceanography* **31(4):** 894 – 900.
- **Sánchez España, J., López Pamo, E., Santofimia, E., Aduvire, O., Reyes, J. and Barettino, D.** (2005) Acid mine drainage in the Iberian Pyrite Belt (Odiel river watershed, Huelva, SW Spain): Geochemistry, mineralogy and environmental implications. *Applied Geochemistry* **20:** 1320 – 1356.
- **Suzuki, T., Fujikura, K., Higashiyama, T. and Takata, K.** (1997) DNA staining for fluorescence and laser confocal microscopy. *The Journal of Histochemistry and Cytochemistry* **45(1):** 49 – 53.
- **Taylor, B. E., Wheeler, M. C. and Nordstrom, D. K.** (1984). Stable isotope geochemistry of acid mine drainage: Experimental oxidation of pyrite. Geochemica et Cosmochimica Acta **48:** 2669 – 2678.
- **van Eeden, E. S., Liefferink, M., and Durand, J. F.** (2009) Legal issues concerning mine closure and social responsibility on the West Rand. *TD The Journal for Transdisciplinary Research in Southern Africa* **5:** 51 – 71.
- **Wang, X., Li, Y., Wang, M., Li, W., Chen, M. and Zhao, Y.** (2014) Synthesis of tunable ZnS-CuS microspheres and visible–light photoactivity for rhodamine B. *New Journal of Chemistry* **38:** 4182 – 4189.
- **Warthmann, R., Vasconcelos, C., Sass, H. and McKenzie, J. A.** (2005) *Desulfovibrio brasiliensis* sp. nov., a moderate halophilic sulfate-reducing bacterium from Lagoa Bermelha (Brazil) mediating dolomite formation. *Extremophiles* **9:** 255 – 261.
- **Winch, S., Mills, H. J., Kostka, J. E., Fortin, D. and Lean, D. R. S.** (2009) Identification of sulfate-reducing bacteria in methylmercury-contaminated mine tailings by analysis of SSU rRNA genes. *Federation of European Microbiological Societies* **68:** 94 – 107.

CHAPTER 4

BEHAVIOURAL STUDIES AND EVALUATION OF ANAEROBIC SULFATE REDUCING COMMUNITIES FOR SULFATE REDUCTION AND METAL PRECIPITATION IN VARIED CONDITIONS

4. BEHAVIOURAL STUDIES AND EVALUATION OF ANAEROBIC SULFATE REDUCING COMMUNITIES FOR SULFATE REDUCTON AND METAL PRECIPITATION PROCESSES IN VARIED CONDITIONS

4.1. Abstract

This chapter is focused on factors that affect the microbial sulfate reduction process. The sulfate reducing capabilities of the enriched sulfate-reducing bacteria (SRB) were tested in PSGM with sulfate concentrations ranging between 2000 mg/L and 4000 mg/L. An average of 72% sulfate reduction was achieved in all experiments with a positive response of SRB to higher sulfate concentrations. Effects of pH and temperature on sulfate reduction were evaluated at pH of 3.5 and 6.2, with temperature of 10ºC and 25ºC. Low pH conditions showed negative effects on sulfate reduction and bacterial growth even when temperature was raised to 25ºC. Optimum SRB activity was observed in the experiment where pH was 6.2 at 25ºC. The preferred carbon source in the enriched SRB between glycerol and sodium lactate was evaluated in the batch operated bioreactors. The best sulfate reduction was observed when glycerol was used as a sole carbon source, as it yielded greater amounts of dissolved sulfide concentrations. Glycerol was then used further as the main carbon source in PSGM. Metal-microbe interactions were evaluated where higher concentrations of zinc (Zn^{2+}) and iron (Fe^{2+}) were introduced into the bioreactors. Results showed 100%, 85% and 40% sulfate reduction in experiments where no metals, 200 mg/L of Fe^{2+} and 200 mg/L of Zn^{2+} were added respectively. Effects of high Zn^{2+} concentrations were similar to those exerted by low pH conditions. However, 90% of Zn^{2+} and 97% Fe^{2+} concentrations were removed from the medium through biogenic precipitation. Precipitates were characterized by Scanning Electron Microscopy (SEM), Transmission Electron Microscopy (TEM) and X-Ray Diffractometer (EDX) which confirmed the presence of biologically induced precipitates.

Keywords: Sulfate-reducing bacteria; Sulfate reduction; Metal-microbe interactions; Batch bioreactors; Biogenic metal precipitation.

4.2. Introduction

The applications of any bacteria for biotechnological purposes require adequate knowledge of the microorganism of choice including the conditions that induce its optimum activity (Chapelle *et al.,* 2009). Bacteria are used for their unique nature of tolerating conditions known to be harsh and extreme to most eukaryotes. Sulfate-reducing bacteria (SRB) are a diverse group of microorganisms studied widely because of the important roles they play in the natural geochemical sulfur cycle (Castro *et al.,* 2000). SRB catalyse the reduction of sulfate (SO_4^{2-}) to sulfide (S^{2-}) in the presence of organic matter under anaerobic conditions which in return reacts with metals forming precipitates. This process takes place when SRB uses sulfate as their final electron acceptor while oxidising the organic compounds (Castillo *et al.,* 2012). This phenomenon is applied in most of the acid mine drainage (AMD) treatment systems where SRB are used to reduce sulfate and precipitate dissolved toxic metals (Moosa *et al.,* 2005).

Various factors can affect and inhibit the sulfate reduction process such as high concentrations of transition metals, low pH conditions, low or high temperatures, unsuitable carbon source for SRB and environmental settings that inhibit the achievement of anaerobic conditions. Improved SRB activity in terms of sulfate reduction when the bacteria is exposed to high sulfate concentrations up to 10 000 mg/L have been reported which implies that sulfate concentration stress improve sulfate reduction activities (Moosa *et al.,* 2002).The optimum temperature and pH for SRB activity are required for SRB to reduce a wide range of sulfate concentrations (Moosa *et al.,* 2002). Various groups of SRB have been reported to optimally grow in anaerobic conditions with temperature ranging between 25ºC and 40ºC and pH values of around 5 and 7 (Castro *et al.,* 2000; Chapelle *et al.,* 2009). Moosa and co-workers (2005) reported insignificant effect on SRB growth at temperature ranges between 20ºC and 35ºC but stated that an increase in magnitude of sulfate reduction rate were observed at 35ºC.

Transition metals such as cadmium (Cd^{2+}) and zinc (Zn^{2+}) in high concentrations can affect bacteria in various ways on a molecular level. The uptake of metals from the solution into the cell is through the transporter proteins or carriers used by the cells to acquire ions for various metabolic activities (Harrison *et al.,* 2007). A large number

of proteins use Zn^{2+} as a structural or catalytic cofactor for their activation and function. At high concentrations, Zn^{2+} binds strongly to the proteins inhibiting the binding of other metals ions such as Fe^{2+} (Carasi *et al.,* 2013). Some of the transition metals catalyse microbial cellular functions which can damage the bacterial DNA resulting in cell death. Most bacteria can sequester excess Zn^{2+} which can irreversibly bind to the bacterial receptors outcompeting Cd^{2+}, Fe^{2+}, copper (Cu^{2+}) or magnesium (Mg^{2+}) ions required for other functions of proteins involved in bacterial growth (Harrison *et al.,* 2007). Zn^{2+}concentrations above 210 mg/L have been reported to be lethal to SRB hence inhibiting sulfate reduction (Castillo *et al.,* 2012). Iron is one the most abundant metals in the earth's crust and results in high Fe^{2+} concentrations in AMD. It has been proven to be less toxic even in high concentrations in the environment because of iron reducing and iron oxidizing bacteria which play vital roles in cycling ferrous (Fe^{2+}) and ferric iron (Fe^{3+}) in the environments (Brown *et al.,* 1999; Onysko *et al.,* 1984). Iron oxidizing bacteria such as *Acidithiobacillus ferrooxidans* induce oxidation process of pyrite (FeS_2) during AMD formation releasing Fe^{3+} in the solution while iron reducing bacteria such as *Shewanella putrefaciens* reduce the Fe^{3+} to Fe^{2+} in anaerobic environments (Nealson and Myers, 1990). The cycling of Fe^{2+} and Fe^{3+} is continuous in most aquifers where anaerobic conditions are created in the sediments at the base of the aquifer (Baumgartner *et al.,* 2006; Brown *et al.,* 1999; Onysko *et al.,* 1984). In such anaerobic environments, SRB such as *Desulfovibrio vulgaris* reduce SO_4^{2-} to S^{2-} while oxidizing 80% of the carbon in the sediments (Baumgartner *et al.,* 2006). In extreme conditions like environments with toxic metals such as Zn^{2+}, microorganisms combine their chemical, physical and physiochemical characteristics to survive the conditions by forming biofilms (Harrison *et al.,* 2007).

Metal precipitation as a result of biogenic S^{2-} reaction with dissolved metal ions play a major role in mitigating toxicity of AMD during biological treatments (Moreau *et al.,* 2013). Factors affecting biogenic sulfate reduction, indirectly affect metal precipitation hence, optimization of sulfate reducing conditions is beneficial for both processes. Metal-microbe interactions between SRB and dissolved metals have been widely studied and different mechanisms of how bacteria precipitate metals have been classified into two mechanisms: intracellular and extracellular metals precipitation (Gadd, 2010; Rathnayake *et al.,* 2010). Bacteria used in bioremediation

of AMD employ various mechanisms such as biosorption, bioaccumulation, bioreduction and biomineralization to remove metals from their dissolution state by precipitation either internally or externally. This is mediated by the release of by-products of bacterial metabolism that reacts with the metals to form precipitates and also internally by sequestering metal ions forming internal precipitates with cellular components or metabolic by-products (Vaughan and Lloyd, 2011).

Maintenance of the optimum conditions in open systems used to treat AMD are impossible hence closed systems are required to create an anoxic environment with other parameters adjusted for growth and activity of SRB to optimally reduce SO_4^{2-} (Moreau *et al.,* 2013). Bench scale bioreactors were used in these studies to characterize SRB communities and their behaviour when exposed to conditions mimicking AMD toxicity. Bioreactors allow maintainable adjustments of conditions in the system to study the behaviour of SRB during sulfate reduction (Moosa *et al.,* 2002). In this section of the study, batch and bioreactor experiments were conducted with varied parameters that are known to affect sulfate reduction by reducing or inhibiting SRB activity in AMD treatments.

4.2.1. Aims and objectives of the chapter

The aims of this section were to study the behaviour of anaerobic sulfate reducing communities enriched from the previous chapter when exposed to different environmental conditions and also to evaluate the behaviour of SRB in the presence of transition metals.

The first objective was to study the behaviour of SRB at elevated SO_4^{2-}, metal (Zn^{2+} and Fe^{2+}) concentrations, low pH values and temperatures in batch experiments. The second objective was to use bench scale bioreactors to evaluate the suitable carbon source for optimum sulfate reduction by the enriched SRB community in optimized conditions. The final objective was to study the metal-micro interactions of SRB with elevated metal concentrations in optimized conditions and also to characterize the metal precipitates formed in these interactions using Scanning Electron Microscopy (SEM), Transmission Electron Microscopy (TEM) and X-Ray Diffractometer (EDX).

4.3. Materials and methods

4.3.1. Preparation and maintenance of cultures for the microbial-metal interaction experiments

Since the enriched bacterial consortia from the three study sites contained different species of SRB, the enrichments were co-cultured by using 5 mL portions from each tertiary enrichment cultures (Site-Ex, Site-Ka, Site-Po and Sludge) and inoculated into 80 mL of Postgate medium (PSGM) and anaerobic sulfate reducing medium (ASRM) respectively. After 10 days of incubation at 30ºC, the microbial cells were subjected to Live/Dead cell staining described in section 3.3.4.2. From each of the two cultures, 10 mL were mixed and used as the 20% (v/v) inoculum into 80 mL PSGM which was selected to be used in the metal-microbe interaction experiments. Mixed microbial consortia were maintained anaerobically in PSGM by inoculating 40 mL of the active consortia into 160 mL of fresh medium prepared according to section 3.3.6.1.

The carbon source used in these experiments was changed from sodium lactate to glycerol as described by Bertolino and co-workers (2014) who reported 90% sulfate reduction when using either glycerol or sodium lactate. The active cultures were inoculated into freshly prepared media after 20 days while incubating at 30ºC. Bigger volumes of cultures were prepared by inoculating 20% (v/v) from the active culture into 80% (v/v) of the medium volume to makeup the required volumes for the subsequent experiments while maintaining the active cultures in 200 mL volumes. The 20 days incubation period was reduced to 15 days due to the detection of higher numbers of dead cells after the 20 days periods. Maintenance and preparations of the consortia were done at 30ºC as they were enriched in the previous chapter.

4.3.2. Batch experiments

4.3.2.1. Microbial sulfate reduction of inclining concentrations

Sulfate reduction potential of the enriched SRB was tested by inoculating the mixed consortia in PSGM with varied sulfate concentrations. The medium contained 1455.6 mg/L of sulfate concentration as part of the medium composition and was supplemented with additional sulfate solution to attain concentrations of 2000, 2500, 3000 and 4000 mg/L. The sulfate stock solution of 10 000 mg/L was prepared by dissolving 2.892g of $FeSO_4.7H_2O$ into 100 mL of de-oxygenated water into a vial which was opened and closed in the anaerobic chamber (COY- Laboratory Product INC. 14500 COY DR. Grass Lake, MI49240) to avoid oxidation of the Fe^{2+} which precipitates when dissolved in the presence of oxygen. Sulfate reduction of each culture in the medium was monitored by determining sulfate concentrations every 5 days for 20 days according to the procedure described in section 3.3.3.2.

4.3.2.2. Effects of pH and temperature on sulfate reduction

The effect of pH and temperature on sulfate reduction was evaluated at two pH values (optimum and low) and two temperature conditions lower than the ones enriched in. PSGM was prepared as described section 3.3.6.1 and adjusted according to the diagram in Figure 4.1 before autoclaving the vials. Each vial containing 160 mL of fresh medium was inoculated with 40 mL of the culture and incubated at their respective temperatures. Five parameters: sulfate concentrations ($[SO_4^{2-}]$), sulfide concentrations ($[S^{2-}]$), pH, oxidation reduction potential (ORP) and optical density (OD) were monitored on a daily basis from the day of inoculation until the twentieth day of the experiment.

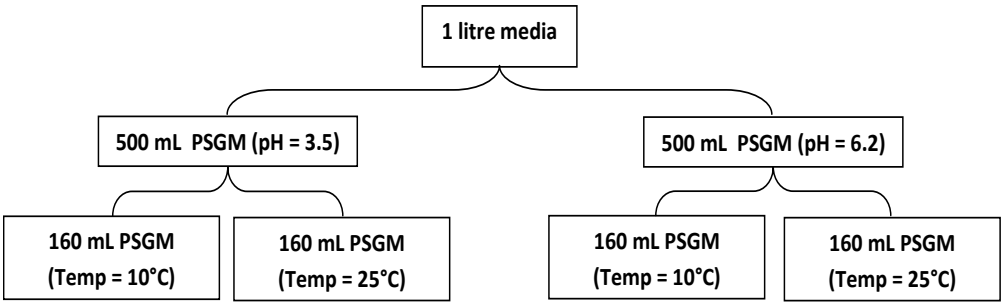

Figure 4.1: Preparation flow diagram and selected parameters for evaluating sulfate reducing activity of the enriched SRB.

Sulfate concentrations were determined as described in section 3.3.3.2. Prior to sample analysis, dissolved sulfides were precipitated by adding 1 mL of the sample in a 1.5 mL Eppendorf tube containing 100 µL of zinc Acetate, vortexed and centrifuged at 14 000 *x g* for 10 minute then the supernatant was used for sample analysis. Sulfite concentrations were determined as described in section 3.3.3.3. Samples were immediately added into cuvettes each containing 375 µL of zinc acetate to precipitate the dissolved sulfides before they re-oxidises back to sulfates. The pH and ORP of the cultures were determined by the use of ExStik®II – EC500 and ExStik® – RE300 probes respectively as described in section 3.3.3.1.

4.3.2.2.1. Optical density measurements

Microbial growth was monitored by determining optical density (OD) using the absorbance of the cultures at 600 nm with a spectrophotometer (SpectronicR® GENEYS™ 5). The spectrophotometer readings were blanked with 1.5 mL of fresh PSGM followed by the absorbance readings of culture (1.5 mL). Care was taken before samples were analysed to ensure homogenous suspension.

4.3.2.3. Effects of high metal concentrations on sulfate reduction

Effect of high Zn^{2+} and Fe^{2+} concentrations on sulfate reduction were evaluated by monitoring the sulfate reduction rates at temperature of 25ºC and pH of 6.2. Adaptation of SRB to high concentrations of heavy metals is vital as their adaptability will determine their potential to be used in the bioremediation processes (Haferburg and Kothe, 2007). Zn^{2+} and Fe^{2+} were selected to be used in these metal-microbe interaction studies because normally AMD has elevated levels of Fe^{2+} due to the abundance of pyrite in the earth's crust (Baker and Banfield, 2003) and Zn^{2+} concentrations above 210 mg/L were reported to have inhibitory effects of sulfate reduction mediated by SRB (Castillo *et al.,* 2012). These metals were also selected to extend the knowledge regarding their interaction with SRB in anaerobic environments.

Stock solutions with concentrations of 10 000 mg/L of Zn^{2+} and Fe^{2+} were prepared separately by dissolving 4.43 g of $ZnSO_4.7H_20$ and 4.97 g of $FeSO_4.7H_2O$

respectively in 100 mL volumes of de-oxygenated Milli-Q water in the anaerobic chamber as described in section 4.3.2.1 done for sulfate stock solutions. Five 80 mL vials were used with 40 mL of PSGM (pH 6.2) and the target metal concentrations outlined in Table 4.1 were calculated and added prior to inoculation with the mixed consortium. Three kinetic parameters ($[SO_4^{2-}]$, $[S^{2-}]$ and pH) were monitored for 15 days as described in section 4.3.2.2. The vials were incubated aerobically at 25ºC in a bench top incubator and samples were taken on random days to reduce oxygen intrusion in the vials during sampling.

Table 4.1: Metal (Fe^{2+} and Zn^{2+}) concentrations in the batch cultures.

Sample set up	**Fe^{2+} (200 mg/L)**	**Fe^{2+} (100 mg/L)**	**Zn^{2+} (200 mg/L)**	**Zn^{2+} (100 mg/L)**
No metals + Inoculum	-	-	-	-
100 mg/L Zn^{2+} + Inoculum	-	-	-	+
200 mg/L Zn^{2+} + Inoculum	-	-	+	-
Fe200 mg/L Fe^{2+} + Inoculum	+	-	-	-
100 mg/L Zn^{2+} & Fe + Inoculum	-	+	-	+

4.3.3. Bioreactor studies

4.3.3.1. Carbon source selection

Two carbon sources: sodium lactate and glycerol used for SRB growth in the previous experiments were evaluated for optimum bacterial growth and sulfate reduction activity in the media with elevated sulfate concentrations in automated bioreactors. PSGM was used as the medium of choice for both carbon sources. The bioreactors were operated at 25ºC and the pH in both cultures was maintained at 6.2. These conditions were maintained automatically by the bioreactor system.

4.3.3.1.1. The Sixfors bioreactor setup

Sixfors HT (INFORS AG CH-4103 Bottminingen / Switzerland) bioreactors depicted in Figure 4.2 were used to improve the cultivation conditions and optimize the sulfate reduction process. The six bioreactors each with maximum capacity of 300 mL can be operated simultaneously while varying conditions or components in each. The equipment has a pH control function that regulates the addition of acid or base to the

required set pH value. Temperature can also be maintained at a set point as well as the stirrer speed in each bioreactor. The system is also equipped with a gas inlet and outlet control for each reactor connected to a dissolved oxygen (DO) sensor. This permits that any gas of choice can be flushed through the culture in the reactors. The discussed functions can be set and automated to operate for more than a month even when the power is unintentionally shutdown as it is connected to an external battery.

The system components: glassware, tubes and metal parts were washed and autoclaved at 120ºC for 10 minutes. The system was assembled according to the instructions in its manual. PSGM (pH = 6.2) with different carbon sources prepared to a total volumes of 1 L in separate Schott bottles, one containing either sodium lactate or glycerol as described in section 3.3.6.1. The media had a final sulfate concentration of 2 500 mg/L for each reactor. All openings of the reactors were sealed with air tight designated metal stoppers and tubes were sealed with cable ties at the ends. A pH probe was calibrated for each reactor and immersed in the media. DO probes immersed in the media and connected to the system were calibrated by bubbling with filtered air until 100% DO reading was reached and subsequently bubbled with oxygen free nitrogen gas till all the oxygen was released from the media until 0% DO readings were recorded. The gas tubes were then sealed leaving no opening on the bioreactors. The media in the bioreactors were autoclaved at 120ºC for 20 minutes and allowed to cool. However, all media were again flushed with the filter sterilized nitrogen gas to eliminate any oxygen to ensure 0% DO state for SRB metabolisms. The bioreactors were connected to the sixfors system and turned on. For each bioreactor, 15 mL deoxygenated hydrochloric acid (0.5 M of HCl) and sodium hydroxide as base (0.5 M of NaOH) reservoirs in 20 mL vials were connected to the system for pH control in each reactor during operation. A 25 mL syringe filled with nitrogen gas was used as a pressure release plunger connected to each vial for when the solution is pumped from the vial into the reactor, the gas in the syringe replaces the volume of solution without creating any vacuum. The 0% DO state was restored by bubbling filtered nitrogen gas (through 0.02 µm syringe filter) prior to inoculation.

Figure 4.2: Sixfors fermenters (INFORS AG CH-4103 Bottminingen / Switzerland) used for the bioreactor studies.

4.3.3.1.2. Bioreactors inoculation, start up, operation and termination

The bioreactors already installed and filled with respective media (160 mL in each) were inoculated with 40 mL of a 15 days old inoculum prepared as described in section 3.3.6.2. The cultures were injected into the bioreactors through a sampling tube and then sealed with a T-shaped sampling valve. The system was then automated to operate with a constant stirrer speed of 50 rpm, at a temperature of 25ºC and maintained pH of 6.2 in the cultures. The sixfors bioreactors were operated in a batch mode for 16 days without stoppage. Daily sampling was done for the first 12 days followed by random sampling days to compensate for low culture volumes in the reactors.

DO percentages and pH values were recorded from the sixfors system. OPR values, SO_4^{2-} and S^{2-} concentrations were determined as discussed in section 4.3.2.2. After the 16 days of bioreactor operation period, the bioreactors were stopped by first sealing the acid and base tubes, followed by the stirrer and switching off of the pH and DO monitoring systems. The cultures in the reactors were aspirated into water washed, autoclaved and deoxygenated vials and visual analysis was done on the cultures.

4.3.3.2. Metal-microbe interactions studies in the bioreactors

After the best carbon source was selected, the metal-microbe interactions were evaluated by the use of the Sixfors bioreactors in optimized conditions (pH of 6.2 and temperature of 25ºC). PSGM was used with glycerol as the main carbon source preferred for the enriched bacteria. The same metals (Fe^{2+} and Zn^{2+}) that were used in section 4.3.2.3 were selected for the metal-microbe interaction studies. Bioreactor setup and inoculations were done as described in section 4.3.3.1.1 and 4.3.3.1.2 respectively. The bioreactors were operated in a batch mode with either 200 mg/L of Zn^{2+}(R1) or 200 mg/L of Fe^{2+} (R2) added to the media through the sampling tube. Two other reactors with similar condition but without any metals were also setup where no pH control was employed (R3) and another with pH control set at 6.2 (R4). The monitoring and parameter analysis was carried out daily for 20 days.

4.3.3.2.1. Sampling and analysis

Sampling from these four bioreactors was done daily to monitor the kinetic parameters (pH, DO, ORP, [SO_4^{2-}], [S^{2-}], [Fe^{2+}], [total iron] (Fe_T) and [Zn^{2+}]) and after every fifth day, 10 mL samples were harvested from each bioreactor for carbon source and molecular analysis. Sampling and analysis was done as described in section 4.3.2.2 for SO_4^{2-} and S^{2-} concentrations and ORP determination. DO concentrations were recorded but not controlled in all reactors whereas the pH of 6.2 was set and maintained by the system in 3 (R1, R2 and R4) of the 4 reactors.

Concentrations of dissolved metals (Fe^{2+}, Total iron (Fe_T) and Zn^{2+}) were determined by colorimetric analysis using the HACH spectrophotometer (DR900) according to the protocol provided by the manufacturer. Fe^{2+} concentrations were determined according to method 255 (Iron, Ferrous. 1,10-Phenanathroline Method[1]), Fe_T concentrations were determined according to method 265 (Iron, Total. USEPA[1] FerroVer® Method[2]) and Zn^{2+} concentrations were determined according to method 780 (Zinc. USEPA[1] Zincon Method[2]). Samples used for metal concentrations analysis were taken from the sampling port and 1.5 mL of each sample was added in Eppendorf tubes and centrifuged for 10 minutes at 14 000 *x g* to precipitate metal sulfide precipitates before they dissociate. The supernatants were used for the analysis of dissolved metal concentrations.

4.3.3.2.2. Carbon source analysis

Glycerol concentrations were determined every 5th day by High Performance Liquid Chromatography (HPLC). HPLC analysis was carried out on an Agilent 1200 instruments with pump, autosampler and refractive index detection. The analytical column was an Aminex HPX 87H from Biorad and the mobile phase of 5 mM H_2SO_4 pumped at a rate of 0.6 mL/min was used. Samples were taken in 2 mL Eppendorf tubes filled to the brim and centrifuged at 14 000 *x g* and the supernatants were used to determine glycerol concentrations using the constructed standard curve depicted in Figure 4.3. Fresh glycerol containing PSGM was used as a standard curve stock solution for dilutions

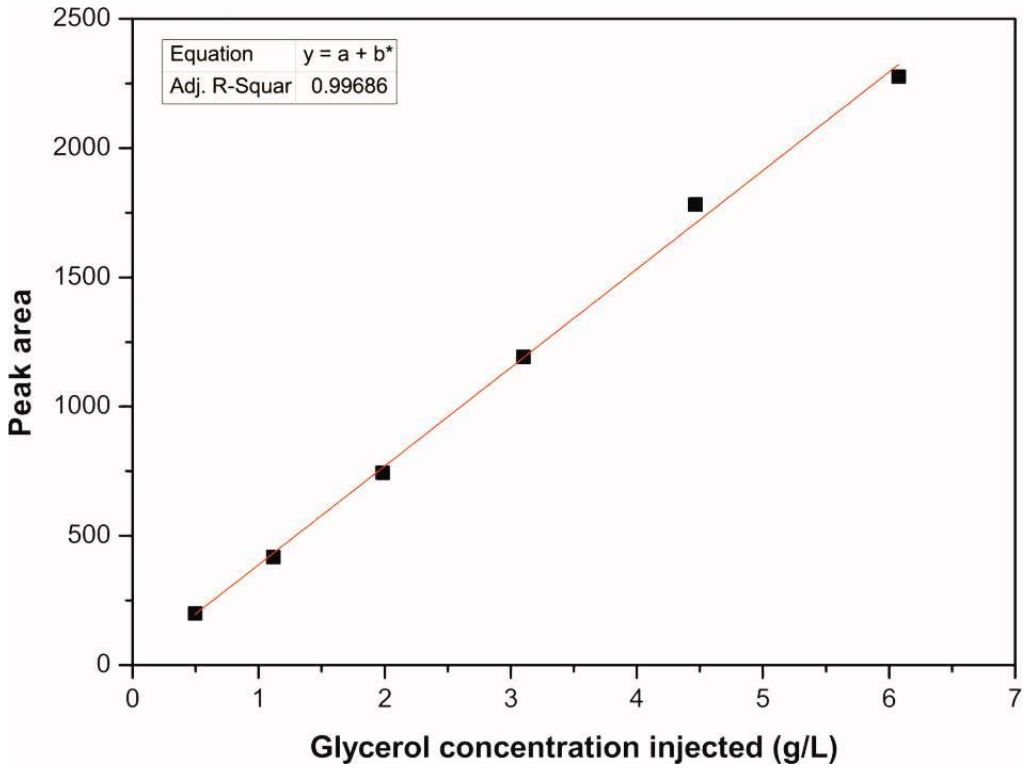

Figure 4.3: HPLC standard curve relating glycerol peak area to the amount of sample injected into the HPLC column.

4.3.3.3. Molecular analysis of metals tolerant microorganisms

Molecular analysis was done on samples taken in 5 days intervals. A total of 16 samples (4 samples from each reactor) were analysed. Genomic DNA was extracted from these culture samples according to the procedure described in section 3.3.5.1. Amplification of the partial 16S rRNA gene fragments were done according to section 3.3.5.2. Denaturation gradient gel electrophoresis (DGGE) was done to evaluate the microbial diversities in the cultures according to the procedure described in section 3.3.5.3. DGGE bands were excised and processed for sequencing.

4.3.3.4. Morphological and mineralogical characterization of precipitates

4.3.3.4.1. Samples preparation

The cultures from the four bioreactors were subjected to lyophilisation as described in section 3.3.6.9. The powdered samples were each divided into three portions and sent for analysis by SEM-EDS, TEM-EDS and XRD.

4.3.3.4.2. Scanning Electron Microscopy coupled to Energy Dispersed X-ray Spectroscopy (SEM-EDS)

SEM was used to visualize the metal-microbe interactions morphologically. Semi quantitative determination of elements concentrations in the precipitates was done by Energy Dispersed X-ray Spectroscopy (EDS) coupled to SEM. The powdered samples were mounted onto copper grids and coated with carbon prior to analysis. The analysis was performed by the SEM-EDS (Joel JSM-7800F Field Emission SEM) with high resolution equipped with Oxford Aztec EDS and Gatan Mono CL4 at the Centre of Microscopy at the University of the Free State. Analysis was performed as described in section 3.3.6.9.

4.3.3.4.3. Transmission Electron Microscopy coupled to Energy Dispersed X-ray Spectroscopy (TEM-EDS)

TEM (Philips CM100. Mega View III, Soft Imaging System) coupled to EDS at the Centre of Microscopy at the University of the Free State was used to study the interaction of metals and microorganisms to intercellular level. Since the electron beam generated in the TEM can pass through thin samples yielding high resolution images. With greater than 1000 000 x achievable magnifications of TEM, bacterial cells, precipitated organic and inorganic particles, as well as their interactions, were easily visualized. Only the Zn^{2+} containing sample was mounted onto a copper grid and then subjected to the analysis by TEM.

4.3.3.4.4. X-Ray Diffractometer analysis (XRD)

The qualitative analysis of the crystalized minerals was done on both metals (Zn^{2+} and Fe^{2+}) containing samples by the Panalytical Empyrean X-ray Diffractometer (XRD) at the Department of Geology at the University of the Free State. XRD was used to identify the neoformed phase minerals that resulted during the biogeochemical process in the bioreactors.

4.4. Results and discussions

4.4.1. Culture preparations for the metal-microbe interaction

The successfully enriched consortia from the three study sites were used in this chapter for the metal-micro interaction studies. The consortia enriched in ASRM were co-cultured in one vial and similarly with those enriched in PSGM as described in section 4.3.1. On day 10 of the incubation period, the samples were subjected to Live/Dead cell staining technique to check the viability of the co-cultured cells. Viable cells with various morphologies were observed in both cultures depicted in Figure 4.4 A and B. After day 20, the two culture consortia in PSGM and ASRM were further mixed and co-cultured in PSGM. Likewise, on the tenth day of incubation, Live/Dead cell staining was employed and the viable cells with diverse morphologies were observed as notable in Figure 4.4 C. Since there were almost 100% viable cells in the cultures when analysed on the tenth day, the incubation period was reduced by five days to fifteen days. The final cultured consortia were maintained in PSGM with 15 days intervals of cultivation periods. The PSGM was selected for the subsequent experiments due to its properties such as development of a black colour in the medium indicating the presence and activity of SRB compared to when cultivated in ASRM. The black colour develops when SRB generate hydrogen sulfide (H_2S) which reacts with iron (Fe^{2+}) forming black precipitates of iron monosulfide (FeS). The iron in the cultures is from the AMD samples which contained high iron concentrations. Maintaining the viable SRB in PSGM prevents loss of some microbial groups that cannot re-adapt to grow after being cryopreserved (Bosso *et al.,* 2009). The black medium colour that results when growing the enriched consortia in PSGM faded away during the maintenance passaging resulting in a grey colour depicted in Figure 4.4 D which is almost similar to the one observed while enriching SRB in ASRM. This can be due to the decreasing iron concentrations primarily from the AMD water used as inoculum for primary cultures during the enrichments studies. The PSGM used to maintain the consortia contained glycerol as the main carbon source due to its low costs and preference for experimental upscaling for bioreactors operated in either continuous or batch modes as done by Bertolino and co-worker (2014).

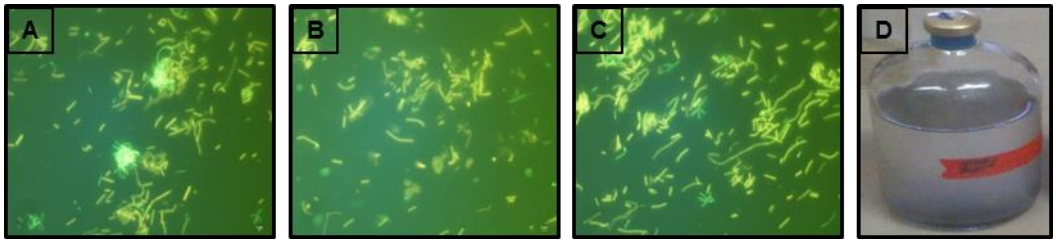

Figure 4.4: Live/Dead staining images (A to C): A: Co-cultured consortia in PSGM, B: Co-cultured consortia in ASRM and C: Secondary co-cultured consortia from cultures depicted in A and B. D: Consortia maintained in PSGM for downstream experiments.

4.4.2. Batch experiments

4.4.2.1. Microbial sulfate reduction of inclining concentrations

The microbial consortia were exposed to higher sulfate concentrations as described in section 4.3.2.1 to determine if the enriched SRB could reduce sulfate concentrations up to 4000 mg/L. The tests were conducted anaerobically in 100 mL cultures for 20 days with determination of sulfate concentrations every five days of the incubation. The sulfate reduction results in Table 4.2, showed positive response of the SRB to high sulfate concentrations as 70% of the highest sulfate concentrations were reduced over a period of 20 days. The calculations of the sulfate reduction percentages were done by using the overall reduced amount and the highest recorded concentration in each experiment. An average of 72.6% sulfate reduction was achieved for all experiments. However, 100% sulfate reduction was not achieved even in a culture that contained the lowest concentrations. This also showed that the reduction rates were not influenced by an increase in sulfate concentration ranges. The incomplete sulfate reduction activity was therefore not because of the toxicity of the sulfate concentrations but probably due to oxidation of sulfide back to sulfate during sampling or other sulfate reduction affecting parameters such as pH and energy source depletion (Bosso *et al.,* 2014). All cultures in the vials turned black within 5 days of incubation and this was due to the presence of Fe^{2+} that was introduced with the supplement sulfate solution as it was prepared by dissolving $FeSO_4.7H_2O$ which dissociate into ferrous iron (Fe^{2+}) and sulfate (SO_4^{2-}) as outlined in Equation 4.1 (Kobylin *et al.,* 2011). The addition of Fe^{2+}

in the environment, promote the formation of metal sulfides such as FeS. This process serves an indication of biogenic sulfate reduction process as the formed precipitates depend mainly of the presence of hydrogen sulfide (biogenic in this case). The oxidation of the neoformed phase mineral (FeS) by oxygen, allow the re-dissolution of the precipitates increasing sulfate concentrations in the solution (Davison, 1991). The fluctuating trend of sulfate in the batch experiment could possibly be due to the re-oxidation of the reduced and unstable sulfide.

Equation 4.1: $FeSO_4.7H_2O \leftrightarrow Fe^{2+} + SO_4^{2-} + 7H_2O$

The behaviour of SRB in this preliminary experiment showed the potential of reducing sulfate at higher concentrations in mine drainages like those collected from the study sites which had sulfate concentrations below 4000 mg/L. Biogenic sulfate reduction was also observed by Moosa and co-workers (2005) at sulfate concentrations around 10 000 mg/L in a continuous system. This proved that SRB can reduce sulfate at higher concentrations and could be considered in remediation.

Table 4.2: Sulfate reduction efficacy of SRB consortium.

Day	Test 1: 2000 mg/L	Test 2: 2500 mg/L	Test 3: 3000 mg/L	Test 4: 4000 mg/L
0	1850	2100	2900	3750
1	1900	2300	3050	3000
5	1850	2200	2900	4000
10	1550	750	2000	1850
15	1750	800	1850	1500
20	500	550	1000	1200
Removed [SO_4^{2-}]	1400	1750	2050	2800
Mathematical [SO_4^{2-}] Reduction %	73.7%	76.1%	70.7%	70%

4.4.2.2. Effects of low pH and temperature on sulfate-reduction

Sulfate reduction is a complex process which can be affected by a variety of parameters. Sulfate concentrations, pH, temperature, metals, the availability and type of electron donor, as well as sulfide concentrations can exert an inhibitory effect on the sulfate reduction process (Moosa *et al.,* 2005). Effects of pH and temperature on sulfate reduction were investigated in batch experiments as described in section

4.3.2.2 and shown in Figure 4.1. The experiments were conducted for 20 days with daily analysis to determine the pH, OD, ORP, [SO_4^{2-}] and [S^{2-}] in each culture incubated at its respective temperature.

Like any bacterial community, SRB require optimal growth conditions to effectively reduce sulfate. Varied environmental conditions mimic the climatic conditions in natural environments that change seasonally whereas the pH variations represent the AMD and non-acid mine drainage (NMD) conditions. Most SRB grow optimally at pH values above 4 and temperatures between 25ºC and 40ºC. The inoculum used in this study contained SRB from both AMD and NMD and with their combined characteristics; their tolerance to lower pH and temperature could be improved.

According to the results, the best bacterial growth was observed in a culture with pH of 6.2 incubated at 25ºC as seen from Figure 4.5 A. The experiment conducted at a pH of 6.2 but incubated at 10ºC also showed good bacterial growth based on the OD readings especially when compared to cultures incubated at both 10ºC and 25ºC with pH of 3.5. These results showed that there were changes in the densities of the cultures even if it might not have been bacterial growth entirely and the pH is showed to be the main controlling factor of bacterial growth or activity in these conditions.

The metabolic processes of SRB allow the release of H_2S in the medium and promote formation of bicarbonates which increase the pH of the medium according to Equation 4.2 (Castillo *et al.,* 2012) and also evident in Figure 4.5 C.

Equation 4.2: $$SO_4^{2-} + 2H_2CO \leftrightarrow H_2S + 2HCO_3^-$$

The redox couple SO_4^{2-}/S^{2-} had a reverse correlation with the ORP evolution which dropped below -200 mV in a culture grown at a pH of 6.2 and 25ºC as it can be seen in Figures 4.5 B, D and E. The ORP values below -100 mV create optimal SRB growth conditions hence promoting the biogenic sulfate reduction as seen in Figure 4.5 B and D. Similar correlations of SO_4^{2-} and S^2, pH and ORP was evident in cultures incubated in conditions with a pH of 3.5 as depicted in Figures 4.5 B, C, D and E. The minimum drop of ORP and stabilization of pH were observed in the two cultures with a pH of 3.5 and the one with pH of 6.2 at 10ºC. The ORP and pH profiles showed negative effects exerted by low pH and temperature on SRB activity to perform sulfate reduction and sulfide formation. The SO_4^{2-} and S^2 evolution was

more visible in the experiment with optimal conditions (25ºC and pH of 6.2). The overall sulfate reduction percentages were: 95%, 33%, 33% and 47% for cultures incubated at 25ºC with pH values of 6.2 and 3.5 and cultures incubated at 10ºC with pH values of 6.2 and 3.5 respectively.

According to the results, it can be noted that some of the sulfide produced was lost probably through the gaseous H_2S gas formation which escaped during sampling at lower pH conditions especially within the first 10 days of the experiment. This can be attributed to the low concentrations of sulfide which do not balance stoichiometrically with the reduced sulfate concentrations. The sulfide production trends correlated directly with pH values which dictate the form of sulfide present in the culture. At low pH values, sulfide is present in a gaseous form and at high pH values is in a liquid form and dissolved thus detected in high concentrations in the culture with a pH of 6.2 incubated at 25ºC. Temperature had lesser effects on sulfide production compared to low pH conditions. Maximum sulfite formation was observed in the culture with pH of 6.2 incubated at 25ºC. Second most sulfide concentrations were detected in the culture incubated at 10ºC and pH of 6.2 which had twice as much as the sulfide formed in cultures with pH of 3.5 incubated at both 10ºC and 25ºC as shown in Figure 4.5 F showing three profiles set aside for clear comparison.

On the other hand, the microbial growth and activity in the experiment at a pH of 6.2 incubated at 10ºC did not correlate with the sulfate reduction as expected. Sulfate concentrations were reduced similar as in the culture with a pH of 3.5. The high OD readings in this culture perhaps represent the formation of precipitates and biofilm as a strategy for bacterial adaptation to the varied conditions from the optimum SRB conditions. Since the inoculum was obtained from natural environments, different bacterial species cohabiting with SRB are also likely to grow as the environmental conditions permit their growth with a suitable carbon and energy source supplied in the medium. This was supported by the ORP values and sulfide concentrations which showed poor sulfate reducing activity because of the growth of SRB and other bacterial species co-cultured in the consortium. The experiments showed the presence of SRB even though the sulfate reduction in three of the four experiments was insignificant because of the effects of low pH and temperature which exerted inhibitory characteristics.

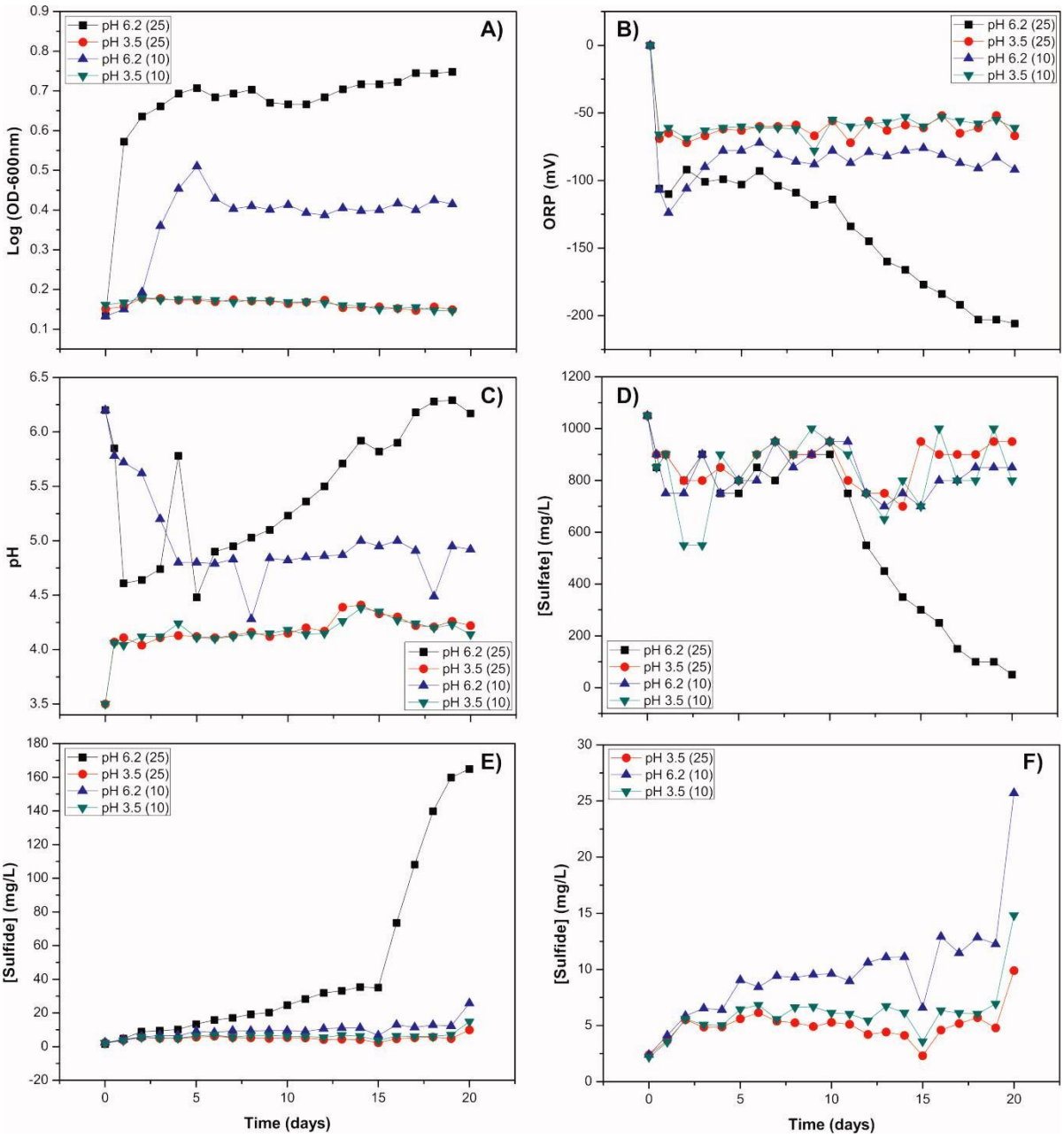

Figure 4.5: Parameter profiles monitored in four batch experiments to evaluate the effects of pH and temperature on SRB. A: Microbial growth curves, B: ORP profiles, C: pH profiles, D: sulfate reduction profiles, E: sulfide formation profiles and F: sulfide formation profiles of cultures grown at a pH of 3.5 (25ºC) and two cultures both grown at temperature of 10ºC in pH of 6.5 and 3.5.

4.4.2.3. Effects of high metal concentrations on sulfate reduction

Interaction of SRB and high metal concentrations was evaluated by growing the co-cultured consortia in media containing various metal concentrations as described in section 4.3.2.3. Metal ions such as Zn^{2+}, Cd^{2+} and manganese (II) ions (Mn^{2+}) can be inhibitory to the bacterial processes including sulfate reduction. These transition metals can negatively affect the bacterial enzyme production processes and their functions in the cell. DNA transcription is one of the processes mostly affected by metal ions which in turn affect the bacterial growth and inactivate some enzymes resulting in the loss of cellular function (McDevitt *et al.,* 2011). In this section of the study, effects of elevated Zn^{2+} and Fe^{2+} concentrations on sulfate reduction were evaluated. The effects were determined by monitoring biological sulfate reduction and sulfide formation in the cultures containing Zn^{2+} and Fe^{2+} in various concentrations for a period of 15 days with random days of sampling and analysis. Fluctuations of pH were also monitored in all cultures including the one without metals to check the effects of metals addition on the pH of the culture. Previously determined optimal sulfate reducing conditions (pH of 6.2 and temperature of 25ºC) were mimicked to acquire best bacterial growth. The maximum Fe^{2+} concentrations (200 mg/L) used in this experiment are moderate and on a level typically of that found in most AMD even though SRB has demonstrated tolerance of up to 800 mg/L of Fe^{2+} (Fortin *et al.,* 2002). In contrast, Zn^{2+} was selected because of its toxicity even at moderate concentrations of 150 mg/L (Carasi *et al.,* 2013).

The media with cultures in the vials changed colour within the first 5 days of incubation and on day 12, precipitates and gas bubbles in some cultures containing metals were observed as depicted in Figure 4.6 A. According to the obtained results, acidic conditions were stabilized below a pH of 5.5 in all experiments as shown in Figure 4.6 B. The sulfate reduction process was affected differently in all experiments as well as the sufide production rates, as seen from Figure 4.6 C and D respectively. Sulfate reduction percentages in the five experiments were all below 55% which is poor for SRB growing at optimum conditions. Three possible reasons responsible for the effects could be:

1. Microbial diversity of the inoculum

The bacteria in the cultures compete for the same carbon source and other growth factors which could become a limiting factor when depleted hence lowering the sulfate reduction rate by SRB. The intrusion of oxygen during sampling was possibly sufficient for minimal sulfide oxidation but bacterial communities related to the iron-reducing bacteria (*Acidobacterium capsulatum*) which were detected in the consortium could have had a major impact in re-oxidizing sulfide back to sulfate. In the iron containing cultures, the iron-reducing bacteria utilised the low oxygen concentrations in the vials to facilitate ferric iron (Fe^{3+}) reduction to ferrous iron (Fe^{2+}) while utilizing the organic matter (Luef *et al.,* 2013). During these processes, SRB compete for the carbon source with the rest of the bacteria growing in the cultures hence affecting growth and activity of SRB (Christensen *et al.,* 2002). In the experiments without metals, the presence of sulphur-oxidizing bacteria such as *Sulfuritalea hydrogenivorans,* also detected in the consortium, could be the cause of the low sulfate reduction and sulfide formation as it counteracts the activity of SRB by oxidizing thiosulfate ($S_2O_3^{2-}$), elemental sulfur (S^0) and H_2S (Kojima and Fukuli, 2011). The sulfide oxidation reaction limits the presence of sulfide in the solution making it seems like no sulfate reduction is taking place. This is the reason the stoichiometric imbalance of the reduced sulfate and the formed sulfide did not correlate in the solution. In Zn^{2+} containing cultures, inhibitory effects of the metal possibly contributed to the poor sulfate-reduction.

2. pH effect

In all cultures, the pH was below 5.5 from day 2 until the last day of experiments. During the ferric iron (Fe^{3+}) reduction process outlined in Equation 4.3, carbon dioxide (CO_2) and hydrogen protons (H^+) are generated contributing in the lowering of pH in the system as it was observed in iron containing experiments. Furthermore, according to Equation 4.4, the H^+ are generated during metal-sulfide precipitation which contributes to the lowering of the pH in the metals containing cultures. The low pH in the positive control without metals could be due to the release of H^+ generated during hydrogen sulfide oxidation according to either Equation 4.5 or 4.6. During these reactions, organic carbon gets oxidized and either sulfate or elemental sulfur result with carbonates.

Equation 4.3: $$Fe^{3+} + CH_2O + H_2O \leftrightarrow Fe^{2+} + CO_2 + H^+$$

Equation 4.4: $$H_2S + M^{2+} \leftrightarrow MS_{\downarrow} + 2H^+$$

Equation 4.5: $$H_2S + 2CO_2 + 2H_2O \rightarrow SO_4^{2-} + 2[CH_2O] + 2H^+$$

Equation 4.6: $$H_2S + 2CO_2 + 2H_2O \rightarrow S^0 + 2HCO_3^- + 4H^+$$

3. Zinc concentration

Tolerance of SRB to Zn^{2+} concentrations has been correlated with the environmental conditions from which they have been isolated. Utgikar and co-workers (2003) reported the toxicity of Zn^{2+} on SRB from 65 mg/L and the inhibitory effects at 170 mg/L, while Babich and Stotzky (1978) reported the growth inhibitory effects of Zn^{2+} at 654 mg/L concentrations. Castillo and co-workers (2012) also reported tolerance of SRB to over 260 mg/L of Zn^{2+} in anaerobic environments. One of the three bacterial (SRB) sources in this study contained zinc concentrations of 3.53 mg/L which are quiet low to inhibit growth of SBR hence the consortium could be highly susceptible to elevated concentrations of Zn^{2+}. According to the obtained results, 100 mg/L of Zn^{2+} did not have significant effects on bacterial growth as the sulfate-reduction was similar to the positive control. Low Zn^{2+} concentrations may not negatively affect bacterial growth because Zn^{2+} is one of the micronutrients that bacteria use for their structural proteins and a catalytic cofactor in their metabolic activities (Cerasi *et al.,* 2013). According to Figure 4.6 C and D culture with 200 mg/L of zinc showed the lowest sulfide production and poor sulfate reduction. This shows that the SRB were affected by elevated Zn^{2+} concentrations in the solution probably due to the propensity of Zn^{2+} to form stable complexes with proteins (Irving and Williams, 1948). High intracellular concentrations of Zn^{2+} competes with other metal ions such as Mn^{2+} by binding and blocking the active sites of some proteins in a conformation that prevents entry of metals that activates other proteins. This inhibitory effects, shows the possible effect of high (200 mg/L) Zn^{2+} concentrations in the culture which resulted in poor sulfate reduction and sulfide formation. The stable low pH values in Zn^{2+} containing cultures further indicated the possible toxicity of higher Zn^{2+} concentrations in the medium. The results support the speculations that 200 mg/L of Fe^{2+} does not negatively affect the sulfate reduction process compared to the toxicity and inhibitory effects showed by 200 mg/L of Zn^{2+}.

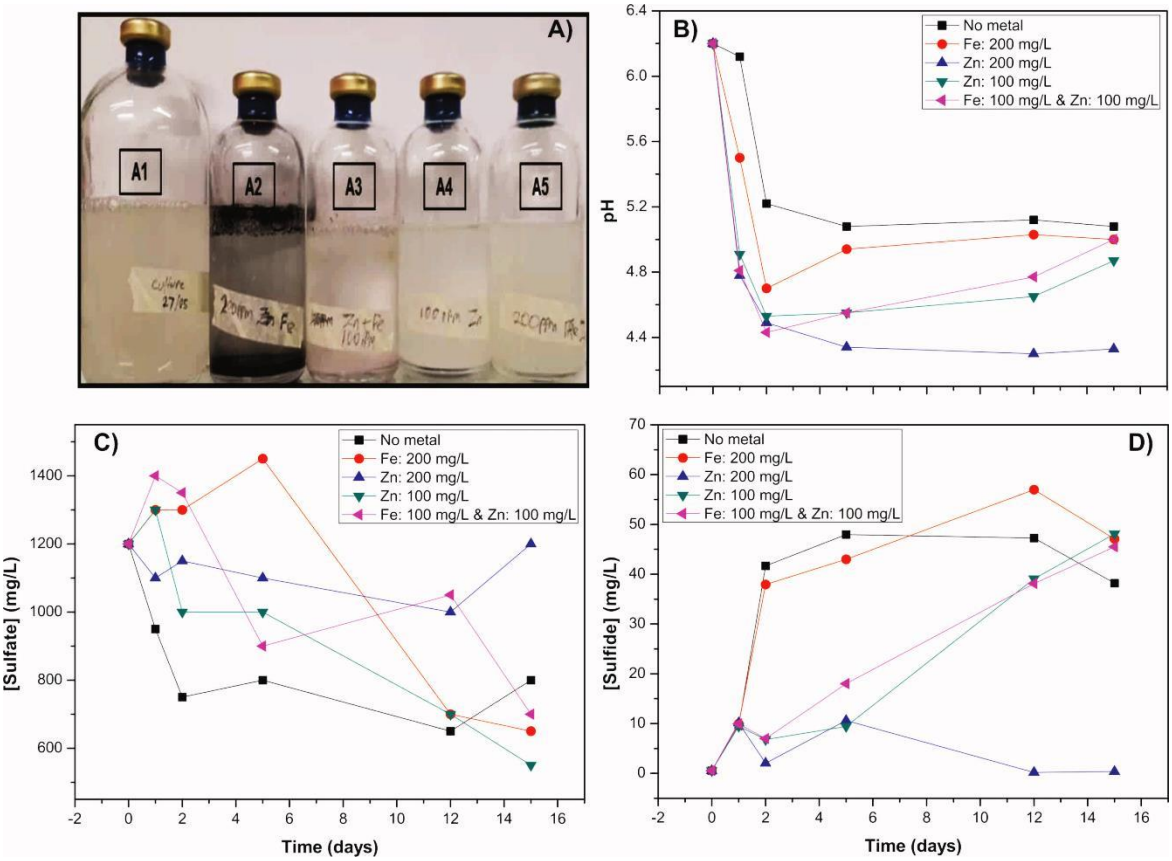

Figure 4.6: Vials containing cultures used in batch experiments of the metal effects on sulfate reduction and profiles of monitored parameters. A: Vials containing cultures at day 12. A1: Culture with no metals, A2: Culture with 200 mg/L of Fe^{2+}, A3: Culture with 100 mg/L of Fe^{2+} and 100 mg/L of Zn^{2+}, A4: Culture with 100 mg/L of Zn^{2+} and A5: Culture with 200 mg/L of Zn^{2+}. B: pH profiles, C: sulfate reduction profiles and D: sulfide formation profiles.

4.4.3. Bioreactor studies

4.4.3.1. Carbon source selection

Two carbon sources were tested for their effective usage by SRB to reduce over 2000 mg/L of sulfate in a closed automated system to maintain the optimum sulfate-reduction conditions. Sixfors bioreactors (INFORS AG-4103 Bottminingen /Switzerland) equipped with temperature, pH control and DO monitoring system was used to perform the carbon source evaluation experiments as described in section 4.3.3. The bioreactors were operated for 11 days with daily monitoring followed by

random days of analysis till day 20. The bioreactors were terminated and cultures were removed from the bioreactors into sterile vials due to the detection of an unexpected high oxygen intrusion in the reactor containing the culture growing on sodium lactate as a carbon source depicted in Figure 4.7 D. The pH in the two cultures was maintained at 6.2 with the upper limit of 6.5 and lower limit of 5.7 set to initiate the pH adjustments. The DO was monitored without any adjustments. Sulfate reduction profiles depicted in Figure 4.7 A, showed a total of 98.2% and 89% sulfate reduction in glycerol and sodium lactate containing cultures respectively. The glycerol was a better carbon source to the SRB growth as over a maximum of 2500 mg/L of sulfate was reduced compared to when using sodium lactate as a donor where over 2000 mg/L of sulfate was reduced.

The sulfate reduction was evident in both experiments. However, the sulfide formation profile depicted in Figure 4.7 B was not comparable with the sulfate reduction profiles. Stoichiometrically, it is known that sulfate reduction to sulfide formation have a ratio of 1:3 (Barton and Fauque, 2009). Since the pH was maintained at 6.2, sulfide should theoretically be in solution but results show that no significant sulfide was produced in culture growing on sodium lactate. This is possibly due to the conversion of sulfate into thiosulfate and possibly elemental sulfur instead of sulfide (Krämer and Cypionka, 1989). This phenomenon could also be due to the sulfide oxidation reaction catalysed by sulfur-oxidizing bacteria such as *Sulfuritalea hydrogenivorans* (Watanabe *et al.,* 2014). The activity of this bacterium would oxidize the sulfide to elemental sulfur or polysulfide, which could not be detected with the methylene blue method hence low sulfide concentrations in sodium lactate containing culture prevailed. The reduced sulfur species could act as electron acceptor of SRB due to the sulfate depletion in solution, therefore generating excess amounts of sulfide in the medium as observed in the culture growing on glycerol (Muyzer and Stams, 2008). In addition, the reduction process of elemental sulfur, polysulfide and sulfate to sulfide, could promote the drop in ORP to -250 mV as observed in Figure 4.7 C.

In the experiment with sodium lactate, there was an increase in the sulfide concentration on the fifth day which was insignificant but faster in the experiment with glycerol. The sulfide started declining after day 15 when sulfate was almost depleted. The decline in sulfide could be due to the sulfur-oxidizing bacteria utilizing

sulfide to promote their growth. The ORP values were stabilized after day 5 between -50 and -150 mV in sodium lactate containing culture and around -250 mV in the glycerol containing culture. This could be another reason for low sulfide detection in sodium lactate containing culture where conditions promote incomplete degradation of the carbon source and incomplete sulfate reduction resulting in other sulfur reduced species rather than sulfide (Bertolino *et al.*, 2014; Muyzer and Stams, 2008).

The sulfide generation profiles depicted in Figure 4.7 B supported the use of glycerol as the preferred carbon source. The sulfate reduction rate in both cultures was relatively high as seen in Figure 4.7 A. By day 10, both cultures had reduced over 2000 mg/L of sulfate. However, the sulfide generation rates were not comparable as the culture grown on glycerol generated 7 times more sulfide concentrations compared to the amount detected in the culture grown on sodium lactate.

The overall results showed sulfide production hindrances when using sodium lactate as the carbon source. The ability of SRB to utilize glycerol as the main carbon source to reduce over 98% of sulfate with subsequent formation of sulfide is a success in pipeline to use glycerol to grow SRB and use it as the main carbon source for future experiments.

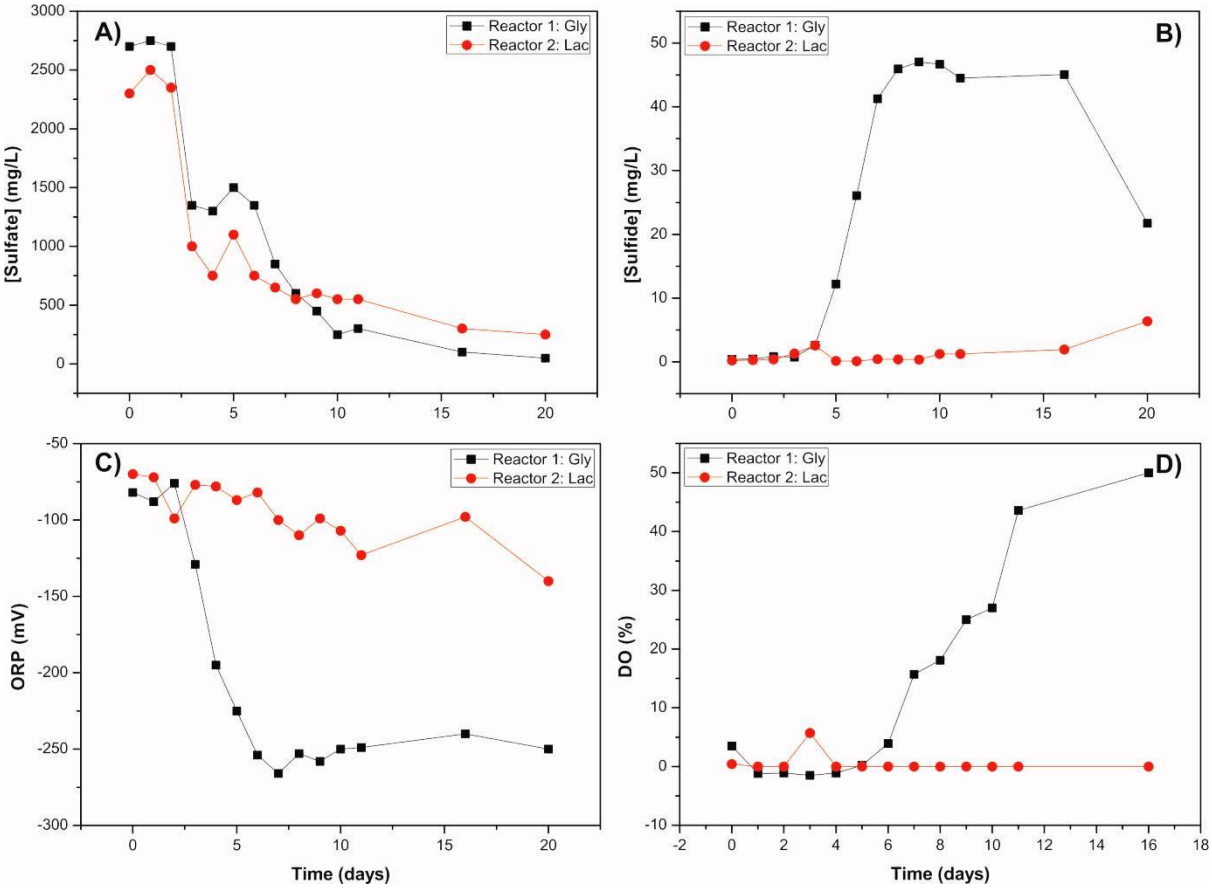

Figure 4.7: Profiles showing evolutions of parameters yielded by two cultures with different carbon sources: glycerol and sodium lactate. A: sulfate reduction profiles, B: sulfide formation profiles, C: ORP profiles and D: DO profiles.

4.4.3.2. Metal-microbe interactions

Metal-microbe interactions between SRB and high concentrations of Zn^{2+} and Fe^{2+} were studied in bioreactors at pre-determined optimum sulfate reducing conditions (pH of 6.2 and a temperature of 25ºC) in PSGM. Simultaneously, the effect of maintaining pH at 6.2 for sulfate reduction was also evaluated by growing SRB in a pH controlled environment and another without pH control. Four reactors (R1 to R4) were operated as described in section 4.3.3.2.

The conditions in R2 and R4 were better according to the preliminary experiments conducted previously in the vials. In R2, tolerance to elevated Fe^{2+} concentration (200 mg/L) at controlled pH (6.2) was evaluated whereas in R4 no metals were added and the pH of the culture was maintained at a constant range between 5.7

and 6.7. Conditions in R1 and R3 were unfavourable for sulfate reduction hence their impact on SRB was evaluated. In R1, effects of elevated concentration of Zn^{2+} (200 mg/L) at controlled pH (6.2) was evaluated whereas in R4, no metals were included in the culture and no pH was controlled.

Sulfate reduction results, represented in Figure 4.8 A, revealed 100% sulfate-reduction attained on day 11 of the incubation in the reactor containing no metals (R4) with the pH maintained at 6.2. In the same reactor (R4), highest sulfide concentrations of 57 mg/L formed as a result of complete sulfate reduction seen in Figure 4.8 B. The sulfide concentrations were produced at a faster rate after day 5 which correlated with the sulfate reduction rate at the same time interval. From day 5 onwards till day 10, sulfate was reduced till it got depleted as environmental conditions were supporting its reduction noted by the lowering of ORP from -169 mV to -304 mV seen in Figure 4.8 C which was the lowest ORP in all experiments.

The carbon source (glycerol) in this experiment was almost used completely within 10 days shown on Figure 4.8 H. An increase in ORP was observed accompanied by a rapid decline in sulfide concentration after day 10 which supports other bacterial processes such Sulfide-oxidizing bacteria (SOB) that utilizes the reduced hydrogen sulfide as well as fermentative bacteria that are capable of utilizing acetate that forms from incomplete utilization of glycerol (Willrodt *et al.,* 2014).

In R2 experiment, the second best SRB was observed where 85% of sulfate concentrations were reduced. Maximum sulfite production of over 45 mg/L which was almost similar to the trend of sulfate reduction and sulfide formation observed in R4 but at slower rates. Exponential sulfide formation was also observed between days 5 and 10 followed by a rapid decrease from over 45 mg/L of sulfide to less than 5 mg/L. According to these findings, Fe^{2+} seems to be less toxic to the enriched consortia and have a minimal impact on sulfate reduction as 100% sulfate reduction was unattainable in its presence. Depletion of the carbon source was observed at day 15 and dissolved oxygen DO showed an introduction of oxygen to a maximum of up to 30% between day 10 and 18 but had no significant effect on sulfate reduction and sulfide formation processes. The sulfide produced in the system was sufficient to precipitate almost all the Fe^{2+} as 97% of it was removed from the solution shown in Figure 4.8 F. The oxygen intrusion possibly during sampling is the reason for

dissolution of small amounts of Fe^{2+} detected between day 10 and 20 as seen on Figure 4.8 G. Concentrations of both Fe^{2+} and Fe^{3+} represented by low concentrations of total iron (F_T) were simultaneously precipitated showing minimal chances of Fe^{2+} oxidation.

In R1 and R3 containing 200 mg/L of Zn^{2+} and no metals without pH control respectively, both showed less than 40% sulfate reduction with less than 20 mg/L of sulfide production. The poor sulfate reduction and sulfide formation observed in R1 confirms the toxicity of Zn^{2+} on the activity of SRB even when the pH and temperature are optimal which is similar to what was observed in the batch experiments. In contrast to the batch experiments, Zn^{2+} concentrations were determined daily in the bioreactor studies and a maximum of 90% Zn^{2+} was removed showing that the controlled pH had positive impacts on the precipitation of zinc sulfide (ZnS). Even though 90% of Zn^{2+} was removed from the solution shown in Figure 4.8 E, over 60% of the sulfate was not reduced by the microbial activity. Low ORP values (below -150) were observed in the system which aided sulfate reduction and sulfide production which quickly reacted with dissolved Zn^{2+}, this resulted in a rapid lowering of Zn^{2+} concentrations between day 3 and 10. Fluctuations of ORP values were observed which correlated with fluctuating concentrations of sulfate, sulfide and zinc in the system. The Zn^{2+} toxicity at 200 mg/L could have also affected other bacteria which limited the utilization of carbon source. Other metals precipitation mechanisms like bioaccumulation, bio-sorption and internal bio-mineralization could have taken place.

Finally, the culture in R3 could not reduce more than 40% of the sulfate concentration due to the low pH that stabilized at between 4.5 and 5.5 as seen in Figure 4.8 D. This could mean that the bacteria metabolized glycerol at a faster rate as seen in Figure 4.8 H where glycerol was detected to be zero at day 10. This fast utilization of the carbon source could be due to the conversion of the glycerol to other forms like butyrate, propionate or acetate which is usable to other bacterial groups hence creating the carbon source utilization with SRB and other bacteria that grow anaerobically. Utilization of these converted carbon sources results in production of H^+, CO_2 and more acetate outlined in Equation 4.7 to 4.12 (Muyzer and Stams, 2008) which do not favour sulfate reduction process. ORP values in this

system dropped from -74 to -221 between day 0 and day 10 followed by a rapid increase to above -50 which does not support sulfate reduction. The low pH did affect the growth and sulfate reduction activity of SRB as it did in the batch experiments.

Equation 4.7: $Propionate^- + 3H_2O \rightarrow Acetate^- + HCO3^- + H^+ + 3H_2$

Equation 4.8: $Butyrate^- + 2H_2O \rightarrow 2Acetate^- + H^+ + 2H_2$

Equation 4.9: $Lactate^- + 2H_2O \rightarrow Acetate^- + HCO_3^- + H^+ + 2H_2$

Equation 4.10: $2Lactate^- \rightarrow 3Acetate^- + H^+$

Equation 4.11: $Acetate^- + SO_4^{2-} + 3\,H^+ \rightarrow 2\,CO_2 + 1.5\,H_2S + 2\,H_2O$

Equation4.12:

$$Butyrate^- + 1.5\,SO_4^{2-} + 3\,H^+ \rightarrow Acetate^- + 2\,CO_2 + 1.5\,H_2S + 2\,H_2O$$

The sequential trend of sulfate reduction, sulfide formation and then sulfide reduction in cultures inoculated with a consortia enriched from different environments can be attributed to the diverse bacterial groups present in the culture that perform all three processes. Similar trends were reported by Castillo and co-workers (2012) and this was attributed to SRB and methanogens present in a culture that grew under anaerobic conditions. The results in this section widen the knowledge of effects that metals and pH have on sulfate reduction process aided by SRB in an anaerobic environment.

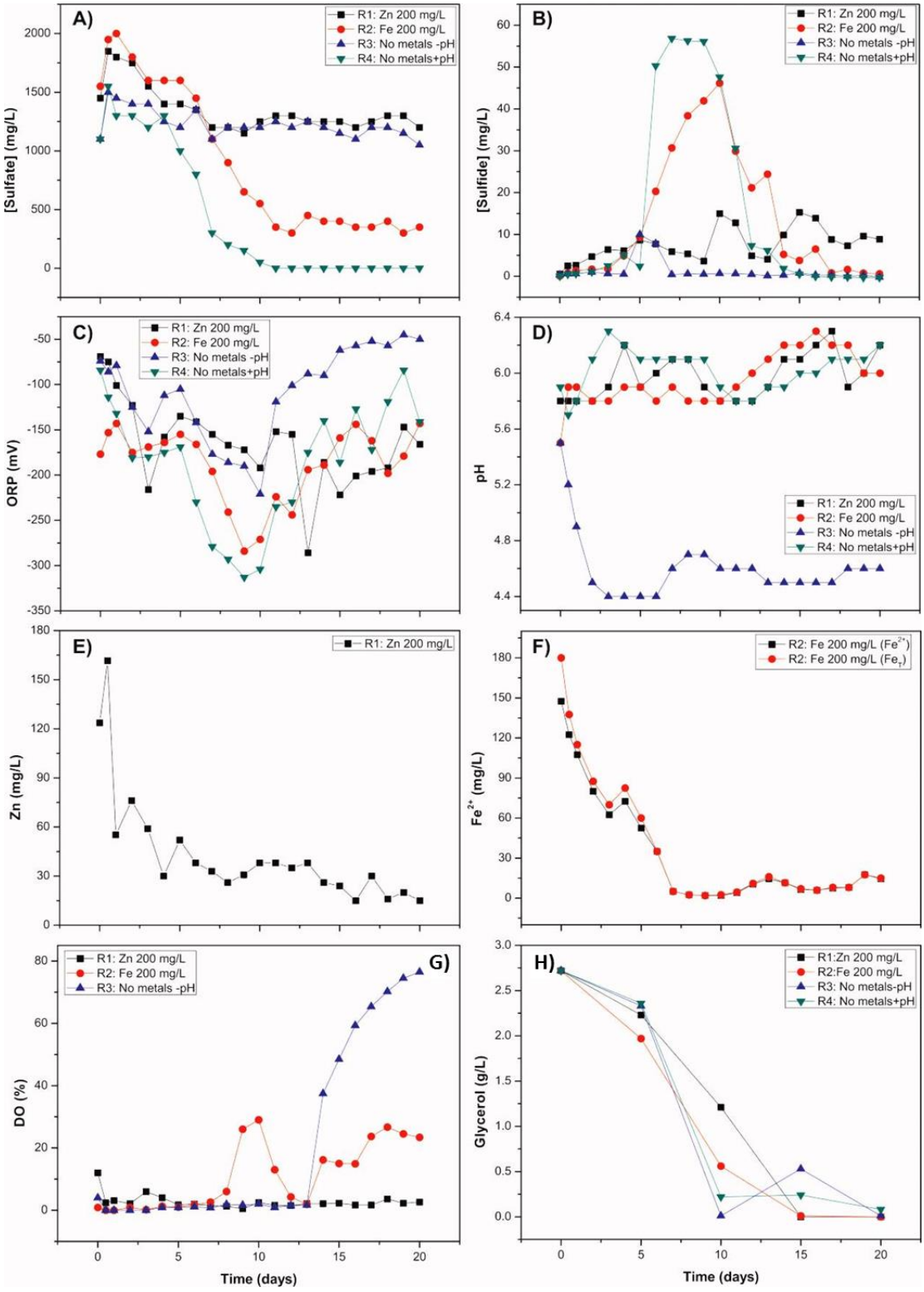

Figure 4.8: Profiles showing evolutions of parameters yielded by four cultures with different metal concentrations and pH control effects on bacterial growth. A: sulfate reduction profiles, B: sulfide generation profiles, C: ORP profiles, D: pH profiles, E: Zn^{2+} reduction profile, F: Fe^{2+} reduction profile, G: DO profiles and H: Glycerol quantification profiles done by HPLC.

4.4.3.3. Molecular analysis of metals tolerant microorganisms

4.4.3.3.1. Genomic DNA extraction and 16S rRNA amplification

Molecular analysis was done to identify dominant bacterial groups associated with higher metals concentrations and pH control. Genomic DNA was successfully extracted from the 16 samples (4: from R1, 4: from R2, 4: from R3, 4: from R4 from the reactors) and the inoculum used in the reactors.

The extracted gDNA was subjected to PCR analysis to amplify partial 16S rRNA fragments from all 17 samples as described in section 4.4.3.3.1. The amplicons with expected band size of approximately 600 base pairs (bp) are depicted in Figure 4.9 showing four groups of samples from the bioreactors collected in 5 days intervals and the inoculum amplicon. The results showed successful amplification of the partial 16S rRNA gene fragment in all samples.

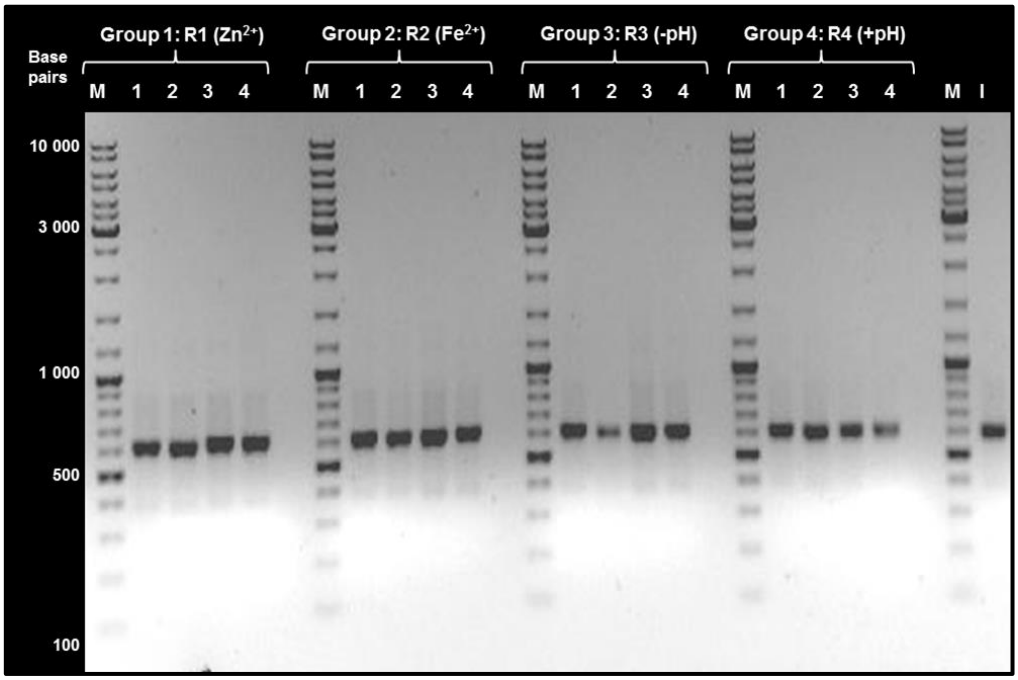

Figure 4.9: Amplificons of the 16S rRNA fragments from the extracted gDNA of bioreactor samples on a 1% (w/v) agarose gel stained with EtBr. Group 1: R1 samples, Group 2: R2 samples, Group 3: R3 samples and Group 4: R4 samples. Lane M: DNA standard Marker (O'GeneRuler^{TM} Ladder Mix), Lane 1: day 5, Lane 2: day 10, Lane 3: day 15, Lane 4: day 20 and Lane I: Inoculum used for the bioreactors.

4.4.3.3.2. Denaturation Gradient Gel Electrophoresis (DGGE)

The PCR products of the 16 reactor samples were subjected to DGGE analysis as described in section 4.3.3.3. The DGGE profiles of the metals containing samples are depicted in Figure 4.10 and the DGGE profiles for the varied pH samples are depicted in Figure 4.11. Visible and dominant bands were excised, sequenced and the sequences were subjected to BLAST analysis against the NCBI database. The sequencing results are recorded in Table 4.3 and 4.4. The first four lanes in Figure 4.10, represents microbial communities in the bioreactor which had 200 mg/L of Fe^{2+} which showed an interesting microbial shift detected by bands appearing and disappearing in lanes of samples analysed on different days. According to the sequencing results, on day 5, Iron reducing bacteria were present in the culture but it was not seen from day 10 onwards. Various microbial species like *Desulfotomaculum* sp., *Dethiosulfatibacter* sp. and *Clostridium* sp. known to contribute in the sulfate reduction process were detected in the metals containing cultures. Irrespective of the suggested toxicity of 200mg/L of Zn^{2+} on bacterial metabolism, a diverse microbial community was observed in the culture analysed represented by the last four lanes on Figure 4.10.

DGGE profiles depicted in Figure 4.11 represent the microbial communities in cultures from bioreactors without metals and varied pH controls. Microbial shifts in both cultures were not as severe as observed in the metal containing cultures. However, from a culture which its pH was controlled, represented by the last four lanes, *Clostridium beijerinkii* was detected only in day 5 and 15. DGGE profiles of the samples from the bioreactor with pH control are represented by the first four lanes of Figure 4.11, results showed thicker and visible bands showing the high concentrations of the represented microbial species (Campbell *et al*., 2009) compared to the few intense bands in the culture without pH control. This shows the positive effects of keeping pH constant to support microbial growth. Various strains of *Desulfovibrio* spp. were detected as part of the microbial communities in the pH varied bioreactors as one representative of the SRB. Some of the novel anaerobic bacteria like *Bacteroides* sp. (Hatamoto *et al.,* 2014), were also detected in the cultures showing a great diversity of the enriched consortium. Some of the unexpected enteric bacteria like *Enterobacter* sp, *Pantoea* sp and *Klebsiella* sp. all

belonging to the Enterobacteriaceae family (Delétoile *et al.,* 2009) were detected in the cultures.

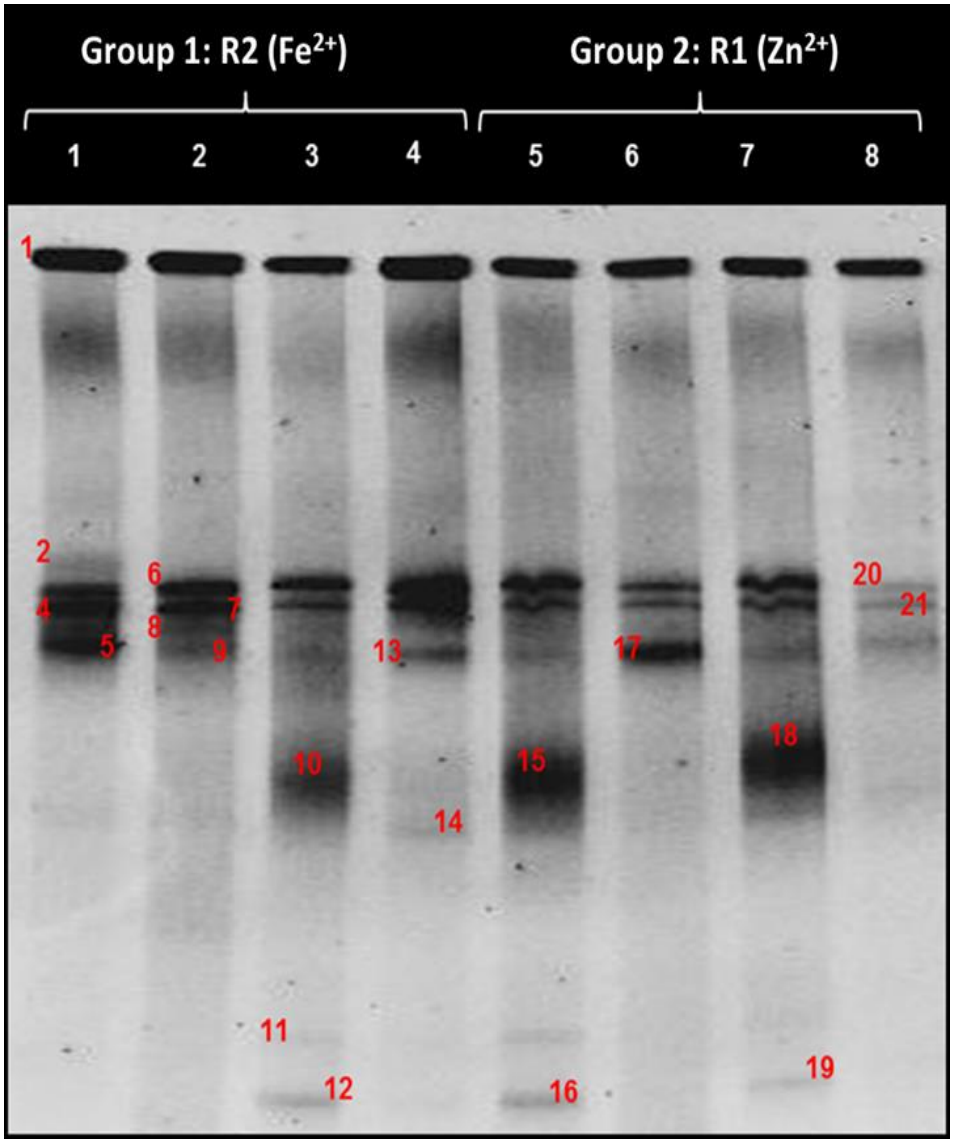

Figure 4.10: DGGE profiles of consortia incubated in reactors with metals (R1: Inoculum, 200 mg/L Zn^{2+} and pH control and R2: Inoculum, 200 mg/L Fe^{2+} and pH control).

Group 1 (Fe^{2+}): Lane 1: R2 – day 5, Lane 2: R2 – day 10, Lane 3: R2 – day 15, Lane 4: R2 – day 20.

Group 2 (Zn^{2+}): Lane 5: R1 – day 5, Lane 6: R1 – day 10, Lane 7: R1 – day 15, Lane 8: R1 – day 20.

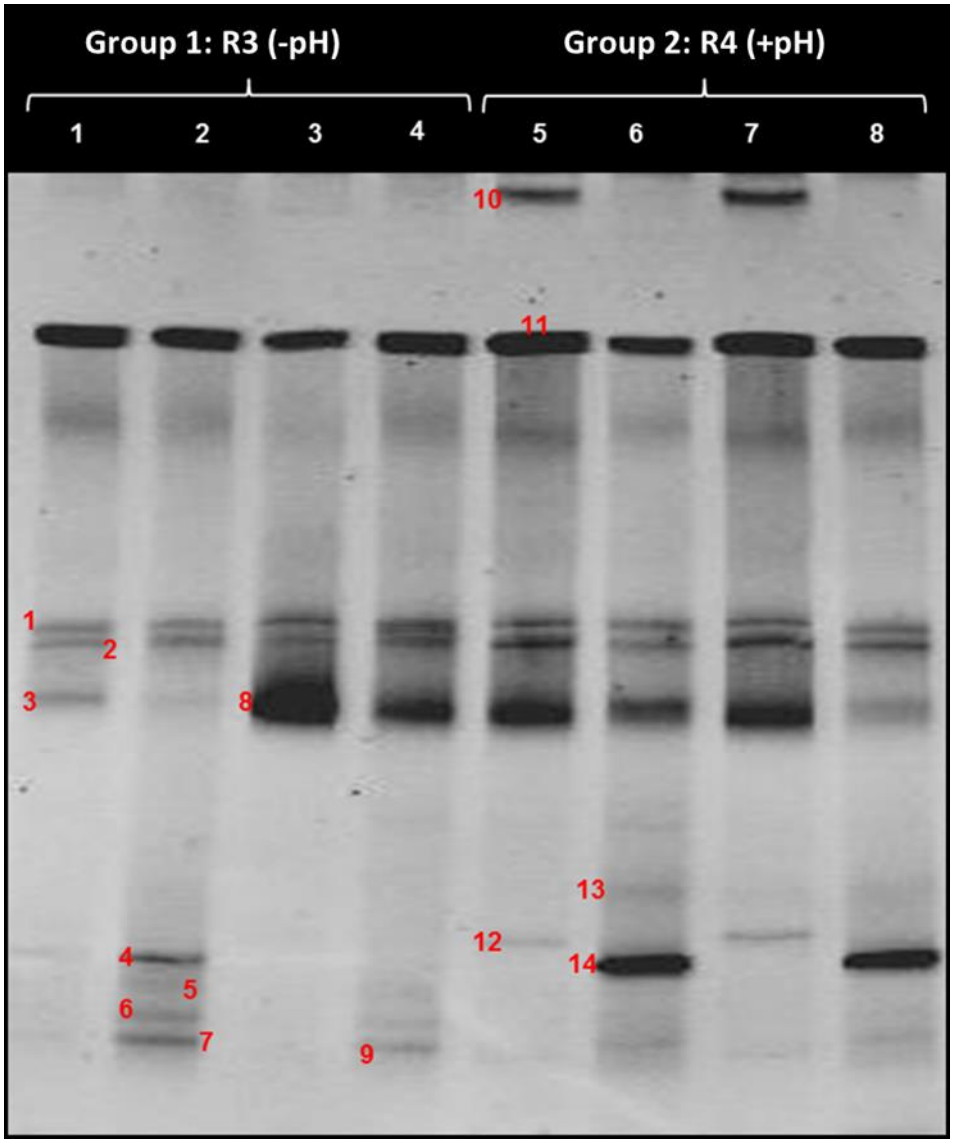

Figure 4.11: DGGE profiles of consortia incubated in reactors with (R3: Inoculum, no metals and no pH control and R4: Inoculum, no metals and pH control).
Group 1 (-pH): Lane 1: R3 – day 5, Lane 2: R3 – day 10, Lane 3: R3 – day 15, Lane 4: R3 – day 20.
Group 2 (+pH): Lane 5: R4 – day 5, Lane 6: R4 – day 10, Lane 7: R4 – day 15, Lane 8: R4 – day 20.

Table 4.3: Sequencing results obtained from the BLAST analysis for samples obtained from bioreactors with metals (R1 and R2).

Band N.o	Accession N.o	Description	E-Value	Max ID %
1	NR_125463.1	*Bacteroides luti* strain UasXn-3 16S ribosomal RNA gene, partial sequence	8.00E-88	88%
2	FJ269062.1	Iron-reducing bacterium enrichment culture clone HN56 16S ribosomal RNA gene sequence	1.00E-157	87%
4	KC011365.1	Uncultured anaerobic bacterium clone OTU18 16S ribosomal RNA gene, partial sequence	0	93%
5	NR_029315.1	*Anaerofilum agile* strain F16S ribosomal RNA gene, partial sequence	2.00E-10	93%
6	NR_111998.1	*Pantoea agglomerans* strain JCM1236 16S ribosomal RNA gene, partial sequence	0.00E+00	95%
7	NR_041309.1	*Dethiosulfatibacter aminovorans* strain C/G2 16S ribosomal RNA gene, complete sequence	1.00E-38	80%
8	NR_026409.1	*Desulfotomaculum guttoideum* strain DSM 4024 16S ribosomal RNA gene, partial sequence	3.00E-64	76%
9	NR_125464.1	*Anaerobacterium chartisolvens* strain T-1-35 16S ribosomal RNA gene, partial sequence	1.00E-142	85%
10	NR_116574.1	*Vagococcus acidifermentans* strain AC-1 16S ribosomal RNA geen, partial sequence	7.00E-34	90%
11	HE610795.1	*Raoultella planticola* partial 16S rRNA gene, strain BD18C2ACC-S22	0.00E+00	99%
12	GQ417196.1	Uncultured *Raoultella* sp. clone F1Sjun.33 16S ribosomal RNA gene, partial sequence	0.00E+00	99%
13	AB742106.1	Uncultured Firmicutes bacterium gene for 16S rRNA partial sequence, clone: BS-B7	0.00E+00	99%
14	KC331191.1	*Clostridium* sp. BEN5 16S ribosomal RNA gene, partial sequence	0.00E+00	99%
15	KM822773.1	*Enterococcus faecalis* 16S ribosomal RNA gene, partial sequence	6.00E-30	94%
16	FJ432002.1	*Klebsiella* sp. HQ-3 16S ribosomal RNA gene partial sequence	0.00E+00	99%

17	JX575923.1	Uncultured *Pseudoflavonifractor* sp. clone b10-114 16S ribosomal RNA gene, partial sequence	0.00E+00	99%
18	AB854169.1	*Enterococcus faecalis* gene for 16S ribosomal RNA, partial sequence, strain: ALS13	0.00E+00	100%
19	HE610792.1	*Raoultella planticola* partial 16S rRNA gene, strain BD18C2ACC-S08	0.00E+00	99%
20	JN371682.1	Uncultured Firmicutes bacterium clone C3-27 16S ribosomal RNA gene, partial sequence	1.00E-07	95%
21	CP006777.1	*Clostridium beijerinckii* ATTCC 35702, complete genome	0.00E+00	99%

Table 4.4: Sequencing results obtained from the BLAST analysis for samples obtained from bioreactors with and without pH control (R3 and R4).

Band N.o	Accession N.o	Description	E-Value	Max ID %
1	FJ269054.1	Iron-reducing bacterium enrichment culture clone HN19 16S ribosomal RNA gene, partial sequence	1-138	84%
2	KF726918.1	Uncultured bacterium clone ANS_TL2F07 16S ribosomal RNA gene, partial sequence	0	90%
3	AB742106.1	Uncultured Firmicutes *bacterium* gene for 16S rRNA, partial sequence, clone: BS-B7	0	84%
4	FJ865473.1	*Desulfovibrio* sp. 12ML3 16S ribosomal RNA gene, partial sequence	2.00E-26	83%
5	AY691544.1	*Pantoea agglomerans* strain ChDC YP2 16S ribosomal RNA gene, partial sequence	0	99%
6	KM253185.1	*Enterobacter* sp. ST 2-11 16S ribosomal RNA gene, partial sequence	0	99%
7	LK391629.1	*Enterobacter cloacae* partial 16S rRNA gene, isolate L2	0	100 %
8	KC873196.1	Uncultured bacterium clone S43_023 16S ribosomal RNA gene, partial sequence	3.00E-34	88%
9	CP006777.1	*Clostridium beijerinckii* ATCC 35702, complete genome	0	99%
10	AF079506.1	*Denitrobacterium detoxificans* strain NPOH3 16S ribosomal RNA gene, complete sequence	0	95%
11	KM495668.1	*Vibrio alginolyticus* strain PASKS160 16S ribosomal RNA geen, partial sequence	3.00E-09	78%

12	KF601943.1	*Desulfovibrio* sp. C1 16S ribosomal RNA gene, partial sequence	0	95%
13	JQ316226.1	*Rhodococcus* sp. AMF3539 16S ribosomal RNA gene, partial sequence	0	99%
14	KF536746.1	*Desulfovibrio marrakechensis* strain HAQ-7 16S ribosomal RNA gene, partial sequence	0	99%

4.4.3.4. Morphological and mineralogical characterization of precipitates

Samples collected at the end of the bioreactor operations depicted in Figure 4.12, were subjected to mineralogical characterization. The dried samples were prepared as described in section 4.3.3.4.1 and subjected to analysis by SEM-EDS, TEM-EDS and XRD.

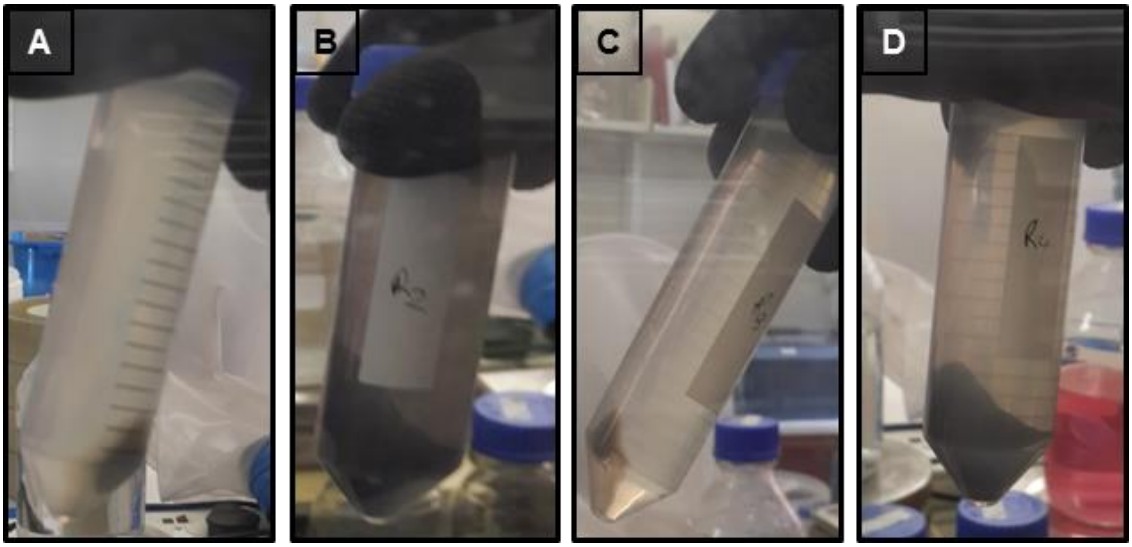

Figure 4.12: Centrifuged samples before lyophilisation. A: R1 (Inoculum, 200 mg/L Zn^{2+} and pH control), B: R2, (Inoculum, 200 mg/L Fe^{2+} and pH control), C: R3 (Inoculum, no metals and no pH control) and D: R4 (Inoculum, no metals and pH control).

4.4.3.4.1. Scanning Electron Microscopy coupled to Energy Dispersed X-ray Spectroscopy (SEM-EDS)

SEM was used to study the morphological properties and metal-microbe interactions as described in section 4.3.3.4.2. The backscattering mode of the SEM was used to capture the micrographs of particles with more density than brightness and can be differentiated easily by this mode. The EDS function of the SEM was used to quantify the elemental compositions of the precipitates.

SEM micrographs and EDS spectrum of R1 (200 mg/L of Zn^{2+}) sample analysis are shown in Figure 4.13. Two different bacterial cells are observed in Figure 4.13 A and B indicated with red arrows, one with white particles around it and the other with white particles on it. The white colour represents metals when using the backscattering mode of SEM (Castillo *et al.,* 2012). The mechanism of metal precipitation around the microbial cells is called bio-mineralization which is an indirect microbial metals precipitation strategy. This happens when the microbial cell releases by-products from their metabolic activities which react with dissolved metal ions around them demonstrated in Figure 4.13 A (Spadafora *et al.,* 2010). In contrast, precipitation mechanism where metal ions are associated with the bacterial cells is called biosorption and is demonstrated in Figure 4.13 B (Suzuki and Banfield, 2004). This happens when the metal ions adhere to the microbial cell through precipitation with lipids in the bacterial cell walls (Dunham-Cheatham *et al.,* 2011). Bioaccumulation is possible in this case where the metal ions pass through the cell wall and membrane to form precipitates within the microbial cell. These mechanisms have been previously reported by Vaughan and Lloyd (2011). Figure 4.13 B, shows particles similar to those observed by Matlakowska and co-workers (2012) which were identified as zinc sulfide precipitates. Figure 4.13 B was further magnified to Figure 4.13 C and single targeted particle indicated by a red circle on the bacterium cell was analysed with EDS to determine the elemental compositions of the particle. EDS spectrum results analysis are shown in Figure 4.13 D which revealed the elemental composition of the precipitates summarised in Table 4.5. Dominant elements in the particle were phosphate, oxygen, iron and zinc which proves that the precipitates were formed from mainly zinc which was present in higher concentrations.

Beside the highest zinc content in the precipitates, the phosphate and oxygen were also present in high quantities showing the possibility of the particles being generated from the organic compounds and microbial cell wall. As expected, zinc (highlighted in blue) was the most dominant metal in the composition of the precipitates followed by low concentrations of iron probably from the inoculum. Sulfur was also detected in the precipitates which is probably from the SRB activity during the sulfate reduction process. The high concentrations of sodium and chloride in the precipitates are from the NaOH and HCl titrated in the bioreactor to balance the pH during the 20 days operation period. The results showed successful microbial Zn^{2+} precipitation in a batch operated bioreactor with optimum sulfate reduction conditions.

SEM-EDS micrographs of R2 (200 mg/L of Fe^{2+}) sample analysis are depicted in Figure 4.14 A-B showing various bacterial morphologies and metal precipitates. The morphological properties of metal precipitates depicted in these micrographs were previously observed by Folk (2005) during studies on pyrite formation and they were identified as dispersed grains from framboidal pyrite which are the precursor particles in pyrite formation observed specifically in Figure 4.14 B. The section with framboidal particles was magnified and one particle was analysed by EDS (on the circled area) of Figure 4.14 C to identify the elemental composition of the particles. The EDS spectrum from Figure 4.14 C is depicted in Figure 4.14 D and the quantified components of the precipitates are outlined in Table 4.6. Iron was the only transition metal detected in the EDS results (highlighted in orange) as expected which confirms the morphological analysis of the precipitates. The EDS results also show total iron in the precipitates to comprise over 60% of the components. The presence of iron and sulfur (highlighted in yellow) served as a confirmation that the precipitate contain iron sulfide, with additional elements acquired from the PSGM. As observed in the zinc sample analysis, sodium and chloride were also dominant as a result of pH control.

SEM micrographs of R3 and R4 (no metals) samples analysis are depicted in Figure 4.15 A to C. All micrographs showed highly compact biofilms observed with precipitates of different sizes and shapes. Figure 4.15 A was captured without the backscatter mode which resulted in its dull intensity while Figure 15 B and C had

brighter colours indicating presence of precipitated metals in low concentrations according to visual analysis. The various microbial morphologies observed in these samples reveals the consortium complexity observed in previous microscopic analysis of the enrichments.

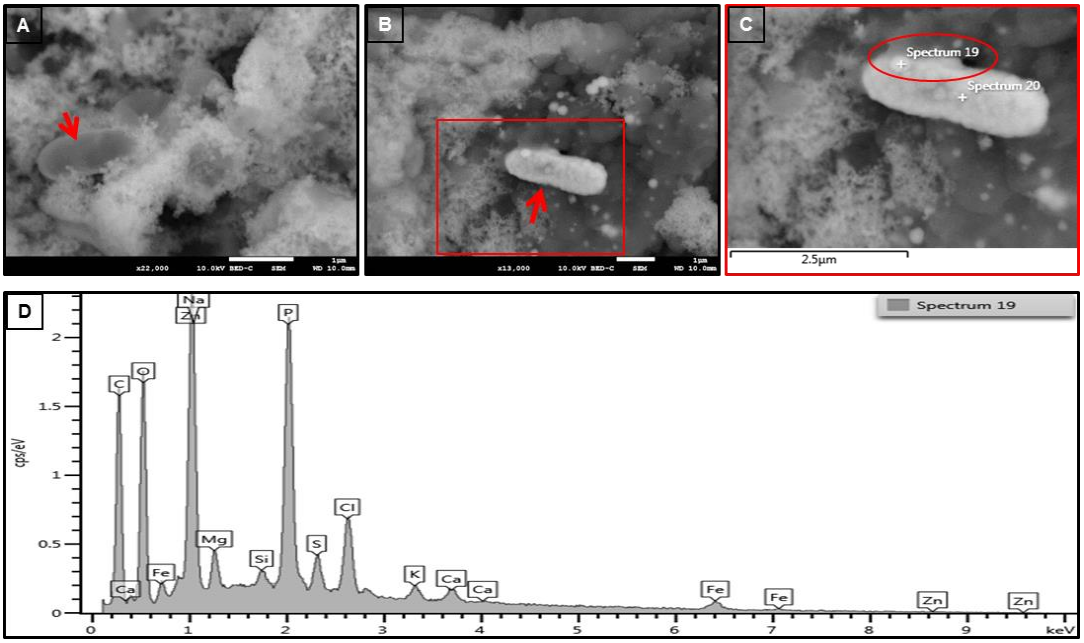

Figure 4.13: SEM micrographs and EDS spectrum of sample harvested from a bioreactor with 200 mg/L of Zn^{2+} (R1). A and B: SEM micrographs showing bacterial cells, C: magnified red square in B and D: SEM-EDS analysis spectrum of the circled particle.

Table 4.5: SEM-EDS results showing elemental composition of the precipitates in the Zn^{2+} sample (R1).

Element	Apparent Concentration	Wt%
O	2.19	19.49
Na	0.54	5.15
Mg	0.18	2.39
Si	0.08	0.95
P	2.6	20.56
S	0.27	3.3
Cl	0.68	8.38
K	0.19	2.12
Ca	0.22	2.49
Fe	0.84	11.74
Zn	1.25	23.42
Total:		100

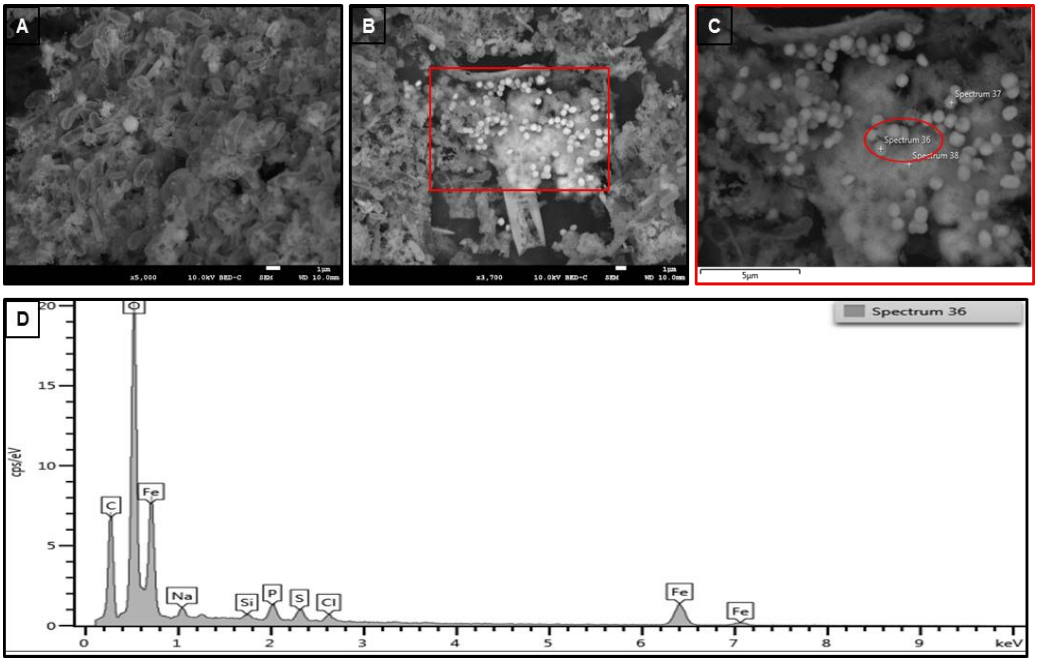

Figure 4.14: SEM micrographs and EDS spectrum of sample harvested from a bioreactor with 200 mg/L of Fe^{2+} (R2). A and B: SEM micrographs, C: magnified red square in B and D: SEM-EDS analysis spectrum of the circled particle in C.

Table 4.6: SEM-EDS results showing elemental composition of the precipitates in the Fe^{2+} sample (R2).

Element	Apparent Concentration	Wt%
O	8.87	30.46
Na	0.19	1.49
Si	0.07	0.53
P	0.47	2.36
S	0.26	1.85
Cl	0.16	1.21
Fe	7.21	62.11
Total:		100.00

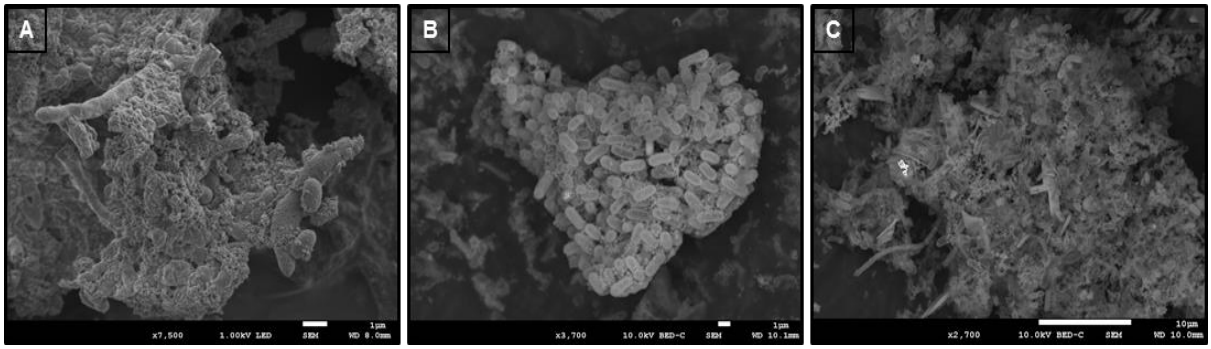

Figure 4.15: SEM micrographs of samples harvested from bioreactors with no metals. A to C: SEM micrographs showing bacterial biofilm from the bioreactors (R3 and R4).

4.4.3.4.2. Transmission Electron Microscopy coupled to Energy Dispersed X-ray spectroscopy (TEM-EDS)

Zn^{2+} containing sample from R1 was analysed further by TEM with the aim of determining the effect Zn^{2+} had on bacterial cells according to section 4.3.3.4.3. Bacterial cells with different morphologies were observed under the TEM as depicted in Figure 4.16 A and B. Short filamentous shaped bacteria with different colour intensities were observed. The dark colour appearing on the TEM micrograph means that the particles are solid enough to inhibit electrons from passing freely through them (Azobou *et al.,* 2007) thus the darker bacterial cells contain metals where there are black spots or shading indicated by red arrows. In TEM micrograph A, the bacterial cell is entirely black indicating precipitation of metals over the cell wall and presumably within the cell. The two microbial metal precipitation mechanisms (biomineralization and biosorption or bioaccumulation) observed during the SEM analysis were also observed in the TEM analysis. Elevated Zn^{2+} concentrations in bioaccumulation can lead to rapid cell death because of the excess zinc ions precipitating within the cell (Azabou *et al.,* 2007; Voughan and Lloted, 2011). The bacterial cell in TEM micrograph B, indicated by a blue arrow, contained black spots inside the cell showing the immobilization of metals within its cell wall also precipitated metals through the bioaccumulation mechanism. Qualitative analysis of the encircled particle was done by TEM-EDS and according to the summarized estimates of elemental concentrations in Table 4.7, zinc was found to comprise over 50% of the precipitate components which is what was expected, however not in such

high concentrations. The TEM results further proved the successful microbial metal precipitation which was also observed by SEM analysis.

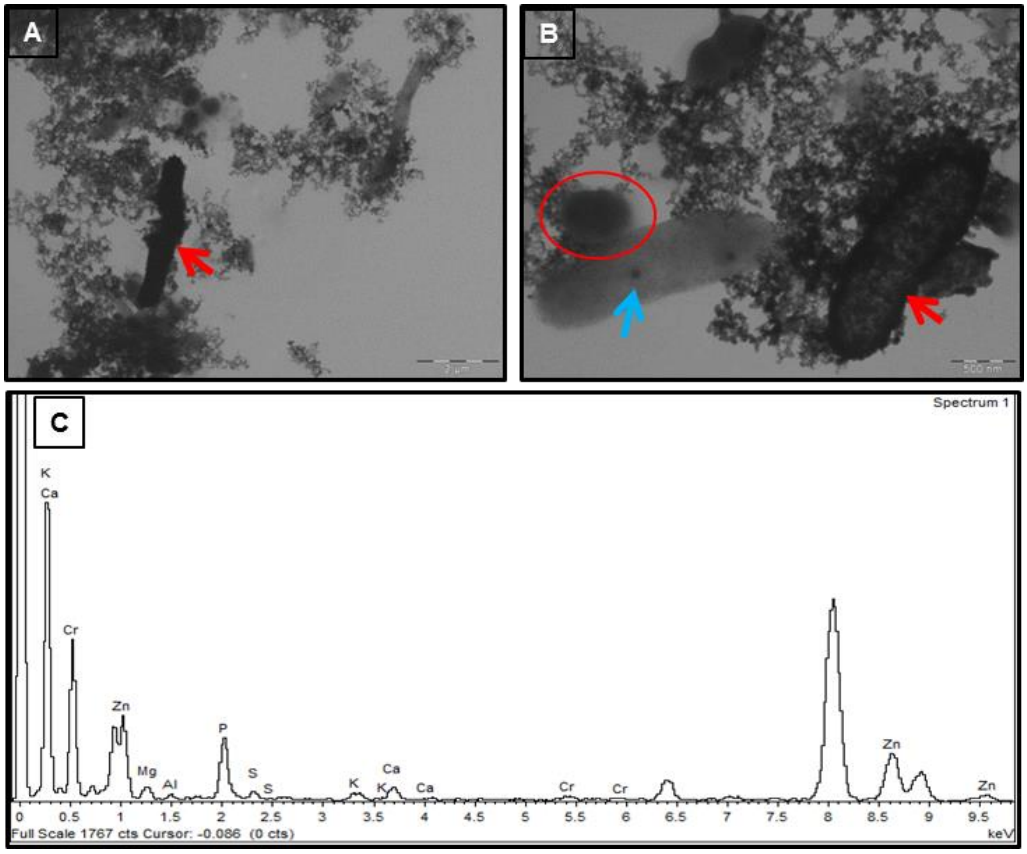

Figure 4.16: TEM micrographs and EDS spectrum of Zn^{2+} containing sample from a bioreactor with 200 mg/L of Zn^{2+} (R2). A and B: TEM micrographs, C: TEM-EDS analysis spectrum of the encircled area in red.

Table 4.7: TEM-EDS results showing elemental composition of the precipitates in the Zn^{2+} containing sample analysed on spectrum.

Element	Weight%	Atomic%
Mg K	4.48	8.1
Al K	1.78	2.89
P K	25.93	36.79
S K	3.16	4.33
K K	3.36	3.78
Ca K	5.84	6.4
Cr K	2.55	2.16
Zn K	52.9	35.56
Totals	100	

4.4.3.4.3. X-Ray Diffraction analysis

The phase crystalline minerals contained in the samples from the experiments with metals were analysed by XRD as described in section 4.3.3.4.4. In the experiment where Zn^{2+} was involved, neoformed phase minerals were evaluated and identified by the use of XRD. Phase mineral such as Wurtzite with a chemical formula of ZnS was detected when the zinc containing sample was analysed. This is one of the phase minerals that form zinc precipitates before sphalerite (ZnS) could form completely. Halite (NaCl), was detected in the analysis indicating formation of precipitates from other medium components rather than the metal sulfides precipitates. The results correlated with the SEM data which both confirm the existence of biogenic sulfate-reduction and metals precipitation. XRD results for the Fe^{2+} containing sample, revealed the presence of vivianite with a chemical formula of $Fe_3(PO_4)_2.8H_2O$. Similar to the Zn^{2+}, the vivianite is a phase mineral which forms from the iron precipitates with other medium components before pyrite could form. The phase minerals detection by XRD, further validates the biologically induced metal precipitation in an anaerobic condition.

4.5. Conclusions

In this chapter, the behaviour of anaerobic sulfate reducing communities were evaluated under harsh and moderate to optimal conditions to understand the adaptation processes involved during sulfate reduction. The sulfate reduction reaction is a complex process and as a result, can be affected by a variety of parameters. The sulfate concentrations, pH, temperature, the availability and type of electron donor, as well as metals and sulfide all can have inhibitory effect on sulfate reduction.

Initially, the enriched consortia were evaluated for sulfate reduction capabilities by being exposed to higher sulphate concentrations (2000 to 4000 mg/L). The SRB showed positive response to high sulfate concentrations, although, the sulfate reduction percentages did not exceed 72%. Furthermore, it was confirmed that the sulfate reducing activity improved when the sulphate concentrations were increased in batch experiments. This meant that the metabolisms of the SRB improved when the bacteria were stressed with high sulfate concentrations.

The inhibitory effects of pH and temperature on the sulfate reduction reactions play crucial roles in the SRB growth. According to the selected temperature (10-25ºC) and pH (3.5-6.2) used in the experiments, low pH was found to be more inhibitory to sulfate reduction even at higher temperature (25ºC). In experiments with pH of 6.2, bacterial growth and activity were optimal at 25ºC while the negative effects of low pH and low temperature were observed. Signs of other bacterial growth rather than SRB were observed at optimal temperature (25ºC) that co-habited with SRB since the inoculum used was a consortium of enrichments. Because of this, the utilization of the carbon source amongst the bacteria could have been the reason for poor sulfate reduction.

The availability and type of electron donor was among the factors evaluated for sulfate reduction processes and SRB growth. Two carbon sources were tested: glycerol and lactate, in PSGM with sulfate concentrations of more than 2000 mg/L. The bioreactors were operated in regulated environmental conditions (pH range of 5.7 and 6.5 and temperature of 25ºC). The results showed that glycerol was a better carbon source for the bacterial community under evaluation.

Finally, the effects of Zn^{2+} and Fe^{2+} on sulfate reduction were evaluated in both serum vials and bioreactor (with pH and temperature control) experiments with maximum concentrations of 200 mg/L of both metals. The conditions in the reactors improved the sulfate reduction results with subsequent precipitation of up to 97% of Fe^{2+} and 90% of Zn^{2+} zinc from the solution. Metal inhibitory effects on sulfate reduction were more in Zn^{2+} containing experiments where less than 40% of sulfate was reduced compared to 85% of the sulfate reduced in Fe^{2+} containing experiments. However, with the same inoculum, 100% sulfate reduction was achieved where no metals were added in a bioreactor operated at 25ºC with a pH of 6.2. Molecular analysis of the cultures revealed the presence of various SRB species and other bacteria that cohabited with SRB in these conditions.

Metal sulfide precipitates were characterized by SEM, TEM and XRD where evidence of biogenic metal precipitation was confirmed. Framboidal pyrite and shpalerite precursors were identified using SEM-EDS and their identification was confirmed by TEM with micrographs showing varied precipitation mechanisms of SRB. Metal compounds such as wurtzite and vivianite were detected with XRD showing definite Zn^{2+} and Fe^{2+} biologically induced precipitation. The acquired knowledge from this study can be applied in the upscaling of the sulfate reduction processes as a contributing process of biological AMD remediation. The data can also be used to formulate the equations to model the upscaling systems.

4.6. References

- **Azabou, S., Mechichi, T. and Sayadi, S.** (2007) Zinc precipitation by heavy-metal tolerant sulfate-reducing bacteria enriched on phosphogypsum as a sulfate source. *Mineral Engineering* **20(2):** 173 – 178.
- **Babich, H. and Stotzky, G.** (1978) Toxicity of zinc to fungi, bacteria and coliphages: Influence of Chloride Ions. *Applied and Environmental Microbiology* **36(6):** 906 – 914.
- **Baker, B. J. and Banfield, J. F.** (2003) Microbial communities in acid mine drainage. *Federation of European Microbiological Societies* **44:** 139 – 152.
- **Barton, L. L. and Fauque, G. D.** (2009) Biochemistry, physiology and biotechnology of sulfate-reducing bacteria. *Advances in Applied Microbiology* **68:** 41 – 88.
- **Baumgartner, L. K., Reid, R. P., Dupraz, C., Decho, A. W., Buckley, D. H., Spear, J. R., Przekop, K. M. and Visscher, P. T.** (2006) Sulfate reducing bacteria in microbial mats: Changing paradigms, new discoveries. *Sedimentary Geology* **185:** 131 – 145.
- **Bertolino, S. M., Melgaco, l. A., Sá, R, G. and Leão, V. A.** (2014) Comparing lactate and glycerol as a single-electron donor for sulfate reduction in fluiized bed reactors. *Biodegradation* **25(5):** 719 – 733.
- **Bosso, O., Lascourreges, J. F., Le Borgne, F., Le Goff, C. and Magot, M.** (2009) Characterization by culture and molecular analysis of the microbial diversity of a deep subsurface gas storage aquifer. *Research in Microbiology* **160(2):** 107 – 116.
- **Brown, C., Coates, J. and Schoonen, M. A. A.** (1999) Localized sulfate-reducing zones in a coastal plain aquifer. *Ground Water* **37(4):** 505 – 516.
- **Campbell, J. H., Clark, J. S. and Zak, J. C.** (2009) PCR-DGGE comparison of bacterial community in fresh and archived soil sampled along a Chihuahuan desert elevational gradient. *Microbial Ecology* **57:** 261 – 266.
- **Castillo, J., Pérez-López, R., Caraballo, M. A., Nieto, J. M., Martins, M., Costa, M. C., Olías, M., Cerón, J. C. and Tucoulou, R.** (2012) Biologically-induced precipitation of sphalerite-wurtzite nanoparticles by sulfate-reducing

bacteria: Implications for acid mine drainage treatment. *Science of the Total Environment* **423:** 176 – 184.

- **Castro, H. F., Williams, N. H. and Ogram, A.** (2000) Phylogeny of sulfate-reducing bacteria. *Federation of European Microbiological Societies* **31:** 1 – 9.
- **Cerasi, M., Ammendola, S. and Battistoni, A.** (2013) Competition for binding in the host-pathogen interaction. *Frontiers in cellular and Infection Microbiology* **3:** 1 – 7.
- **Chapelle, F., Bradley, P. M. Thomas, M. A. and McMahon, P. B.** (2009) Distinguishing iron-reducing from sulfate-reducing conditions. *Ground Water* **47(2):** 300 – 305.
- **Christensen, B. B., Haagensen, J. A. J., Heydorn, A. and Molin, S.** (2002) Metabolic commensalism and competition in a two-species microbial consortium. *Applied and Environmental Microbiology* **68(5):** 2495 – 2502.
- **Davison, W.** (1991) The solubility of iron sulphides in synthetic and neutral waters at ambient temperatures. *Aquatic Sciences* **53(4):** 309 – 321.
- **Delétoile, A., Decré, D., Courant, S., Passet, V., Audo, J., Grimont, P., Arlet., G. and Brisse, S. (2009**) Phylogeny and identification of *Pantoea* species and typing of *Pantoea agglomerans* strain by multilocus gene sequencing. *Journal of Clinical Microbiology* **53(2):** 300 – 310.
- **Dunham-Cheatham, S., Rui, X., Bunker, B., Menguy, N., Hellmann, R. and Fein, J.** (2011) The effect of non-metabolizing bacterial cells on the precipitation of U, Pb and Ca phosphate. *Geochemica et Cosmochimica Acta* **75:** 2828 – 2847.
- **Folk, R. L.** (2005) Nannobacteria and the formation of framboidal pyrite: Textural evidence. *Hhh***14(3):** 369 – 374.
- **Fortin, D., Rioux, J. P. and Roy, M.** (2002) Geochemistry of iron and sulfur in the zone of microbial sulfate reduction in mine tailings. *Water, Air and Soil Pollution: Focus* **2(3):** 37 – 56.
- **Gadd, G. M.** (2010) Metals, minerals and microbes: geomicrobilogy and bioremediation. *Microbiology* **156:** 609 – 643.
- **Haferburg, G. and Kothe, E.** (2007) Microbes and metals: interactions in the environment. *Journal of Basic Microbiology* **47(6):** 453 – 467.

- **Harrison, J. J., Ceri, H. and Turner, R. J.** (2007) Multimetal resistance and tolerance in microbial biofilms. *Nature Reviews Microbiology* **5:** 928 – 938.
- **Hatamoto, M.**, **Kaneshiqe, M., Nakamura, A. and Yamaquchi, T.** (2014) Bacteroides luti sp. nov., an anaerobic, cellulolytic and xylanolytic bacterium isolate from methanogenic sludge. *International Journal of Systematic and Evolutionary Microbiology* **64(5):** 1770 – 1774.
- **Hoek, J., Canfield, D., Reysenbach, A. L. and Iverson, L.** (2006) A Bioreactor for growth of sulphate-reducing bacteria: online estimation of specific growth rate and biomass for the deep-sea hydrothermal vent thermophile *Thermodesulfatator indicus. Microbial Ecology* **58:** 470 – 478.
- **Irving, H. and Williams, R. J. P.**(1948) Order of stability of metals complexes. *Nature* **162:** 746 – 747.
- **Kakooei, S., Ismail, M. C. and Ariwahjoedi, B.** (2012) Mechanism of microbiologically influenced corrosion: A Review. *World Applied Sciences Journal* **17(4):** 524 – 531.
- **Kobylin, P. M., Sippola, H. and Taskinen, P. A.** (2011) Thermodynamic modelling of aqueous Fe(II) sulfate solutions. *CALPHAD: Computer Coupling of Phase Diagrams and Thermodynamics* **35:** 499 – 511.
- **Kojima, H. and Fukuli, M.** (2011) Sulfuritalea hydrogenivorans gen. nov., sp. nov., a facultative autotroph isolated from a freshwater lake. *International Journal of Systematic and Evolutionary Microbiology* **61:** 1651 – 1655.
- **Krämer, M. and Cypionka, H.** (1989) Sulfate formation via ATP sulfurylase in thiosulfate-and sulfite-disproportionating bacteria. *Archives of Microbiology* **151(3):** 232 – 237.
- **Luef, B., Fakra, S. C., Csencsits, R., Wrighton, K. C., Williams, K. H., Wilkins, M. J., Downing, K. H., Long, P. E., Comolli, L. R. and Banfield, J. F.** (2013) Iron-reducing bacteria accumulate ferric oxyhydroxide nanoparticle aggregates that may support planktonic growth. *The International Society for Microbial Ecology Journal* ***7*****:** 338 – 350.
- **Matlakowska, R., Sktodowska, A. and Nejbert, K.** (2012) Bioweathering of kupferschiefer black shale (Fore-Suetic Monocline, SW Polan) by indigenous bacteria: implication for dissolution and precipitation of minerals in deep

underground mine. *Federation of European Microbiological Societies* **81:** 99 – 110.

- **McDevitt, C. Ogunniyi, A. D., Valkov, E., Lawrence, M. C., Kobe, B., McEwan, A. G. and Paton, J. C.** (2011) A molecular mechanism for bacterial susceptibility to zinc. *Plos Pathogens* **7(11):** 1 – 9.
- **Moosa, S., Nemati, M. and Harrison, S. T. L.** (2002) A kinetic study on anaerobic reduction of sulphate, Part I: Effect of sulphate concentration. *Chemical Engineering Science* **57:** 2773 – 2780.
- **Moosa, S., Nemati, M. and Harrison, S. T. L.** (2005) A kinetic study on anaerobic reduction of sulphate, part II: incorporation of temperature effects in the kinetic model. *Chemical Engineering Science* **60:** 3517 – 3524.
- **Moreau, J. W., Fournella, J. H. and Banfield, J. F.** (2013) Quantifying heavy metals sequestration by sulfate-reducing bacteria in an acid mine drainage-contaminated natural wetland. *Frontiers in Microbiology* **4(43):** 1 -10.
- **Muyzer, G. and Stams, A. J.** (2008) The ecology and biotechnology of sulphate-reducing bacteria. *Nature reviews Microbiology* **6:** 441 – 454.
- **Nealson, K. H. and Myers, C. R.** (1990) Iron reduction by bacteria: A potential role in the genesis of banded iron formation. *American Journal of Science* **290:** 35 – 45.
- **Onysko, S. J., Kleinmann, R. L. P. and Erickson, P. M.** (1984) Ferrous iron oxidation by *Thiobacillus ferrooxidans*: inhibition with benzoic acid, sorbic acid and sodium lauryl sulfate. *Applied and Environmental Microbiology* **48(1):** 229 – 231.
- **Rathnayake, I. V. N., Megharaj, M., Bolan, N. and Naidu, R.** (2010) Tolerance of heavy metals by Gram positive soil bacteria. *International Journal of Civil and Environmental Engineering* **2(4):** 191 – 195.
- **Spadafora, A., Perri, E., Mckenzie, J. A. and Vasconcelos, C.** (2010) Microbial biomineralization processes forming morden Ca:Mg carbonate stromatolites. *Sedimentology* **57:** 27 – 40.
- **Suzuki, Y. and Banfield, J. F.** (2004) Resistance to, and accumulation of, uranium by bacteria from a uranium-contaminated sites. *Geomicrobiology Journal.* **21:** 113 – 121.

- **Utgikar, V. P., Tabak, H. H., Haines, J. R. and Govind, R.** (2003) Quantification of toxic and inhibitory impact of copper and zinc on mixed cultures of sulfate-reducing bacteria. *Biotechnology and Bioengineering* **82(3):** 306 – 312.
- **Voughan, D. J. and Lloyd, J. R.** (2011) Mineral-organic-microbe interactions: Environmental impacts from molecular to macroscopic scale. *Comptes Rendus Geoscience* **343:** 140 – 159.
- **Watanabe, T., Kojima, H. an Fukui, M.** (2014) Complete genomes of freshwater sulfur oxidisers Sulfuricella denitrificans skB26 and Sulfuritalea hydrogenivorans sk43H: genetic insight into the sulfur oxidation pathway of betaproteobacteria. *Systematic and Applied Microbiology* **37(6):** 387 – 395.
- **Willrodt, C., David, C., Conelissen, S., Bühler, B., Julsing, M. K. and Schmid, A.** (2014) Engineering the productivity of recombinant *Escherichia coli* for limonene formation from glycerol in minimal media. *Biotechnology Journal* **9(8):** 1000 – 1012.

CHAPTER 5

SUMMARY

5. SUMMARY

5.1. Summary

Acid mine drainage (AMD) or acid rock drainage (ARD) is a global challenge contaminating a lot of the fresh surface and groundwater. The drainage is characterized by low pH, high metal and sulfate concentrations. It is a consequence of most mining activities as lead source of AMD. The metals and sulfate in the drainage result from oxidation of metal sulfide containing rocks also referred to as host rock. Oxidation of the host rock occurs during mining by water and oxygen or naturally where the oxidation process occur through weathering and both processes can be accelerated by iron oxidising bacteria such as *Acidithiobacillus ferrooxidans* and *Leptospirillum ferrooxidans.* The *A. ferrooxidans* catalyses the oxidation of iron containing sulfide minerals such as pyrite and arsenopyrite releasing iron, arsenic and sulfur which gets oxidized into sulfate generating sulfuric acid that lowers the pH of the water. The acidic environment induces dissolution of other metals. In most coal mines, AMD contains some neutralizing minerals such as calcium oxide (lime), calcium carbonate (calcite) and sodium carbonate which raise the pH of the water but do not precipitate all of the metals and sulfate. The pH of water can be raised to between 5 and 8 hence the drainage is termed Non-acid mine drainage (NMD).

Toxic metals in AMD and NMD contaminate streams and rivers where they affect aquatic and terrestrial life. Treatments of these drainages have been developed and characterized into biotic and abiotic systems where chemical and biological methods are used. In this study, attention was given to extending knowledge that can contribute to developing and extending biotic remediation systems where sulfate-reducing bacteria (SRB) are employed to interact with AMD or NMD. SRB are a diverse group of microorganisms used in bioremediation and have been studied widely. SRB play a major role in the reversal process of AMD and NMD formation by reducing the sulfate concentrations. SRB use sulfate as their terminal electron acceptor releasing sulfide in a gas form that dissolves in the solution when the pH is above 4. This process occurs optimally in anaerobic environments and the dissolved sulfide, reacts with dissolved metals in the drainage forming metal sulfide precipitates. The sulfate reduction and metal removal processes from the drainages can be affected by numerous factors and a few discussed were explored and the

knowledge base extended in this study. Environmental conditions always have an effect on most activities performed by biological entities. For sulfate reduction, pH, temperature, carbon source type and availability, metal concentrations and redox conditions have direct effects on SRB activities.

In this study, three mine drainage study sites with generic names: Site-Ex, Site-Ka and Site-Po were selected. Water samples from the three sites as well as a sludge sample from Site-Po were collected and characterized chemically. Drainage from Site-Ex had characteristics of NMD while Site-Ka and Site-Po water samples had AMD characteristics. High concentrations of sulfate and transition metals were detected in the AMD samples. Microscopic analysis revealed high microbial cell counts in NMD and lower cell counts in AMD samples that could most probably be directly related to the diversity and toxicity of metals and low pH of the drainages. Molecular analysis revealed the presence of various SRB species in the drainages and sludge samples including the well-studied *Desulfovibrio* sp. Two media compositions: Postgate medium B (PSGM) and Anaerobic sulfate reducing medium (ASRM) were used to enrich anaerobic bacterial communities. Acclimation process with three passaging intervals of 20 days was conducted in anaerobic serum vials. After the third passaging stage, molecular identification of the enriched cells was performed and results revealed successful enrichment of SRB and other anaerobic (some novel) bacteria within the consortia. Scanning electron microscopy (SEM) was used to morphologically characterize the biogenic precipitates from the tertiary cultures. The SEM results showed bacterial biofilm associated with precipitates similar to those identified as framboid pyrite precursors.

The enriched consortia from the three study sites were co-cultured in PSGM and ASRM respectively. The best bacterial growth was achieved in PSGM which was then used for subsequent experiments as the medium of choice. The sulfate reducing capabilities of the enriched SRB were tested in PSGM with sulfate concentrations ranging between 2 000 mg/L to 4 000 mg/L. An average of 72% sulfate reduction was achieved in all experiments with a positive response of SRB to higher sulfate concentrations. Effects of pH and temperature on sulfate reduction were evaluated at pH of 3.5 and 6.2 and temperatures of 10ºC and 25ºC. Low pH conditions showed negative effects on sulfate reduction activity and bacterial growth

even when temperature was raised to 25ºC. Optimum SRB activity was observed in the experiment where pH was 6.2 at 25ºC. The results confirmed higher sulfate reducing conditions at higher pH (6.2) and temperature (25ºC). The carbon source utilisation by the enriched SRB between glycerol and sodium lactate was evaluated in batch operated bioreactors. The best sulfate reduction activity by SRB was observed when glycerol was used as a sole carbon source yielding greater amounts of dissolved sulfide concentrations. Glycerol was then used further as the main carbon source in PSGM. Metal-microbe interactions were evaluated where higher concentrations of zinc (Zn^{2+}) and iron (Fe^{2+}) were introduced in the bioreactors. Results showed 100%, 85% and 40% sulfate reduction in experiments where no metals, 200 mg/L of iron and 200 mg/L of zinc were added respectively. Effects of high Zn^{2+} concentrations were similar to those exerted by low pH conditions. However, 90% zinc and 97% iron were removed from the medium through biogenic precipitation. Precipitates were characterized by SEM, Transmission Electron Microscopy (TEM), X-ray Diffraction (XRD) and Energy Dispersive X-ray Spectroscopy (EDX) which confirmed the presence of biologically induced precipitates.

Results in this study can be used to model the activity of SRB in evaluated conditions that affect sulfate reduction. The enriched bacterial communities also showed great potential to be used in the up-scaled “reactors” to reduce sulfate concentration while indirectly precipitating dissolved metals in AMD.

Keywords: Acid mine drainage; Sulfate-reducing bacteria; Batch bioreactors; Enrichments; sulfate reduction; Metal microbe interactions.

5.2. Opsomming

Suur myn water (SMW) is ‘n globale probleem wat baie vars oppervlak- en grondwater kontamineer. Die water word gekarakteriseer deur lae pH en hoë metaal- en sulfaat konsentrasies. Dit is die nagevolg van meeste myn aktiwiteite as die hoofsaaklike bron van SMW. Die metale en sulfate in die water is as gevolg van die oksidasie van metaal sulfied wat in sekere minerale voorkom. Die oksidasie van SMW geskied tydens mynwese aktiwiteite as gevolg van die teenwoordigheid van water en suurstof of natuurlik waartydens die oksidasie proses plaasvind deur verwering. Beide prosesse kan versnel word deur yster-oksiderende bakterië soos *Acidothiobacillus ferrooxidans* en *Leptospirillum ferrooxidans*. *A. ferrooxidans* kataliseer die oksidasie van yster bevattende sulfied minerale soos piriet en arsenopiriet, wat lei tot die vrystelling van yster, arseen en swael wat op sy beurt geoksideer word om swaelsuur te produseer wat lei tot die daling van die water se pH. Hierdie lae pH induseer die oplossing van ander metale. In meeste steenkool myne bevat die SMW neutraliserende minerale soos kalsium oksied (kalk), kalsium karbonaat (kalsiet) en natrium karbonaat wat lei tot die styging van die water pH. Hierdie styging in pH verminder egter nie die hoë metaal- en sulfaat konsentrasies nie. Die pH van die water kan verhoog word na tussen 5 en 8, waarna dit verwys word na Nie-suur myn water (NMW).

Toksiese metale wat in SMW en NMW voorkom kontamineer strome en riviere met ‘n negatiewe impak op die akwatiese en terestriële lewe. Behandeling van hierdie water is al ontwikkel en kan gekarakteriseer word as biotiese en abiotiese sisteme waar biologiese en chemiese metodes gebruik word. In hierdie studie, was die aandag gefokus op die uitbreiding van kennis wat kan bydrae tot die ontwikkeling en uitbreiding van biotiese remediasie sisteme waartydens sulfaat-reduserende bakterië (SRB) gebruik word in interaksies met SMW en NMW. SRB is 'n diverse groep mikroorganismes wat in bioremediasie gebruik word en is al wyd bestudeer. SRB speel ‘n groot rol in die omkerings proses van SMW en NMW formasie deurdat dit die sulfaat konsentrasie in die water verlaag. SRB gebruik sulfaat as ‘n terminale electron akseptor, wat lei tot sulfied wat as ‘n gas vrygestel word en opgelos word in die water wanneer die pH steig bo 4. Hierdie proses vind optimaal plaas in anaërobiese toestande waartydens die sulfied dan ook reageer met die opgeloste

metale in die water wat lei tot die vorming van metaal sulfied presipitate. Die sulfaat reduksie en metaal presipiterings prosesse in die water kan geaffekteer word deur verskeie faktore en 'n paar wat bespreek is, is ondersoek en die kennis uitgebrei tydens hierdie studie. Omgewings toestande het altyd ‘n invloed op die meeste aktiwiteite wat deur biologiese entiteite uitgevoer word. Vir sulfaat reduksie om plaas te vind, kan die pH, temperatuur, koolstof bron tipe en beskikbaarheid, metaal konsentrasies en redox toestande ‘n direkte effek hê op SRB aktiwiteite.

Tydens hierdie studie was drie myn water studie areas met generiese name, Site-Ex, Site-Ka en Site-Po geselekteer. Water monsters van die studie areas, asook 'n slyk monster vanaf Site-Po is geneem en chemies gekarakteriseer. Die water vanaf Site-Ex is as NMW en beide die vanaf Site-Ka en Site-Po as SMW gekarakteriseer. Hoë konsentrasies sulfaat en transisie metale was opgespoor in die SMW monsters. Mikroskopiese analiese het gewys dat hoë mocrobiese sel getalle in die NMW voorkom, terwyl laer getalle in die SMW voorkom, wat waarskynlik direk verband kan hou met die diversiteit en toksisiteit van die metale en lae pH van die water. Molekulêre analiese het die teenwoordigheid aangedui van verskeie SRB spesies in die water en slyk monsters wat die wyd bestudeerde *Desulfovibrio* spesie insluit. Twee groei medium komposisies, Postgate medium B (PSGM) en Anaërobiese sulfaat-reduserende medium (ASRM), is gebruik om die anaërobiese bakteriële populasies te verryk. ‘n Akklimasie proses is gevolg met drie passerings intervalle van 20 dae in anaërobiese serum bottels. Na die derde passering, is molkulêre identifikasie van die verrykte selle uitgevoer. Die resultate het gewys op suksesvolle verryking van die SRB asook ander anaërobiese (sommige uniek) bakterië in die konsortium. Skanderings Elektron Mikroskopie (SEM) is gebruik om die biogeniese presipitate van die tersiêre kulture morfologies te karakteriseer. Die SEM resultate het gewys op ‘n bakteriële biofilm wat geassosieer is met presipitate soortgelyk aan die wat geïdentifiseer is as framboïde piriet voorgangers.

Die verrykte konsortiums van die drie studie areas is afsonderlik gekweek in PSGM en ASRM onderskeidelik. Die beste bakteriële groei is bereik in PSGM wat dus in die gevolglike eksperimente gebruik is as die groei medium van keuse. Die sulfaat reduserende vermoë van die verrykte SRB is getoets in PSGM met afsonderlike sulfaat konsentrasies tussen 2000 mg/L en 4000 mg/L. ‘n Gemiddeld van 72%

sulfaat reduksie kon gehandhaaf word in alle eksperimente, met ‘n positiewe reaksie van die SRB op hoër sulfaat konsentrasies. Die effek van pH en temperatuur op sulfaat reduksie is geëvalueer by ‘n pH van 3.5 en 6.2 en temperature van 10°C en 25°C. Lae pH toestande het ‘n negatiewe impak gehad op die sulfaat reduksie aktiwiteit sowel as bakteriële groei, selfs toe die temperatuur toegeneem het na 25°C. Optimale SRB aktiwiteit kon waargeneem word by ‘n pH van 6.2 by 25°C. Die resultate het die verhoogde sulfaat reduserende toestande teen hoër pH en temperature bevestig. Die koolstof bron gebruik deur die SRB tussen gliserol en natrium laktaat is geëvalueer in bioreaktors. Die beste sulfaat reduserende aktiwiteit is waargeneem met die gebruik van gliserol as die enigste koolstof bron, met die hoogste konsentrasie van sulfied in oplossing. Gliserol is verder gebruik as die koolstof bron van keuse in die PSGM. Metaal-mikrobe interaksies is geëvalueer deur hoër konsentrasies Zn^{2+} en Fe^{2+} by die bioreaktors te voeg. Resultate het gewys dat 100%, 85% en 40% sulfaat reduksie plaasgevind het toe 0 mg/L en 200 mg/L yster en 200 mg/L zink onderskeidelik bygevoeg is. Die effek van hoë Zn^{2+} konsentrasies was soortgelyk aan die effek wat lae pH toestande gehad het, terwyl 90% zink en 97% yster egter verwyder kon word deur biogeniese presipitasie. Presipitate is kerakteriseer deur SEM, Transmissie Elektron Mikroskopie (TEM), X-straal Diffraksie (XSD) en Energie Dispersiewe X-straal Spektroskopie (EDX) wat die teenwoordigheid van biologies-geïnduseerde presipitate bevestig het.

Die resultate van hierdie studie kan gebruik word om die aktiwiteit van die SRB vir sulfaat reduksie te modelleer. Die verrykte bakteriële populasies het die potensiaal getoon om gebruik te word in groter skaal “reaktore” om sulfaat konsentrasies te reduseer, terwyl opgeloste metale indirek gepresipiteer word in SMW.

Sleutelwoorde: Suur myn watre; Sulfaat-reduserende bakterie; Bioreaktors; Verrykings; Sulfaat reduksie; Metaal-mikrobe interaksies.